Characterization of Hydrophobically Modified Titanium Dioxide Polylactic Acid Nanocomposite Films for Food Packaging Applications

Naerin Baek

Dissertation submitted to the faculty of the Virginia Polytechnic Institute and State University in partial fulfillment of the requirements for the degree of

Doctor of Philosophy
In
Food Science and Technology

Sean F. O'Keefe, Chair

Young Teck Kim

Joseph E. Marcy

Susan E. Duncan

June 29, 2016
Blacksburg, Virginia

Keywords: titanium dioxide, surface modification, oleic acid, bioplastics polylactic acid, nanocomposites, food packaging, active packaging

Characterization of Hydrophobically Modified Titanium Dioxide Polylactic Acid Nanocomposite Films for Food Packaging Applications

Naerin Baek

ABSTRACT

Titanium dioxide (TiO_2) polymer nanocomposites improve barrier properties to gas and moisture and mechanical strength as well as providing active packaging functions. However, low compatibility between hydrophilic TiO_2 nanoparticles and hydrophobic polymers such as polylactic acid (PLA) causes problems due to the tendency of TiO_2 nanoparticles (TiO_2) to agglomerate and form large clusters. A surface modification of TiO_2 with long chain fatty acid may improve the compatibility between PLA and TiO_2. The goal of this study was to enhance barrier properties of oxygen and water vapor, mechanical strength and add light protecting function to PLA composites by incorporation of oleic acid modified TiO_2 nanoparticles (OA_TiO_2). The objectives of this study were: 1) synthesize TiO_2 and modify surface of TiO_2 with oleic acid, 2) investigate dispersion stability of TiO_2 and OA_TiO_2 in hydrophobic media, 3) incorporate TiO_2 and OA_TiO_2 into a PLA matrix and to characterize properties of TiO_2PLA (T-PLA) and OA_TiO_2 PLA nanocomposite films (OT-PLA), and 4) to determine stability of green tea infusion in T-PLA and OT-PLA packaging model systems during refrigerated storage at 4 ℃ under florescent lightening. TiO_2 was synthesized by using a sol-gel method and the surface of TiO_2 was modified by oleic acid using a one-step method. T-PLA and OT-PLA were prepared by solvent casting. TiO_2 and OA_TiO_2 were analyzed by X-ray diffraction, Fourier transform infrared spectroscopy, thermal analysis and dynamic light scattering. The barrier properties to oxygen and water vapor, morphology, mechanical properties, thermal stability and light absorption properties of T-PLA and OT-PLA were characterized. Dispersion of TiO_2 was

improved in PLA matrix by the surface modification method with oleic acid. OT-PLA had more effective improvements in the barrier properties and flexibility than T-PLA and PLA, but toughness of the films based on Young's modules of OT-PLA was lower than the T-PLA and the PLA. The OT-PLA may have a potential to be used as transparent, functional and sustainable packaging films, but limited use for complete visible and UV-light protection for photosensitized foods.

ACKNOWLEDGEMENT

It is still unbelievable that I am close to finishing my Ph.D. study. It would have never been possible to accomplish this long journey alone during the past three years. There were always those who gave their guidance, support, encouragement, help, smiles and precious time for me. I would like to express my sincere appreciation to those who were there for me during Ph.D. study.

I would like to thank my major advisor Dr. Sean O'Keefe for his guidance, patience, kindness, cheers and financial support during my Ph.D. study. Words are never enough to express my appreciation to him for this great opportunity to purse Master and Ph.D. studies and his extensive knowledge and experience that were always available for me. His trust and encouragement made me move forward and complete this journey. Without him, I would not be in this stage. I would like to thank Dr. Young Kim as a co-advisor for guidance, knowledge and research ideas. Without the research opportunity and experience in his lab as an intern student before started Ph.D. study, this dissertation would not have been possible. I also would like express my appreciation to Dr. Joseph Marcy and Dr. Susan Duncan who shared their precious times, expertise, knowledge and kind help. I feel so grateful that I could work with all of them as my committee members.

I would like to thank the staff, faculty and graduate students in the Food Science and Technology Department. I will always appreciate that I have been helped by FST members during the past years, especially Dr. Hengjian Wang, Melisa Wright, Brian Wiersema for their assistance with using instruments, troubleshooting instrument, and setting up experiments in the pilot plant. I would also like to thank Dr. Ann Norris for helping me use XRD, DSC and Rheometer equipment in Sustainable Biomaterials which played important roles in my studies. I

would like to thank Dr. Katia Rodriguez for ordering lab supplies and her knowledge and suggestions for my research project at Dr.Kim's lab. I would like to thank Stephen McCartney and Chris Winkler at the Institute for Critical Technology and Applied Science Nanoscale Characterization and Fabrication Laboratory for the training of Field Scanning Electron Microscopy and Transmission Electron Microscopy. I want to thank the lab members in Dr. O'Keefe (Renata and Oumoule) and Dr. Kim's labs (Elham, Yoojin and Jun) for the smiles, help, chatting and encouragement.

Warm thanks to previous roommates and friends, Liyun, Eveline, Moonyoung, Boram, Andrew, Seul-yi and Hyun-woo for their support, humor, laughs and warm wishes.

My special and dearest thanks to my parents and my brother for their belief, support, wishes and cheers with their unconditional love and prayers. I feel most fortunate to have them. Without them, it would not have been possible to finish through my Bachelor's, Master of Science and Ph.D. studies in U.S.A.

My final thanks to Food Science and Technology and Water INTERface, INTERdisciplinary graduate education program for the financial support during my Ph.D. study.

TABLE OF CONTENTS

LIST OF ABBREVIATIONS

TiO_2 nanoparticles	TiO_2
Polylactic acid	PLA
Oleic acid	OA
Oleic acid modified TiO_2	OA_TiO_2
TiO_2 PLA nanocomposite films	T-PLA
Oleic acid modified TiO_2 PLA nanocomposite films	OT-PLA
Biobased biopolymer	Biopolymer
X-ray diffraction	XRD
Nanometer	nm
Micrometer	μm
Fourier transform infrared spectroscopy	FTIR
Transmission electron microscopy	TEM
Thermogravimetric analysis	TGA
Dynamic light scattering	DLS
Field emission scanning electron microscopy	FESEM
kV	kilo volt
InLens	inlens detector
X-ray energy dispersive spectrometer system	EDS
Oxygen permeation rate	OPR
Water vapor permeability coefficients	WVP
Differential scanning calorimetry	DSC
Tensile strength	TS

Mega pascal	MPa
Young's modulus	YM
Elongation at break	E
Grass transition temperature	Tg (℃)
Melting temperature	Tm (℃)
Crystallinity	Xc (%)
Melting enthalpy	Δ Hm (j/g)
Cold crystallization enthalpy	Δ Hc (j/g)
(-)-Epigallocatechin Gallate	EGCG
Ready to Drink	RTD
High Performance Liquid Chromatography	HPLC
Lux	lx

CHAPTER 1. INTRODUCTION

Plastics are used in over 40% of total packaging production and nearly half of packaging materials are used for different types of food packaging, such as films, sheets, bottles, cups, tubs and trays etc. [1]. In recent years, there has been growing interest in use of biobased biodegradable polymers for food packaging to reduce fossil energy and accumulation of petroleum-based, non-degradable plastic waste [1, 2]. Currently, biobased and biodegradable polymers are mainly used in disposable containers, utensils and short-term packaging [2, 3]. Among various biobased and biodegradable polymers, polylactic acid, which is produced from synthesis of lactic acid monomers originating from 100% renewable sources such as corn, sugar beets, wheat or other feedstock, is one of the most widely used biobased and biodegradable polymers in applications for food packaging [4]. PLA affords biocompatibility, a safe material for direct food contact, rigidity, hydrophobicity, high transparency, good thermal processability and lower energy costs during manufacturing compared to other biobased and biodegradable polymers for food packaging. However, drawbacks of PLA include low barrier properties of gas and water vapor, brittleness, as well as high cost; thus, PLA use is restricted [4].

Bionanocomposites refer to biopolymer matrices filled with nanostructured material where at least one dimension is smaller than 100 nm [1]. This is one of the innovative packaging strategies that have studied and utilized in recent years to improve mechanical strength, thermal stability, gas barrier properties and to reduce moisture sensitivity by using characteristics of nanomaterials: high surface area to volume ratio, and interfacial adhesion between nanoparticles and polymer matrix [5, 6]. Therefore, bionanocomposite use in food packaging applications has been proposed as one of the innovations and advanced technologies to strengthen physical

properties of biobased and biodegradable polymers as well as to create active and smart packaging systems using the unique properties of nanotechnology [1, 7].

TiO_2 is well known for many years as a white pigment color additive in food packaging materials. Recently, nanosize TiO_2 has been also a popular nanofiller in food packaging because of its non-toxicity, low cost, abundance, and chemical and thermal stability [8]. Particularly, TiO_2 nanomaterials provide properties such as transparently dispersing in polymers providing UV- light blocking properties, self-cleaning effects such as deodorizing, sanitizing and antibacterial activity by photocatalytic activity, reducing permeability of materials and toughening materials [8, 9]. Numerous studies reported that TiO_2 polymer nanocomposites reinforced with TiO_2 nanomaterials effectively inhibit growth of foodborne microorganisms under UV light and UV-blocking films have been developed for photosensitive foods [9-11].

However, low compatibility between hydrophilic TiO_2 nanoparticle surface and hydrophobic polymers such as PLA leads to agglomeration of the particles and formation of large clusters, resulting in reduced efficiency of the nanofiller [12]. Effectiveness of photocatalytic activity, optical properties and UV-blocking properties can be maximized by controlling the size of TiO_2 particles in the nanosize range [12-14].

One of the solutions that has been suggested in other studies is a surface modification of TiO_2 using an appropriate surface modifier and dispersant [15-17]. The surface modification improved dispersion stability between TiO_2 nanoparticles and polymer matrices [15, 18]. When surface modifier and incorporated media has high affinity each other, compatibility between two materials is improved [16].

In this study, the surface of TiO_2 was modified by oleic acid with chloroform as a dispersant. Oleic acid is long chain fatty acid possessing strong hydrophobicity that can change

the hydrophilic surface of TiO_2 to a hydrophobic surface. In addition, we expected using chloroform as a dispersant for oleic acid modified TiO_2 will promote dispersion of oleic acid modified TiO_2 nanoparticles in PLA matrices because oleic acid and PLA are highly soluble in chloroform. In addition, oleic acid is common plasticizer for polymers and functional modifier to improve barrier properties as well as enhancing flexibility of polymers [19-21]. We hypothesized that surface modified TiO_2 with oleic acid can stably disperse in PLA matrices, and PLA nanocomposites reinforced with oleic acid modified TiO_2 nanoparticles might be functional, transparent and sustainable biobased biodegradable polymers that enhance material performances and add UV-light resistance.

Research Objectives

The aim of study is to improve dispersion stability of TiO_2 by surface modification with oleic acid in a PLA matrix and to enhance barrier properties for oxygen and water vapor, improve mechanical strength, and to add a light blocking function to PLA composites by incorporation of oleic acid modified TiO_2 nanoparticles.

Objective 1. Synthesize TiO_2 and modify surface of TiO_2 with oleic acid using an economical and simple method.

Objective 2. Investigate dispersion stability of TiO_2 and oleic acid modified TiO_2 in hydrophobic media.

Objective 3. Incorporate TiO_2 and oleic acid modified TiO_2 in PLA matrices and characterize properties of TiO_2 PLA nanocomposite films and oleic acid modified TiO_2 PLA nanocomposite films.

Objective 4. Determine stability of green tea infusion in TiO_2 PLA and oleic acid modified TiO_2 PLA nanocomposite film packaging models during refrigerated storage at 4 ℃ under florescent illumination.

REFERENCES

1. Rhim, J. W., Park, H. M., & Ha, C. S. (2013). Bio-nanocomposites for food packaging applications. *Progress in Polymer Science*, *38*(10), 1629-1652.

2. Sorrentino, A., Gorrasi, G., & Vittoria, V. (2007). Potential perspectives of bio-nanocomposites for food packaging applications. *Trends in Food Science & Technology*, *18*(2), 84-95.

3. Siracusa, V., Rocculi, P., Romani, S., & Dalla Rosa, M. (2008). Biodegradable polymers for food packaging: a review. *Trends in Food Science & Technology*, *19*(12), 634-643.

4. Jamshidian, M., Tehrany, E. A., Imran, M., Jacquot, M., & Desobry, S. (2010). Poly-Lactic Acid: production, applications, nanocomposites, and release studies. *Comprehensive Reviews in Food Science and Food Safety*, *9*(5), 552-571.

5. De Azeredo, H. M. (2009). Nanocomposites for food packaging applications. *Food Research International*, *42*(9), 1240-1253.

6. Sorrentino, A., Gorrasi, G., & Vittoria, V. (2007). Potential perspectives of bio-nanocomposites for food packaging applications. *Trends in Food Science & Technology*, *18*(2), 84-95.

7. Sanchez-Garcia, M. D., Lopez-Rubio, A., & Lagaron, J. M. (2010). Natural micro and nanobiocomposites with enhanced barrier properties and novel functionalities for food biopackaging applications. *Trends in Food Science & Technology*, *21*(11), 528-536.

8. Bogdan, J., Jackowska-Tracz, A., Zarzyńska, J., & Pławińska-Czarnak, J. (2015). Chances and limitations of nanosized titanium dioxide practical application in view of its physicochemical properties. *Nanoscale Research Letters*, *10*(C.J Moorea), 1-10. doi: 10.1186/s11671-015-0753-2.

9. Llorens, A., Lloret, E., Picouet, P. A., Trbojevich, R., & Fernandez, A. (2012). Metallic-based micro and nanocomposites in food contact materials and active food packaging. *Trends in Food Science & Technology*, *24*(1), 19-29.

10. Gumiero, M., Peressini, D., Pizzariello, A., Sensidoni, A., Iacumin, L., Comi, G., & Toniolo, R. (2013). Effect of TiO2 photocatalytic activity in a HDPE-based food packaging on the structural and microbiological stability of a short-ripened cheese. *Food Chemistry*, *138*(2), 1633-1640.

11. Ghanbarzadeh, B., Oleyaei, S. A., & Almasi, H. (2015). Nanostructured Materials Utilized in Biopolymer-based Plastics for Food Packaging Applications. *Critical Reviews in Food Science and Nutrition*, *55*(12), 1699-1723.

12. Chau, J. L. H., Lin,Y. M., Li, A. K., Su, W. F., Chang, K. S., Hsu, S. L. C., & Li, T. L. (2007). Transparent high refractive index nanocomposite thin films. *Materials Letters, 61*(14), 2908-2910.

13. Buzarovska, A. (2013). PLA nanocomposites with functionalized TiO2 nanoparticles. *Polymer-Plastics Technology and Engineering, 52*(3), 280-286.

14. Silvestre, C., & Cimmino, S. (2013). Ecosustainable polymer nanomaterials for food packaging: innovative solutions, characterization needs, safety and environmental issues. CRC Press.

15. Nakayama, N., & Hayashi, T. (2007). Preparation and characterization of poly (l-lactic acid)/TiO_2 nanoparticle nanocomposite films with high transparency and efficient photodegradability. *Polymer Degradation and Stability, 92*(7), 1255-1264.

16. Arita, T., Ueda, Y., Minami, K., Naka, T., & Adschiri, T. (2009). Dispersion of fatty acid surface modified ceria nanocrystals in various organic solvents. *Industrial & Engineering Chemistry Research*, *49*(4), 1947-1952.

17. Cozzoli, P. D., Kornowski, A., & Weller, H. (2003). Low-Temperature Synthesis of Soluble and Processable Organic-Capped Anatase TiO2 Nanorods. *Journal of the American Chemical Society, 125*(47), 14539-14548. doi: 10.1021/ja036505h.

18. Zhang, L., Chen, L., Wan, H., Chen, J., & Zhou, H. (2011). Synthesis and tribological properties of stearic acid-modified anatase (TiO_2) nanoparticles. *Tribology Letters*, *41*(2), 409-416.

19. Lim, J. H., Kim, J., Ko, J. A., & Park, H. J. (2015). Preparation and Characterization of Composites Based on Polylactic Acid and Beeswax with Improved Water Vapor Barrier Properties. *Journal of Food Science, 80(11)*, E2471-E2477.

20. He, M., Xu, M., & Zhang, L. (2013). Controllable stearic acid crystal induced high hydrophobicity on cellulose film surface. *ACS Applied Materials & Interfaces, 5*(3), 585-591.

21. Lai, H. M., & Padua, G. W. (1998). Water vapor barrier properties of zein films plasticized with oleic acid. *Cereal Chemistry, 75(2)*, 194-199.

CHAPTER 2. LITERATURE REVIEWS

1. Biopolymers for food packaging

The Institute for Bioplastics and Biocomposites (University of Applied Science and Arts Hannover, Germany) and novaInstitute (Hürth, Germany) reported worldwide manufacturing capacity of bioplastics is estimated to increase from 1.7 million tons in 2014 to 7.8 million tons in 2019 [1]. Nearly 70% of total bioplastic market (1.2 million tons) is assigned to the packaging field and production capacity is anticipated to increase to more than 6.5 million tons, which is a more than 80 % increase in 2019 [1].

There has been growing interest in development and utilization of sustainable materials for food packaging due to environmental concerns related to dependence on fossil energy and accumulation of petroleum-based, non-degradable plastic waste [2]. As a result, biobased biopolymers (biopolymers) defined as polymers produced from renewable agricultural sources and decomposed and broken down naturally to biomass and biogases by appropriate moisture, temperature, oxygen and microbial environments. The biopolymers have gained much attention for sustainable food packaging material [2, 3].

Biopolymers can be categorized based on fundamental resources and production methods according to Robertson (2006) [4]. The first category is the biopolymers which are produced from naturally occurring polymers: carbohydrate materials such as cellulose, starch, chitosan, alginate, proteins such as soy, corn zein, wheat gluten, gelatin, collagen and lipids [2-4]. The second category is called as biobased plastics which are biobased and biodegradable polymers [2]. Biobased plastic is produced through synthesis of monomers originated from renewable sources such as corn, rice and other feedstocks. Bioplastic includes polylactic acid, polyglycolic acid, polybuthylene succinate and poly Ɛ-caprolactone [2-4]. As seen Figure 2, polylactic acid (PLA) is commercially available and is one of the most used bioplastics obtained from synthesis

of lactic acid monomers obtained from fermentation of agricultural products such as corn, rice and other feedstocks [5]. The third category is biopolymers such as polyhydroxyalkanoates produced from fermentation and modifications of microorganisms [2, 3]. Although these biopolymers have many potential and beneficial properties that can potentially replace petroleum based non degradable polymers for environmentally friendly materials, these biopolymers have limited use in various applications for food packaging because of poor mechanical strengths, low heat stability, water sensitivity, low barrier property for gas and moisture, high production costs and short shelf life stability [2, 3, 5].

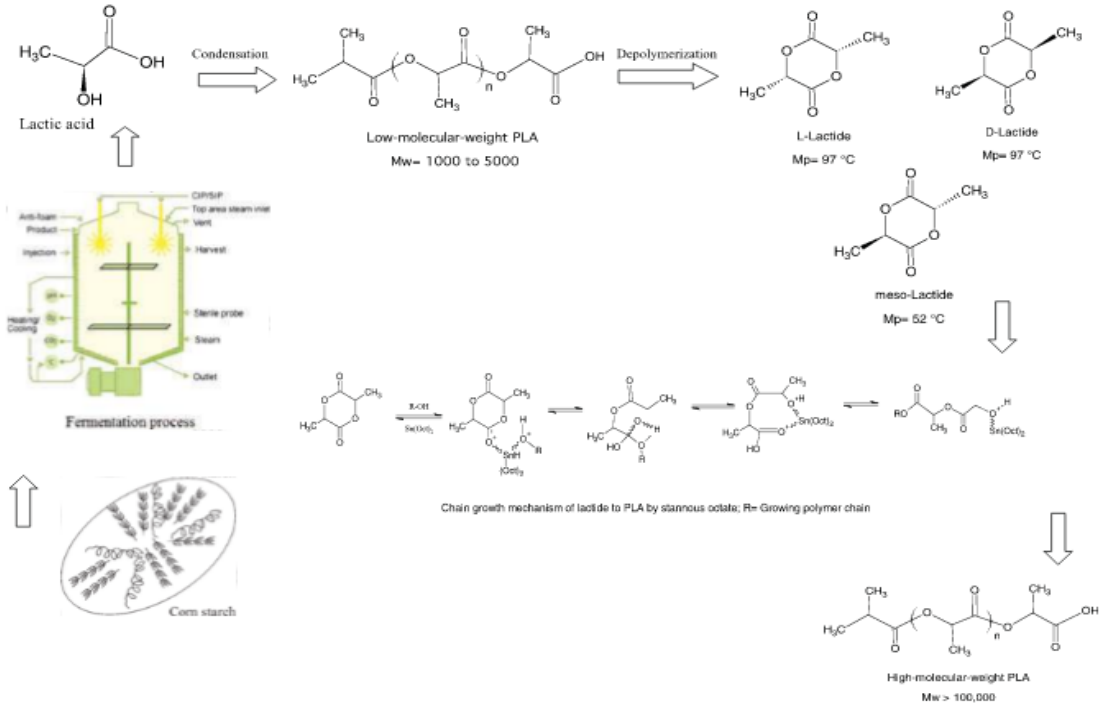

Figure 2. Methods of polylactic acid production [5]. This figure was used with a permission of John Wiley and Sons.

2. Innovative and Advanced Food Packaging Solution for Biopolymers: Polymer Nanocomposites

Bionanocomposites are considered a new class of packaging material: biopolymer matrices enhanced with nanofillers having a least one dimensional size in the nanometer range (1-100 nm) [2, 6].

1) Improvements in mechanical and barrier properties of food packaging

Bionanocomposties exhibited enhanced essential properties of biopolymers such as mechanical strengths, barrier properties to gas and moisture and heat resistance compared to neat biopolymers [7, 8]. Numerous factors influence effective efficiency of nanofillers when they are incorporated into the polymer matrices: structural properties (size, shapes, aspect ratio), mechanical properties (ultimate tensile strengths, elastic modulus), addition amounts of nanofillers, dispersion stability, exfoliation and interfacial properties (compatible ability between nanofillers and polymer matrix) [8]. Due to high surface area to volume ratio of the nanofillers, strong interfacial adhesion between nanoparticles and polymer matrix attributed to produce exceptional properties in the polymer nanocomposites compared to neat polymer composites [8, 9, 10]. Well-distributed nanofillers in polymer matrices is one of the key factors to determine material properties. The Figure 2a. shows how nanofillers make tortuous paths in neat polymers and how barrier properties of polymers are improved by creation of polymer nanocomposites [7].

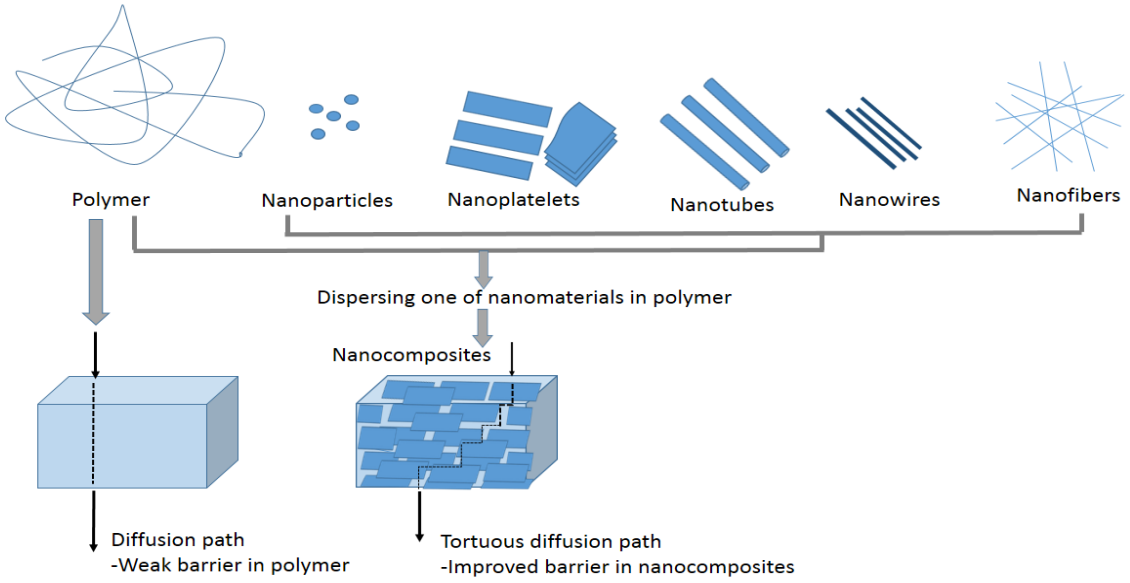

Figure 2a. Schematic illustration how polymernanocompostites are created and enhance barrier properties compared to neat polymer adapted from Mihindukulasuria and Lim (2014) [7]. This figure was used with a permission of Elsevier.

Incorporation of nanofillers influences chain mobility of polymers and creates tortuous diffusion paths. When longer times takes to pass through the tortuous diffusion path, barrier properties of the polymer nanocomposites can be improved [7].

2) Active polymernanocomposites functions

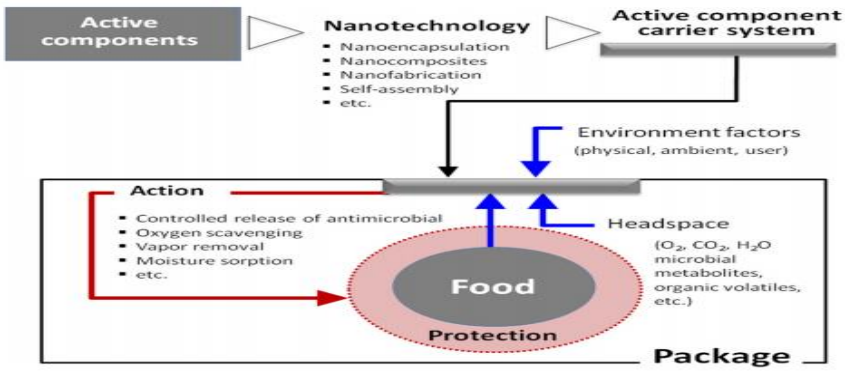

Figure 2b. Schematic illustration of active food packaging system described by Mihindukulasuria and Lim (2014) [7]. This figure was used with a permission of Elsevier.

When it comes to food packaging, active polymer nanocomposties maintain quality of packaged foods and increase shelf life of foods [1], The nanocomposites, which are incorporated with nanomaterial into a polymer matrix in the active food packaging system, release or absorb active compounds such as antimicrobials, preservatives, antioxidants, oxygen scavengers and ethylene gas scavengers into (or internally from) the packaged foods or the external environment [7, 11]. Addition of metal and metal oxides nanoparticles such as titanium oxide, zinc oxide, silver, gold, aluminum and iron oxide are well known antimicrobials that are applied to active packaging [7, 12, 13]. The antimicrobial nanomaterial can inactive microorganism growth; nanomaterial damages cells, interrupting electrons transport, disrupting cell membranes or oxidizing cell components in the direct ways, and producing secondary products of reactive oxygen species or dissolving heavy metal ions in indirect ways under UV lightening [2, 7, 11]. As UV-absorbers, titanium dioxide and zinc oxide, play important roles in hindering UV light and prevention of photo-deterioration of foods in the polymer nanocomposites reinforced with the UV light absorbing nanomaterials [11, 30, 31]. Busola & Lagaron (2012) reported that high density polyethyelene (HDPE) film reinforced with iron containing kaoline as oxygen scavenger produced an efficient active food packaging system that trapped oxygen, as well as building more tortuous diffusion paths [15]. Nanocoating forms active packaing as nanomaterial is applied onto packaging materials and laminated polymer composite layers [7]. For example, metal oxide based nanocoating such as titanium dioxide, iron oxide or zinc oxide improved barrier properties and antimicrobial activity in addition to simultaneously reducing material use and simplifying the film converting process [7].

3) Smart/Intelligent Polymer Nanocomposite Functions

Nanomaterials can be applied to monitor and indicate food quality of packaged foods by providing a visual indicator based on the food quality and condition [7, 11]. Sensors and indicators of nanomaterials fabricated into packaging so that they interact with food components and internal headspace and with external factors in the environment surrounding foods [7]. The fabricated sensors can detect food spoilage organisms and work as oxygen indicators and freshness indicators. Once the sensors detect the food spoilage, it generates color change or other noticeable signs to alert the consumers that quality and shelf life expiration of packaged foods [2, 7, 11, 20]. When a freshness indicator was produced in plastic or paper packaging deposited in 1-10 nm thickness films of silver or copper, it detected volatile sulfide and amine groups from food spoilage and the thin coating responds to the spoilage by developing a dark color [16].

3. TiO_2 Polymer Nanocomposties for Food Packaging

1) TiO_2 nanomaterial:

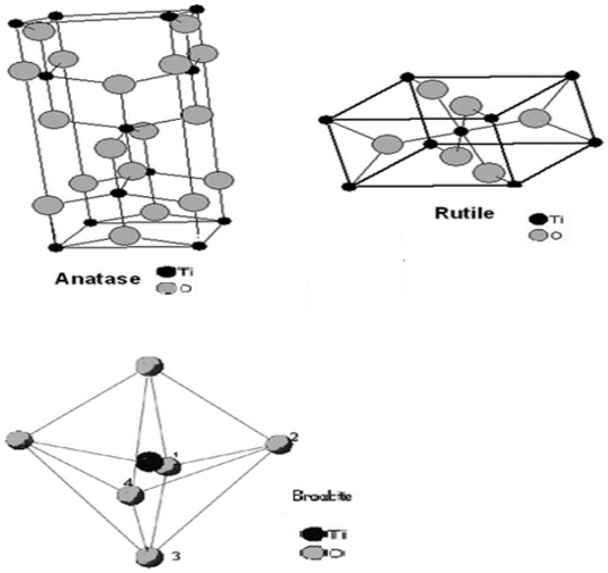

Figure 3a. Crystalline structures of TiO_2: anatase, rutile and brookite forms adapted from Macwan, Dave and Chaturvedi (2011) [25]. This figure is used with a permission of Springer.

TiO_2 has been one of the most well-known color additives in the food industry for several decades [21]. TiO_2 exhibits different properties depending on particle sizes and crystalline structures. TiO_2 nanomaterials have been used in a wide range of applications because of its non-toxicity, highly thermal and chemical stability, inertness, non-corrosiveness, low cost production, abundance, photocatalytic activity under UV-light illumination, UV-light blocking and optical properties [7, 24]. Compared to microsized TiO_2, nano TiO_2 possess much larger active surface to volume ratio as a result of higher UV absorption and higher photocatalytic effects [24, 25]. Also, TiO_2 exhibits three different crystalline phases, anatase, rutile and brookite. Each crystal phases has different stability based on crystal structures and particle sizes [25]. The basic structure of TiO_2 is produced based on octahedral units of TiO_6 [27]. Each different crystal structure of anatse, rutile and brookite is formed by different arrangements and connections of oxygen and Titanium as seen the Figure 3a [25, 27-28].

2) Photocatalytic Activity and UV-Light Absorbance

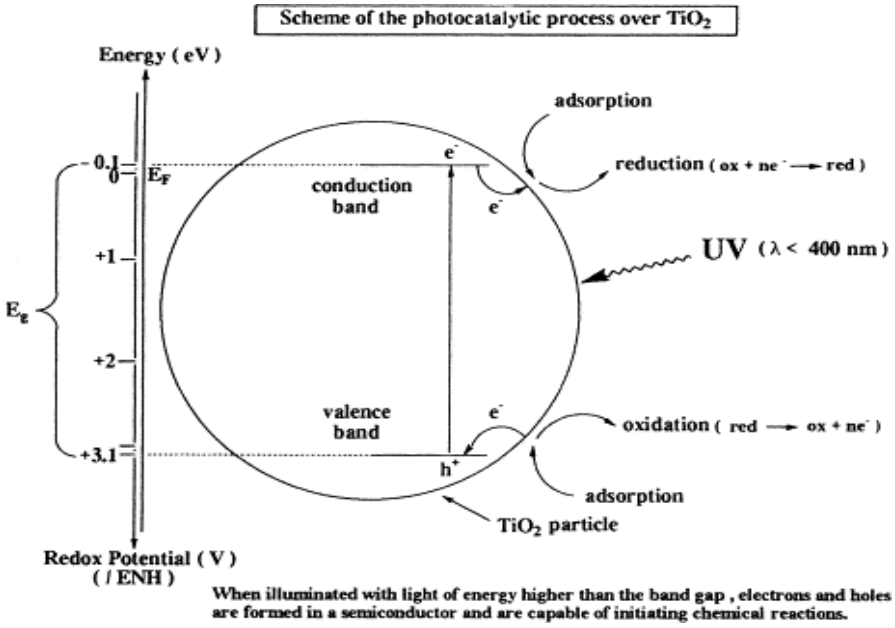

Figure 3b. Illustration of TiO_2 mechanisms for photocatalytic activity adapted from Herrmann (1999) [29]. This figure is used with a permission of Elsevier.

Figure 3b illustrates mechanisms of redox reactions on surface of a TiO_2 photocatalyst. TiO_2 can be activated from a valence band to a conduction band to generate electron hole pairs by illumination with UV light energy of wavelengths smaller than 380 nm (band gap energy higher than 3.2 eV) [8]. Once a pair of electron hole ($h^+ + e^-$) is produced by TiO_2 excitation for valence band (full with electron) to conduction band (free of electron), created electron and oxygen in the conduction band interacts with $O_2^{\cdot -}$ in reduction. Positive electron hole (h^+) and water generates hydroxyl radicals, superoxide anion and hydrogen peroxide and these deactivate and oxidize bacteria, yeast, and mold and decompose to to carbon dioxide, water as well as organic compounds [8, 22, 24, 29]. Valence electron band hole (h^+) works as a powerful oxidant while electron (e-) in conduction band as a reluctant.

In addition, food packaging films incorporated with TiO_2 nanoparticles provide UV protection and prevent/retard packaged food from the photooxdiation under UV-illumination because TiO_2 nanoparticles effectively absorb short wavelengths (as UV light absorber) with high photostability at the same time maintaining the material clarity [8, 30]. Ren, Wang, Gao, Chen, Li and Peng (2015) reported that polyvinyl alcohol/xylan films incorporating TiO_2 nanoparticles obtain efficient UV-light blocking properties [31]. Chitosan/TiO_2 nanotube films also had UV-light shielding property [17]. However, its wide band gap value (3.2eV) limits photocatalytic activity with visible light radiation because it requires high light energy wavelength less than 380 nm [32, 33]. In addition, fast recombination of photogenerated electron hole pairs reduces efficiency of TiO_2 photocatalysis [34]. Metal doping is one of the effective ways to improve photocatlytic activity of TiO_2 from UV light region to visible light region because it reduces the band gap and extends requiring wavelengths [8, 33, 34]. Numerous studies reported that metal dopant including silver and zinc enhanced effectiveness of

photocatalysis of TiO_2 from UV to visible regions by extension of light absorption efficiency using metal dopants [33-36].

3) Antibacterial Activity

TiO_2 polymer nanocomposites have many reports of reduced risks associated with bacteria growth under UV-light. Addition of TiO_2 nanomaterial in polymer packaging material inactivates both gram positive and gram negative bacteria, viruses and molds within various packaged foods. For example, TiO_2 in various forms of nanomaterial such as nanoparticles, nanotubes and nanorods shows significant antimicrobial activity against both gram positive and gram negative bacteria and viruses by photocatalaysis of TiO_2 under UV-illumination [12-16]. Dispersion of nanosize TiO_2 particles in polymer matrices showed higher efficiency and effects in antimicrobial activity than dispersion of microsized TiO_2 nanoparticles in polymer composites [7]. It has been sufficiently studied that polymer incorporated TiO_2 nanoparticles inhibited growth of *E. coli*, mold, *Penicillum* and other microrganisms in vegetables, fruits and breads under UV-irradiation [23, 37-38].

4) Oxygen and Ethylene Scavenging Activity

TiO_2 nanoparticles act as oxygen and ethylene scavengers in food packaging under UV-illumination to keep low oxygen levels and create suitable conditions for oxygen-sensitive foods [18, 19]. When TiO_2 was incorporated into glass and acetate films, it created deoxygenated environment in head space of package, preventing and retarding oxidation and browning processes of foods [7, 39]. Moreover, TiO_2 as a photocatalyst oxidized ethylene gas to water and carbon dioxide, slowing the ripening and maturation of fruits and extending shelf life of fruits and vegetables [7, 8, 21]. Polypropylene films coated with TiO_2 showed effective removal of ethylene gas in horticultural products with nano-sized coated polypropylene [20]. A beneficial

property of TiO_2 ethylene gas scavenger in polymer nanocomposites is that it is not degraded in the reaction and permanently available to remove ethylene gas in the package [7].

REFERENCES

1. Europeon bioplastics (2014) BIOPLASTICS facts and figures. Retrieved from http://www.corbion.com/media/203221/eubp_factsfigures_bioplastics_2013.pdf

2. Rhim, J. W., Park, H. M., & Ha, C. S. (2013). Bio-nanocomposites for food packaging applications. *Progress in Polymer Science*, *38*(10), 1629-1652.

3. Lagaron, J. M., & Lopez-Rubio, A. (2011). Nanotechnology for bioplastics: opportunities, challenges and strategies. *Trends in Food Science & Technology*, *22*(11), 611-617.

4. Robertson, G. L. (2006). Food packaging: principles and practice. 2006. *Taylor & Francis/CRC*

5. Jamshidian, M., Tehrany, E. A., Imran, M., Jacquot, M., & Desobry, S. (2010). Poly - lactic acid: production, applications, nanocomposites, and release studies. *Comprehensive Reviews in Food Science and Food Safety*, *9*(5), 552-571.

6. Kumar, P., Sandeep, K. P., Alavi, S., & Truong, V. D. (2011). A Review of experimental and oodeling techniques to determine properties of biopolymer-Based Nanocomposites. *Journal of Food Science*, *76*(1), E2-E14.

7. Mihindukulasuriya, S. D. F., & Lim, L. T. (2014). Nanotechnology development in food packaging: A review. *Trends in Food Science & Technology*, *40*(2), 149-167.

8. Ghanbarzadeh, B., Oleyaei, S. A., & Almasi, H. (2015). Nanostructured materials utilized in biopolymer-based plastics for food packaging applications. *Critical Reviews in Food Science and Nutrition*, *55*(12), 1699-1723.

9. Sorrentino, A., Gorrasi, G., & Vittoria, V. (2007). Potential perspectives of bio-nanocomposites for food packaging applications. *Trends in Food Science & Technology*, *18*(2), 84-95.

10. De Azeredo, H. M. (2009). Nanocomposites for food packaging applications.*Food Research International*, *42*(9), 1240-1253.

11. Silvestre, C., & Cimmino, S. (2013). Ecosustainable polymer nanomaterials for food packaging: innovative solutions, characterization needs, safety and environmental issues. CRC Press.

12. Duncan, T. V. (2011). Applications of nanotechnology in food packaging and food safety: barrier materials, antimicrobials and sensors. *Journal of Colloid and Interface Science*, *363*(1), 1-24.

13. Espitia, P. J. P., Soares, N. D. F. F., dos Reis Coimbra, J. S., de Andrade, N. J., Cruz, R. S., & Medeiros, E. A. A. (2012). Zinc oxide nanoparticles: synthesis, antimicrobial activity and food packaging applications. *Food and Bioprocess Technology*, *5*(5), 1447-1464.

14. Chaudhry, Q., Scotter, M., Blackburn, J., Ross, B., Boxall, A., Castle, L., ... & Watkins, R. (2008). Applications and implications of nanotechnologies for the food sector. *Food Additives and Contaminants*, *25*(3), 241-258.

15. Busolo, M. A., & Lagaron, J. M. (2012). Oxygen scavenging polyolefin nanocomposite films containing an iron modified kaolinite of interest in active food packaging applications. *Innovative Food Science & Emerging Technologies*, *16*, 211-217.

16. Smolander, M., Hurme, E., Koivisto, M., & Kivinen, S. (2004). Indicator. In (Vol. International Patent WO2004/102185 A1).

17. Díaz-Visurraga, J., Melendrez, M. F., Garcia, A., Paulraj, M., & Cardenas, G. (2010). Semitransparent chitosan-TiO_2 nanotubes composite film for food package applications. *Journal of Applied Polymer Science*, *116*(6), 3503-3515.

18. Molina, J., Sanchez-Salas, J. L., Zuniga, C., Mendoza, E., Cuahtecontzi, R., Garcia-Perez, G., ... & Bandala, E. R. (2014). Low-temperature processing of thin films based on rutile TiO_2 nanoparticles for UV photocatalysis and bacteria inactivation. *Journal of Materials Science*, *49*(2), 786-793.

19. Maneerat, C., & Hayata, Y. (2006). Antifungal activity of TiO 2 photocatalysis against Penicillium expansum in vitro and in fruit tests. *International Journal of Food Microbiology*, *107*(2), 99-103.

20. Maneerat, C., & Hayata, Y. (2008). Gas-phase photocatalytic oxidation of ethylene with TiO_2-coated packaging film for horticultural products. *Transactions of the ASABE*, *51*(1), 163-168.

21. Xiao-e, L., Green, A. N., Haque, S. A., Mills, A., & Durrant, J. R. (2004). Light-driven oxygen scavenging by titania/polymer nanocomposite films. *Journal of Photochemistry and Photobiology A: Chemistry*, *162*(2), 253-259.

22. Kerry, J. P., O'grady, M. N., & Hogan, S. A. (2006). Past, current and potential utilisation of active and intelligent packaging systems for meat and muscle-based products: A review. *Meat Science*, *74*(1), 113-130.

23. Llorens, A., Lloret, E., Picouet, P. A., Trbojevich, R., & Fernandez, A. (2012). Metallic-based micro and nanocomposites in food contact materials and active food packaging. *Trends in Food Science & Technology*, *24*(1), 19-29.

24. Bogdan, J., Jackowska-Tracz, A., Zarzyńska, J., & Pławińska-Czarnak, J. (2015). Chances and limitations of nanosized titanium dioxide practical application in view of its physicochemical properties. *Nanoscale Research Letters*, 10(C.J Moorea), 1-10. doi: 10.1186/s11671-015-0753-2.

25. Macwan, D. P., Dave, P. N., & Chaturvedi, S. (2011). A review on nano-TiO_2 sol–gel type syntheses and its applications. *Journal of Materials Science*, *46*(11), 3669-3686.

26. Lin, H., Huang, C. P., Li, W., Ni, C., Shah, S. I., & Tseng, Y. H. (2006). Size dependency of nanocrystalline TiO_2 on its optical property and photocatalytic reactivity exemplified by 2-chlorophenol. *Applied Catalysis B: Environmental*, *68*(1), 1-11.

27. Cargnello, M., Gordon, T. R., & Murray, C. B. (2014). Solution-phase synthesis of titanium dioxide nanoparticles and nanocrystals. *Chemical Reviews*, *114*(19), 9319-9345.

28. Reyes-Coronado, D., Rodríguez-Gattorno, G., Espinosa-Pesqueira, M. E., Cab, C., de Coss, R. D., & Oskam, G. (2008). Phase-pure TiO_2 nanoparticles: anatase, brookite and rutile. *Nanotechnology*, *19*(14), 145605.

29. Herrmann, J. M. (1999). Heterogeneous photocatalysis: fundamentals and applications to the removal of various types of aqueous pollutants. *Catalysis Today*, *53*(1), 115-129.

30. Hashimoto, A., & Sakamoto, K. (2011). UV-Blocking film for food storage using titanium dioxide. *Food Science and Technology Research*, *17*(3), 199-202.

31. Ren, J., Wang, S., Gao, C., Chen, X., Li, W., & Peng, F. (2015). TiO_2-containing PVA/xylan composite films with enhanced mechanical properties, high hydrophobicity and UV shielding performance. *Cellulose*, *22*(1), 593-602.

32. Ma, J., Wei, Y., Liu, W. X., & Cao, W. B. (2009). Preparation of nanocrystalline Fe-doped TiO_2 powders as a visible-light-responsive photocatalyst. *Research on Chemical Intermediates*, *35*(3), 329-336.

33. Seery, M. K., George, R., Floris, P., & Pillai, S. C. (2007). Silver doped titanium dioxide nanomaterials for enhanced visible light photocatalysis. *Journal of Photochemistry and Photobiology A: Chemistry*, *189*(2), 258-263.

34. Elghniji, K., Atyaoui, A., Livraghi, S., Bousselmi, L., Giamello, E., & Ksibi, M. (2012). Synthesis and characterization of Fe 3+ doped TiO_2 nanoparticles and films and their performance for photocurrent response under UV illumination. *Journal of Alloys and Compounds, 541*, 421-427.

35. Hu, C., Lan, Y., Qu, J., Hu, X., & Wang, A. (2006). $Ag/AgBr/TiO_2$ visible light photocatalyst for destruction of azodyes and bacteria. *The Journal of Physical Chemistry B*, *110*(9), 4066-4072.

36. Akhavan, O. (2009). Lasting antibacterial activities of $Ag–TiO_2/Ag/a\text{-}TiO_2$ nanocomposite thin film photocatalysts under solar light irradiation. *Journal of Colloid and Interface Science, 336*(1), 117-124.

37. Chawengkijwanich, C., & Hayata, Y. (2008). Development of TiO_2 powder-coated food packaging film and its ability to inactivate Escherichia coli in vitro and in actual tests. *International Journal of Food Microbiology*, *123*(3), 288-292.

38. Maneerat, C., & Hayata, Y. (2006). Antifungal activity of TiO_2 photocatalysis against Penicillium expansum in vitro and in fruit tests. *International Journal of Food Microbiology*, *107*(2), 99-103.

39. Xiao-E, L., Green, A. N., Haque, S. A., Mills, A., & Durrant, J. R. (2004). Light-driven oxygen scavenging by titania/polymer nanocomposite films. *Journal of Photochemistry and Photobiology A: Chemistry*, *162*(2), 253-259.

CHAPTER 3. Improvements of Dispersion Stability of TiO_2 Nanoparticles in Hydrophobic Media by Long Chain Fatty Acid Surface Modification

ABSTRACT

TiO_2 nanoparticles have many potential applications, but the high polarity surfaces make TiO_2 nanoparticles less compatible with hydrophobic matrices. TiO_2 nanoparticles were synthesized by a sol-gel method and the surface of TiO_2 nanoparticles was modified with oleic acid by one-step modification. TiO_2 nanoparticles and oleic acid modified TiO_2 nanoparticles were characterized by X-ray diffraction (XRD), Fourier transform infrared spectroscopy (FTIR), transmission electron microscopy (TEM) and thermogravimetric analysis (TGA). Dynamic light scattering (DLS) was used to measure particle sizes of dispersed TiO_2 nanoparticles and oleic acid-modified TiO_2 nanoparticles in solvents of different polarities. TiO_2 nanoparticles and oleic acid-modified TiO_2 nanoparticles were identified as nearly spherical shaped anatase crystals. The diameters of TiO_2 and OA_TiO_2 were estimated to 3-15 nm by TEM. Dispersion of the oleic acid-modified TiO_2 nanoparticles into non polar solvent such as chloroform was more stable than TiO_2 nanoparticles without the modification. Based on the results, the one step surface modification of TiO_2 nanoparticles using oleic acid is an economical and green method to control aggregations by enhancing compatibility between hydrophilic TiO_2 nanoparticles and hydrophobic media.

KEY WORDS
TiO_2, surface modification, dispersion stability

INTRODUCTION

TiO_2 nanoparticles have been an indispensable nanostructured material and have been employed in a wide range of applications due to their unique properties such as: photocatalytic effects, UV light blocking property, low cost, abundance, non-toxicity, environmentally friendliness and thermal and chemical stability [1, 2].

However, TiO_2 nanoparticles have a tendency to adhere together, aggregate and form large clusters due to a high ratio of surface area per volume of the nanoparticles when compared to micro-structured materials [3, 4, 5]. In particular, the hydrophilic TiO_2 nanoparticles make the nanoparticles form severe aggregations when the TiO_2 nanoparticles are incorporated into hydrophobic media. TiO_2 nanoparticles aggregate and form large clusters when incorporated into materials, reducing effective properties such as UV-protective, photocatalytic and optical properties in functional applications [4, 6, 7]. The unstable distributions and aggregations of TiO_2 nanoparticles are a critical problem to overcome. Stable dispersion and controlled size of TiO_2 nanoparticles are desired properties of TiO_2 nanoparticles [7]. Nano-sized TiO_2 particles (1-100nm), which have much larger active surfaces per particle size ratio than micro-sized TiO_2 particles, provide a higher UV absorption rate and a higher photocatalytic activity [1, 4, 8].

Numerous studies over last decade have shown that surface modifications of TiO_2 nanoparticles by adequate modifiers controlled aggregations and improved dispersion stability of TiO_2 nanoparticles into various solvents and functional materials [9, 10, 11]. Solvents have been commonly used as TiO_2 nanoparticles dispersants [13]. Selecting an appropriate surface modifier that is highly compatible with dispersing solvents is one of the most significant factors affecting stable dispersion of TiO_2 nanoparticles into the solvents [10, 13, 14].

Many techniques have been developed to produce and modify surface of TiO_2 nanoparticles to obtain desired crystalline TiO_2 nanostructured material; however, these techniques often require high pressures or high temperatures [15]. Nanotechnology is sometimes limited is use due to its production cost and low production rate.

In this study, we produced oleic acid-surface modified TiO_2 nanoparticles (OA_TiO_2) by one-step surface modification. TiO_2 was produced by a method described by Nakayama and Hayashi (2008) with some changes [16] then the surface of TiO_2 was modified with oleic acid. The surface modification method is a simple, energy saving and inexpensive means of producing pure anatase crystalline TiO_2 nanoparticles even after the surface modification. Particularly, the purpose of this study was to modify surface of TiO_2 nanoparticles with oleic acid in order to improve dispersion stability of TiO_2 nanoparticles in hydrophobic conditions. Oleic acid is an inexpensive, easily obtainable and widely used long chain fatty acid. Long chain fatty acids are widely utilized as surface modifiers and capping agents for producing surface-modified metal oxides because they can be adsorbed onto the surface of metal oxides to attach a dense organic layer [12, 14, 17]. When long chain fatty acids attach to the surface of TiO_2, the surface polarity of TiO_2 nanoparticles can be changed from hydrophilic to hydrophobic, allowing stable dispersion of TiO_2 nanoparticles under hydrophobic conditions [17, 18]. Therefore, oleic acid was shown to be a promising surface modifier of TiO_2 nanoparticles due to the high affinity between oleic acid and hydrophobic media [17]. In addition, the low cost surface modification of TiO_2 nanoparticles by oleic acid may resolve high cost issues with nanotechnology and improve dispersibility of TiO_2 nanoparticles in the functional materials and various applications that require low production cost.

In this study, dispersion stabilities of TiO_2 nanoparticles and oleic acid modified TiO_2 nanoparticles in solvents of various polarities were investigated. The objectives of the study were: 1) to prepare and characterize TiO_2 nanoparticles and oleic acid-surface modified TiO_2 nanoparticles and 2) to determine dispersion stability and measure distributed size of TiO_2 nanoparticles and oleic acid-modified TiO_2 nanoparticles in various solvents.

MATERIALS AND METHODS

MATERIALS

Titanium oxychloride ($TiOCl_2$ xHCl H_2O (HCl: 38-42% Ti: 15%)) was purchased from Sigma Aldrich (St. Louis, MO). Oleic acid (technical grade 90%) was purchased from Alfa Aesar (Wardhill, MA). Ethanol, anhydrous 200 proof, chloroform (HPLC grade) and methanol (HPLC grade) were purchased from Fisher Scientific (Pittsburgh, PA).

Preparation of TiO_2 and surface modification of TiO_2 with oleic acid

Synthesis of TiO_2

TiO_2 nanoparticles were prepared according to a procedure previously reported with some changes [16]. Mixtures of 300 ml of ethanol and 200 ml of distilled water were transferred into a three-neck, flat bottom flask. White precipitated TiO_2 was obtained by dropwise addition of a mixture of 3.8 ml of titanium oxychloride and 17.8 ml of distilled water in the ethanol and distilled water solution under stirring for 3 hours under nitrogen flow at 60 ℃. White TiO_2 paste was collected after centrifugation (Eppendorf 5804 centrifuge, Hauppauge, NY) and washed with distilled water and then methanol. The white TiO_2 paste was dispersed in chloroform, dried in a fume hood at room temperature and in the Fisher Isotemp® Vacuum Oven Model 281 (Pittsburg, PA) at 40 ℃. TiO_2 paste was added into distilled water, methanol, chloroform and toluene to evaluate dispersion stability.

Surface Functionalization of TiO_2 by Oleic Acid (OA_TiO_2)

Wet TiO_2 paste (5g) without the drying process and oleic acid (30 g) ratios of 1:6 (w/w) were added into 100 ml glass bottle and capped tightly. The mixture of TiO_2 paste and oleic acid was sonicated for 10 minutes in a Fisher Scientific FS20 sonication bath (Pittsburgh, PA) and was stirred for 24 hours at room temperature. A light yellow mixture of oleic acid and TiO_2 paste was obtained. OA_TiO_2 paste was collected by centrifugation and washed with methanol to remove nonbound oleic acid. OA_TiO_2 was dispersed in chloroform and dried in a fume hood at room temperature and then dried in the vacuum oven at 40 ℃. OA_TiO_2 paste was added into distilled water, methanol, chloroform and toluene to evaluate dispersion stability.

Characterization of TiO_2 nanoparticles and OA_TiO_2 nanoparticles

Diffraction patterns of TiO_2 and OA_TiO_2 were analyzed on the Bruker D8 Discover X-ray Diffractometer (Madison, WI) operating at 40 kev with a Cu Kα x-ray radiation (λ=15.418 nm). Diffraction patterns of TiO_2 and OA_TiO_2 were collected in a range of reflection angles between 20 and 70° (2θ).

Fourier transform-infrared (FTIR) spectroscopy (Thermo Scientific Nicolet 8700 FT-IR spectrometer, Madison, WI) equipped with an attenuated total reflectance (ATR) crystal was used to collect absorbance of chemical bonds in TiO_2 and OA_TiO_2. A blank background spectrum (32 scans) was collected before every sample. The range of spectra was collected from 4000 to 500cm^{-1} with 64 scans and a resolution of 4cm^{-1}.

Morphology of TiO_2 and OA_TiO_2 was investigated by JEOL 2100 transmission electron microscopy (Peabody, MA) operating at 200 kV. TEM samples were prepared as follows; TiO_2 methanol suspension and OA_TiO_2 chloroform suspension were deposited onto carbon coated 300 mesh copper grids (Ted Pella, Inc, Redding, CA) and air dried to remove solvents.

Thermogravimetric Analysis (TGA) of TiO_2 and OA_TiO_2 was determined using a Q500 TGA (TA instruments, New Castle, DE) equipped with a platinum sample pan for the sample holder. TiO_2 and OA_TiO_2 were dried in a vacuum oven at 40℃ for 24 hours before the TGA analysis. TiO_2 and OA_TiO_2 were heated to 600 ℃ with a constant heating rate 10℃/min under nitrogen flow. Weight loss (% and mg) with temperature (℃) and decomposition temperatures of each sample by derivative weight change were recorded by the TA Instrument Software, Universal Analysis 2000 (New Castle, DE).

Dispersion stability of 0.1 % (w/v) TiO_2 and 0.1 % (w/v) OA _TiO_2 in solvents of various polarities with a different polarity index (distilled water (10.2), methanol (5.1), chloroform (4.1) and toluene (2.4)) were examined [21]. The hydrodynamic diameter sizes of 0.1 % (w/v) TiO_2 in distilled water, 0.1 % (w/v) TiO_2 in methanol and 0.1 % (w/v) OA_TiO_2 in chloroform suspension that showed complete dispersion without sedimentation were measured by dynamic light scattering (DLS) using a Zetasizer Nano Series instrument (Zetasizer Nano ZS, Malvern Instrument Ltd, Malvern, UK). One ml of 0.1 % (w/v) TiO_2 in distilled water, 0.1 % (w/v) TiO_2 in methanol and 0.1 % (w/v) OA _TiO_2 in chloroform suspensions were transferred to glass or polystyrene cuvettes depending on types of the solvent for the DLS measurement. Average hydrodynamic diameter sizes (z-average) of the TiO_2 and OA_TiO_2 suspensions was measured seven times for each sample, prepared in triplicate.

RESULTS AND DISCUSSION

X-Ray Diffraction (XRD)

Figure 1. shows a XRD pattern of synthesized a) TiO_2 and b) the oleic acid-surface modified TiO_2 (OA_TiO_2) nanoparticles. The major peaks of TiO_2 and OA_TiO_2 at 2θ (°) were at 25.15, 38.09, 47.65, 54.86 and 62.77 ° as well as at 25.24, 38.09, 47.74, 54 and 63.28°,

respectively, which agrees with the pure anatase crystalline structures [11, 16, 19, 20]. The average particle sizes of this TiO_2 and OA_TiO_2 from anatase phase peaks (101) of 25.15 and 25.24 at 2θ (°) were estimated to be 4.3 and 4.5 nm, respectively, using Sherrer's formula ($D = 0.9 \lambda / \beta \cos \theta$), with crystallite size (D), full width at half maximum radian (β), wavelength (λ) of radiation (λ=15.418 nm) and Bragg angle (θ) [18].

Transmission Electron Microscopy (TEM)

As seen in the Figure 2a) TiO_2 and 2b) OA_TiO_2 particles were nearly spherical shaped anatase crystals. The diameters of TiO_2 and OA_TiO_2 were estimated to be in the range of 3–15 nm, but some agglomerations of TiO_2 and OATiO_2 nanoparticles were seen in the TEM images of TiO_2 and OA_TiO_2.

Fourier Transform Infrared Spectroscopy (FTIR)

Figure 3. shows the FTIR spectrum of TiO_2, OA_TiO_2 and oleic acid in the range of 4000- 500 cm^{-1}. The stretching vibration ranges of Ti-O-Ti and Ti-OH appeared below 700 cm^{-1} and between 3000 and 3400 cm^{-1}, respectively, in the spectrums of TiO_2 and OA_TiO_2 [7]. Water absorption of TiO_2 was seen at 1610 cm^{-1} in the Figure 3a. In the spectrum of oleic acid (3c), C-H stretching vibrations were presented at 2920 and 2852 cm^{-1}, and carbonyl stretching vibration (C=O) was observed at 1706 cm^{-1}, respectively. Asymmetric and symmetric C-H stretching vibrations of OA_TiO_2 appeared at 2916 cm^{-1} and 2847 cm-1, corresponding to oleic acid in the Figure 3b. Asymmetric and symmetric stretching vibrations of oleate anions in the spectrum of OA_TiO_2 were assigned at 1514 and 1406 cm^{-1}, whereas carbonyl stretching vibration (C=O) of oleic acid at 1710cm^{-1} disappeared due to formation of a bidenate complex [11, 17]. In the Figure 3a, peaks for oleic acid such as carbonyl stretching vibration (C=O),

oleate anions (COO^-) and C-H were not observed in the spectrum of TiO_2. Therefore, oleic acid attachment on TiO_2 was confirmed by the FTIR analysis.

Thermogravimetric Analysis (TGA)

Thermal stability of TiO_2, OA_TiO_2 and oleic acid were determined by TGA. The results of the thermal stability of TiO_2, OA_TiO_2 and oleic acid are shown in the Figure 4. The total weight loss of TiO_2 and OA_TiO_2 were 14.7 % and 25.9%, respectively. The major weight loss of TiO_2 by water evaporation occurred before temperature reached 100 ℃. Oleic acid was nearly all degraded between 200 and 320 ℃. The main thermal decomposition of OA_TiO_2 occurred in the range of 300 and 480 ℃, which is attributed to thermal degradation of oleic acid on TiO_2. Total weight of attached oleic acid on TiO_2 was approximately estimated to 11.2 % based on differences in thermal decomposition rate (%) between OA_TiO_2 and TiO_2 after surface modification [16].

Stability of TiO_2 and OA_TiO_2 in Solvents of Different Polarities

Dispersion stabilities of colloidal solutions of TiO_2 and OA_TiO_2 at 0.1 % (w/v) in various solvents with different polarity index distilled water (10.2), methanol (5.1), chloroform (4.1) and toluene (2.4) are shown in the Table 1 [21]. When TiO_2 or OA_TiO_2 suspensions remained stable without precipitation over one day, 'dispersible' was assigned to the TiO_2 or OA_TiO_2 suspensions. Alternatively, if TiO_2 or OA_TiO_2 suspensions were unstable and formed precipitates, 'non- dispersible' was assigned to the suspensions. If TiO_2 or OA_TiO_2 nano-particles were dispersed at first, but they precipitated out of suspension after one day, they was assigned to 'partially dispersible'. Stable colloidal TiO_2 suspensions were obtained in distilled water and methanol, but the particle agglomerations and precipitations were visually observed in TiO_2 chloroform and toluene suspensions. However, the 0.1 % (w/v) OA_TiO_2 chloroform

suspension was stable over several months. OA_TiO_2 methanol and toluene suspensions were partially dispersed then precipitated out of suspension within one day. OA_TiO_2 was 'non dispersible' in distilled water and formed clusters due to polarity disparity between OA_TiO_2 and water. Dispersion of TiO_2 was improved in non-polar solvent, chloroform, by oleic acid attachment on TiO_2, due to good affinity between oleic acid as a surface modifier and chloroform as a dispersant [14, 17, 22]. This showed that good affinity between surface modifiers and dispersants significantly affected dispersion stability of inorganic nanomaterial in organic media, since the modifiers controlled particle size distribution [13, 14, 23]

Dynamic Light Scattering (DLS) is an efficient instrument to measure hydrodynamic diameters of particles, smaller than 1 μm in suspension, based on light scattering intensity by the Brownian motion of the particles [24, 25]. The average hydrodynamic diameter values of the particle presented z-average values. Only completely dispersed TiO_2 or OA_TiO_2 colloidal suspensions were analyzed by DLS because unstable TiO_2 or OA_TiO_2 suspensions may generate invalid results [25]. The z- average sizes of 0.1 % (w/v) TiO_2 distilled water suspension, 0.1 % (w/v) TiO_2 methanol suspension and 0.1 % (w/v) OA_TiO_2 chloroform suspension were determined.

Nickel et al (2014) defined stable suspensions in his study if the differences of average hydrodynamic diameters and polydispersity index (PDI) are less than 10 %, in at least six repeated internal measurements of the suspension, as well as no visual observation of nanomaterial agglomerations and sedimentation [24]. The TiO_2 distilled water suspension, the TiO_2 methanol suspension and the OA_TiO_2 chloroform suspension remained stable without sedimentation during the DLS measurements. The z-average sizes of the TiO_2 in deionized water and TiO_2 in methanol and the OA_TiO_2 in chloroform were 127, 51 and 128 nm,

respectively. The z-average sizes of TiO_2 and OA_TiO_2 in suspensions were larger than estimating particle sizes of TiO_2 and OA_TiO_2 by TEM. The particle sizes by DLS are usually larger because DLS measured distributed particles with the surrounding surface organic modifier on TiO_2 in suspensions, which are not often perfect spheres, while TEM measures only the core sizes of the particles [14, 25]. In addition, solvents and hydration have an effect upon determining z-average sizes of the particles, while TEM only measures dehydrated spheres of the particles [26].

CONCLUSIONS

The surface modification of TiO_2 with oleic acid was conducted by using a one-step modification. TiO_2 nanoparticles without the surface modification had unstable dispersion, formed agglomeration and precipitated out of nonpolar solvent suspensions such as chloroform and toluene. However, OA_TiO_2 was highly dispersed and stable enough to remain in good dispersion for several months in chloroform. It may be advantageous that the surface modification technique not only requires low energy but also uses a simple method with one step modification method at room temperature. However, OA_TiO_2 was partially dispersed and precipitated out of toluene suspension within one day. It may be limited to use in lower polarity conditions than chloroform. The OA_TiO_2 may be used in hydrophobic conditions possessing a similar polarity of such solvents or materials such as chloroform for enhancing optical properties, photocatalytic effects and UV-protection.

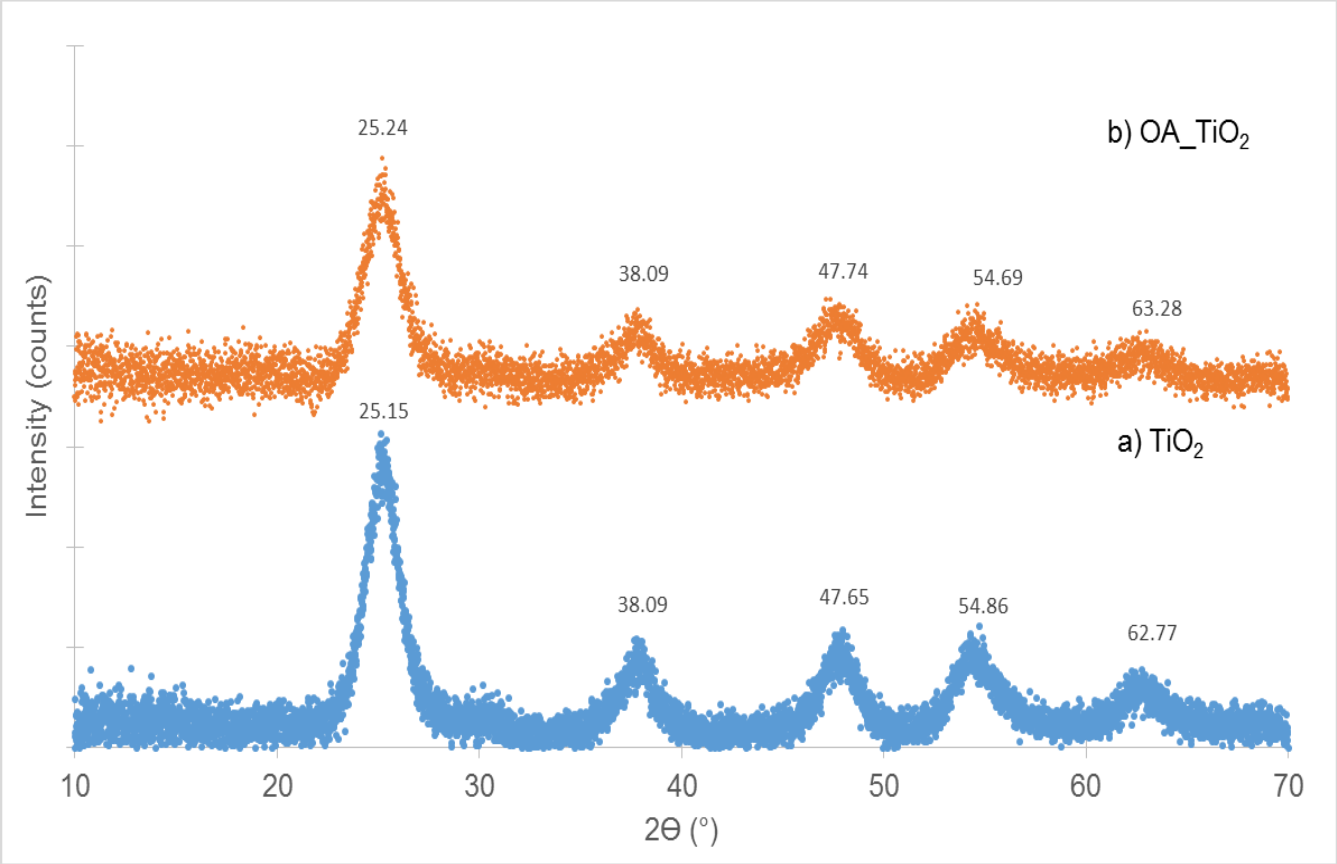

Figure 1. X-Ray Diffraction powder diffraction of a) TiO_2 and b) OA_TiO_2. The major peaks of TiO_2 were at 25.1, 38.1, 47.7, 54.9 and 62.8 ℃ and major peaks of OA_TiO2 were at 25.2, 38.1, 47.7, 54.7 and 63.3 ℃.

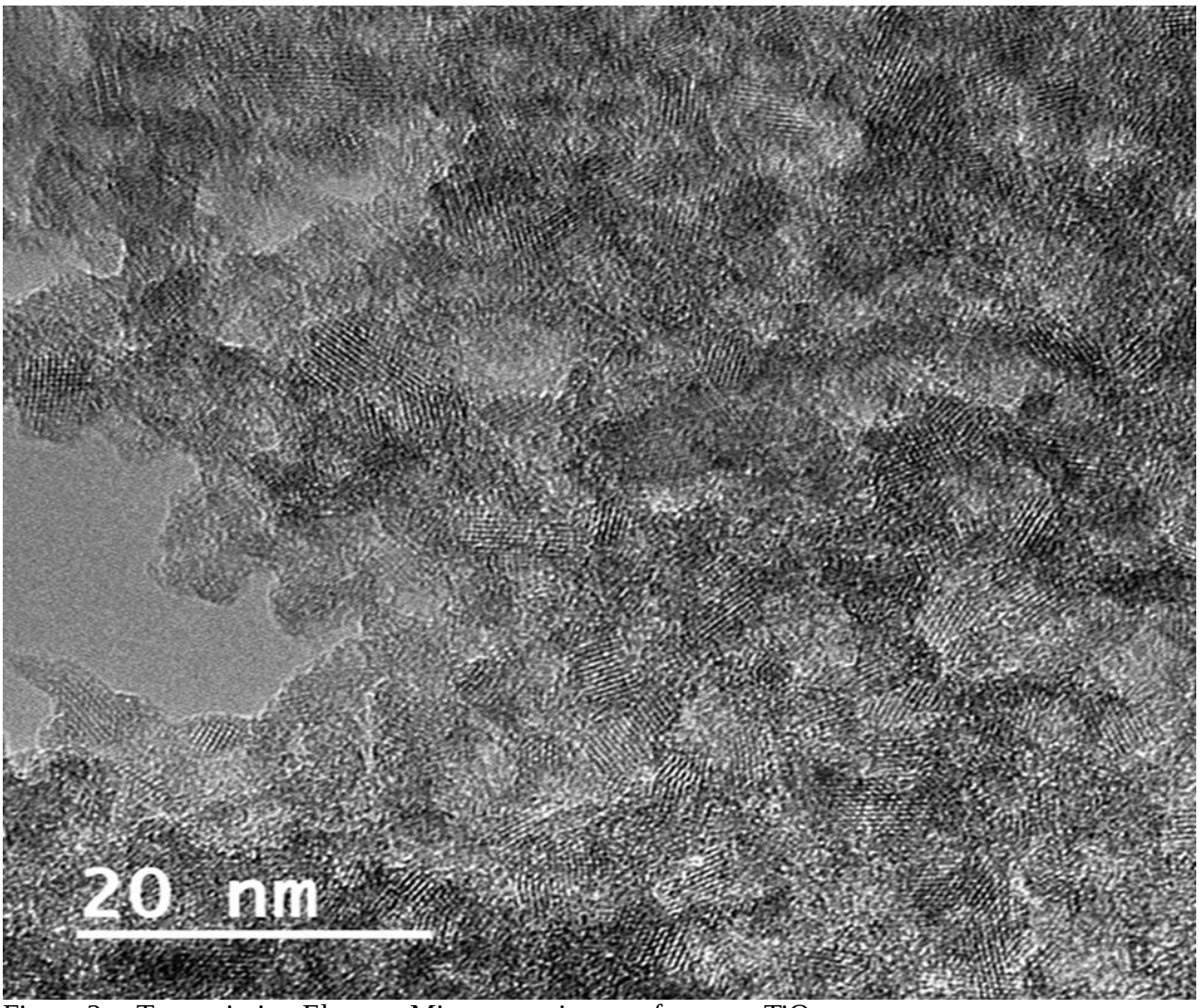

Figure 2a. Transmission Electron Microscopy image of anatase TiO_2

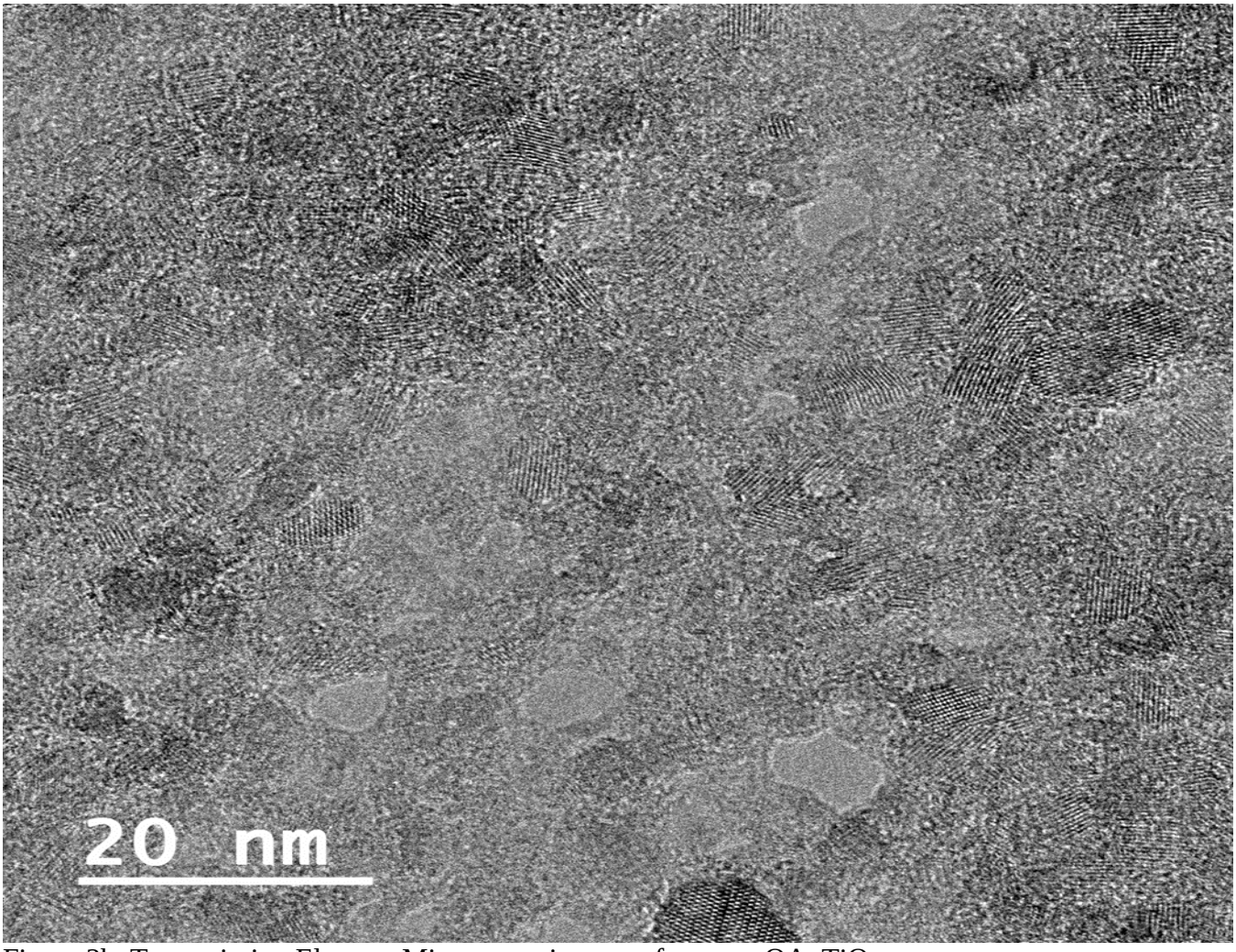

Figure 2b. Transmission Electron Microscopy images of anatase OA_TiO_2

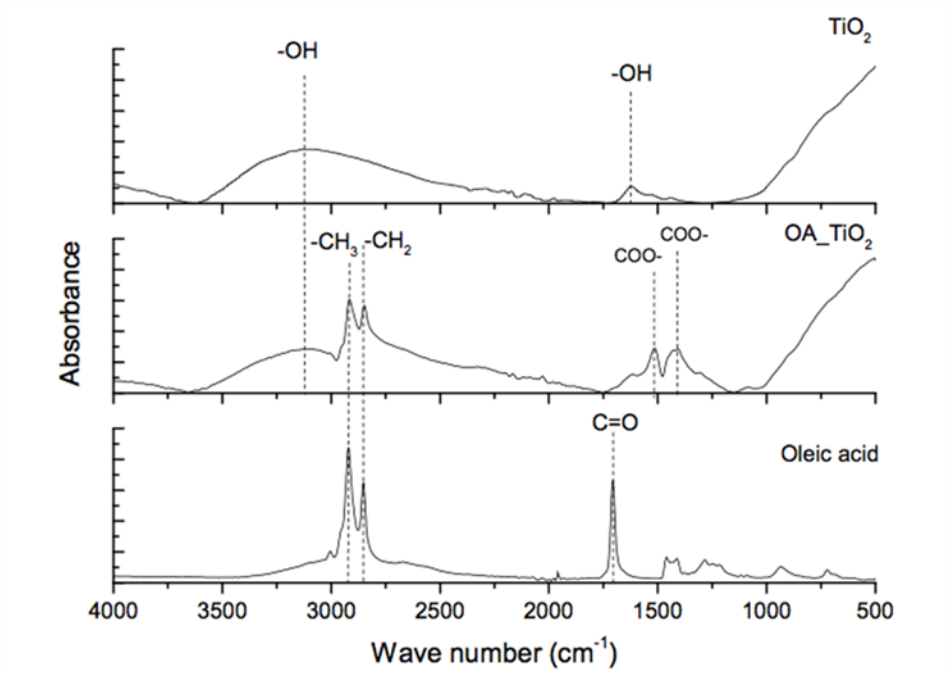

Figure 3. The Fourier transform-infrared (FTIR) -attenuated total reflectance (ATR) of TiO_2, OA_TiO_2 and oleic acid.

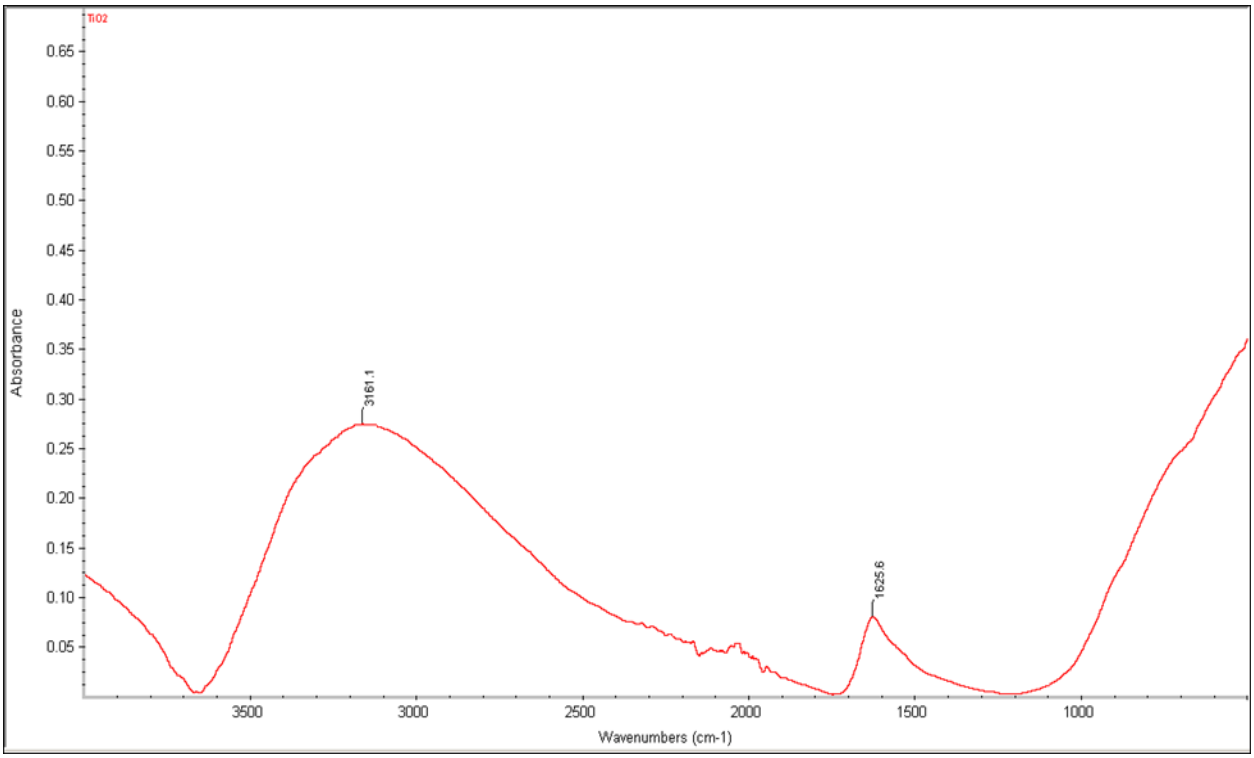

Figure 3a. FTIR spectra of TiO_2

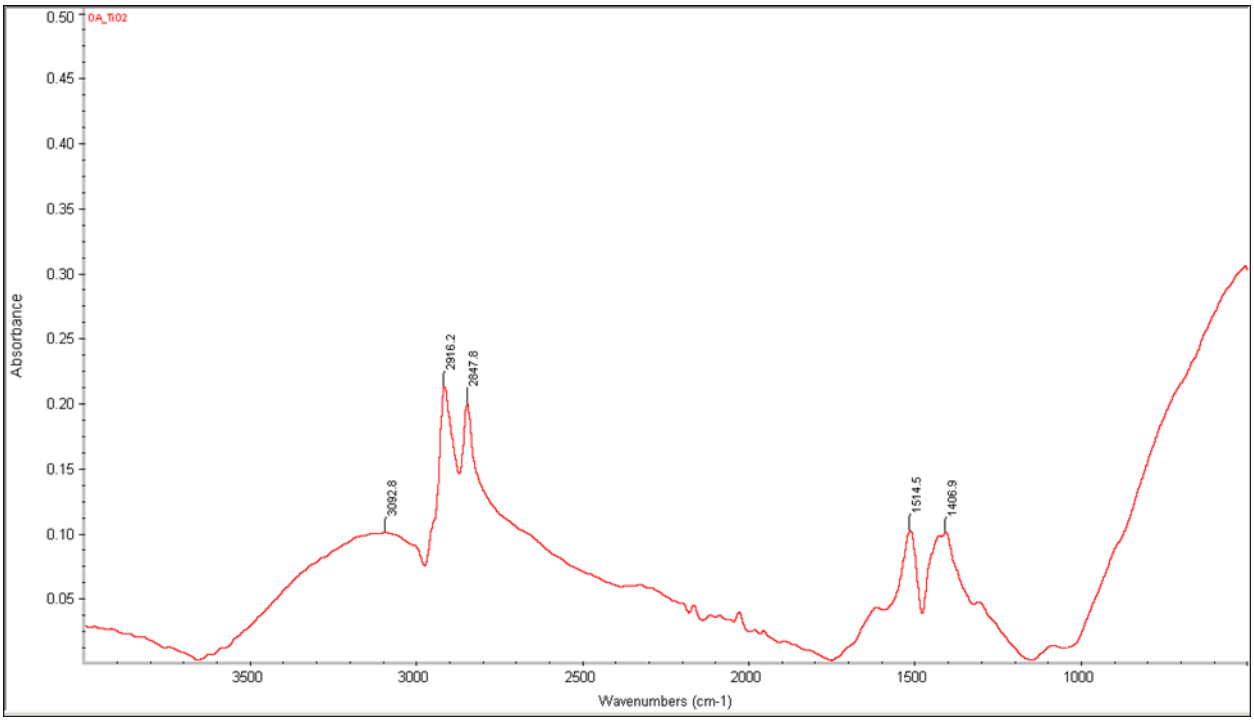

Figure 3b. FTIR spectra of OA_TiO_2.

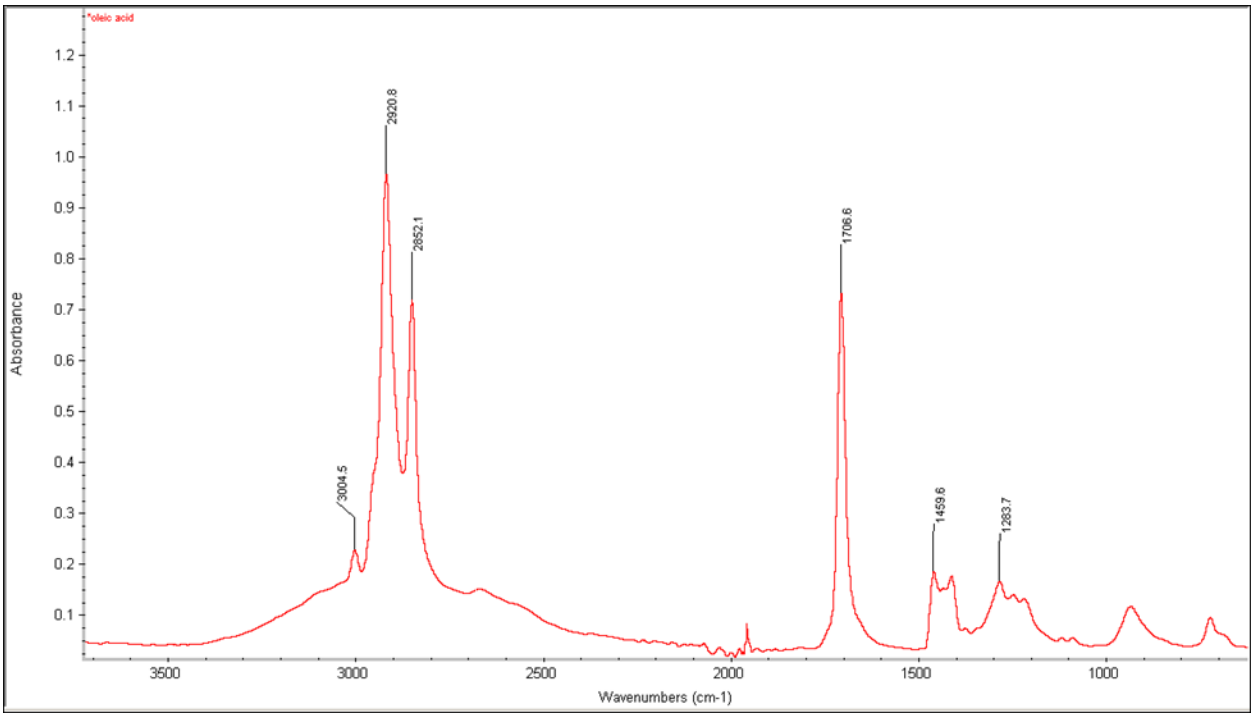

Figure 3c. FTIR spectra of oleic acid.

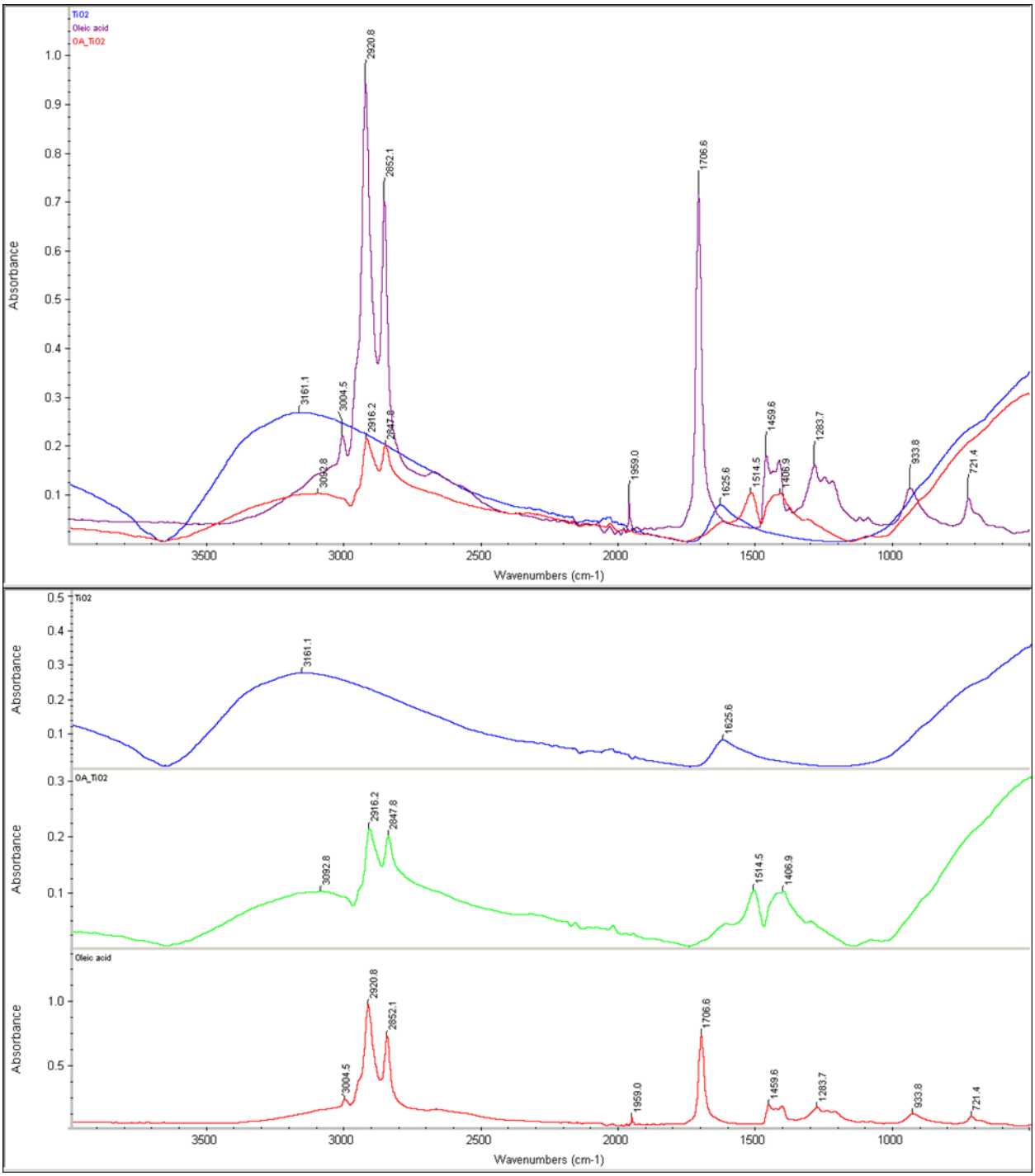

Figure 3d. Overlay and stack FTIR spectra of TiO_2, OA_TiO_2 and oleic acid.

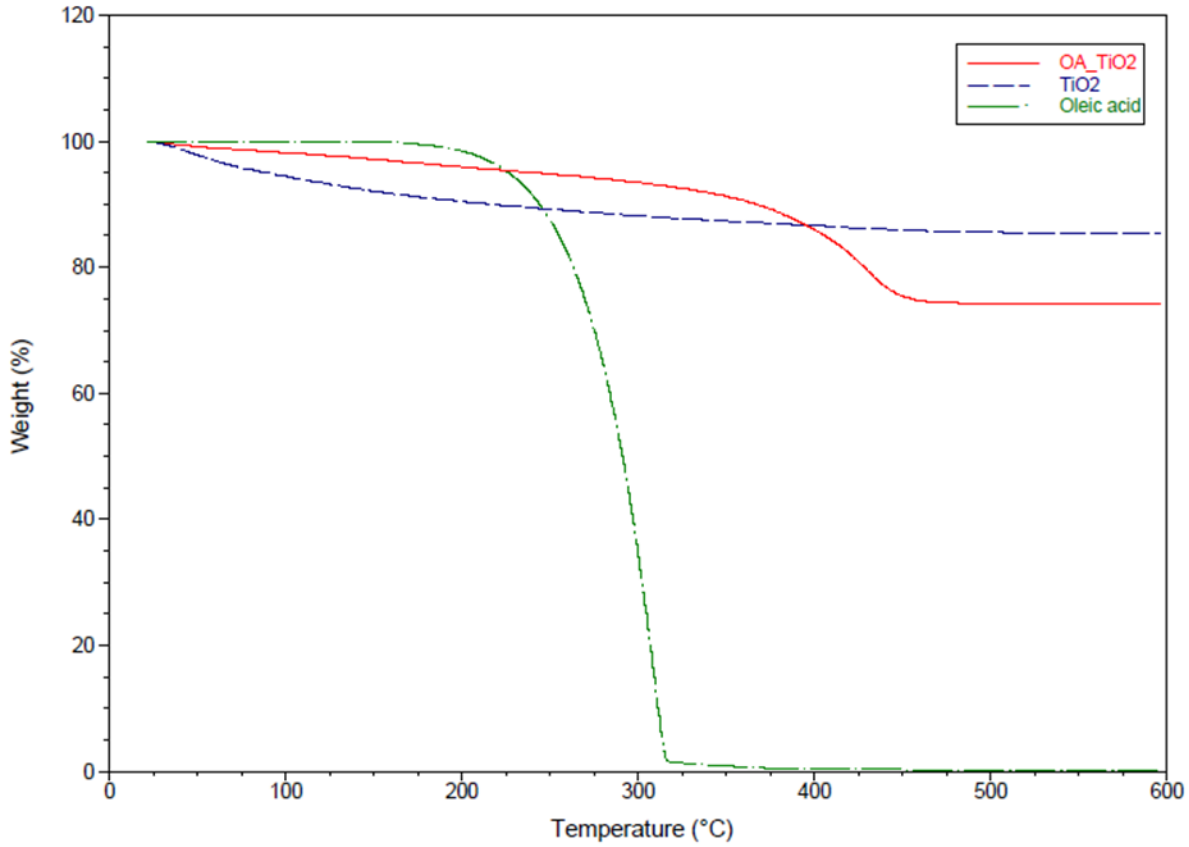

Figure 4. Weight loss of TiO_2, OA_TiO_2 and oleic acid by elevating temperature at 600 ℃

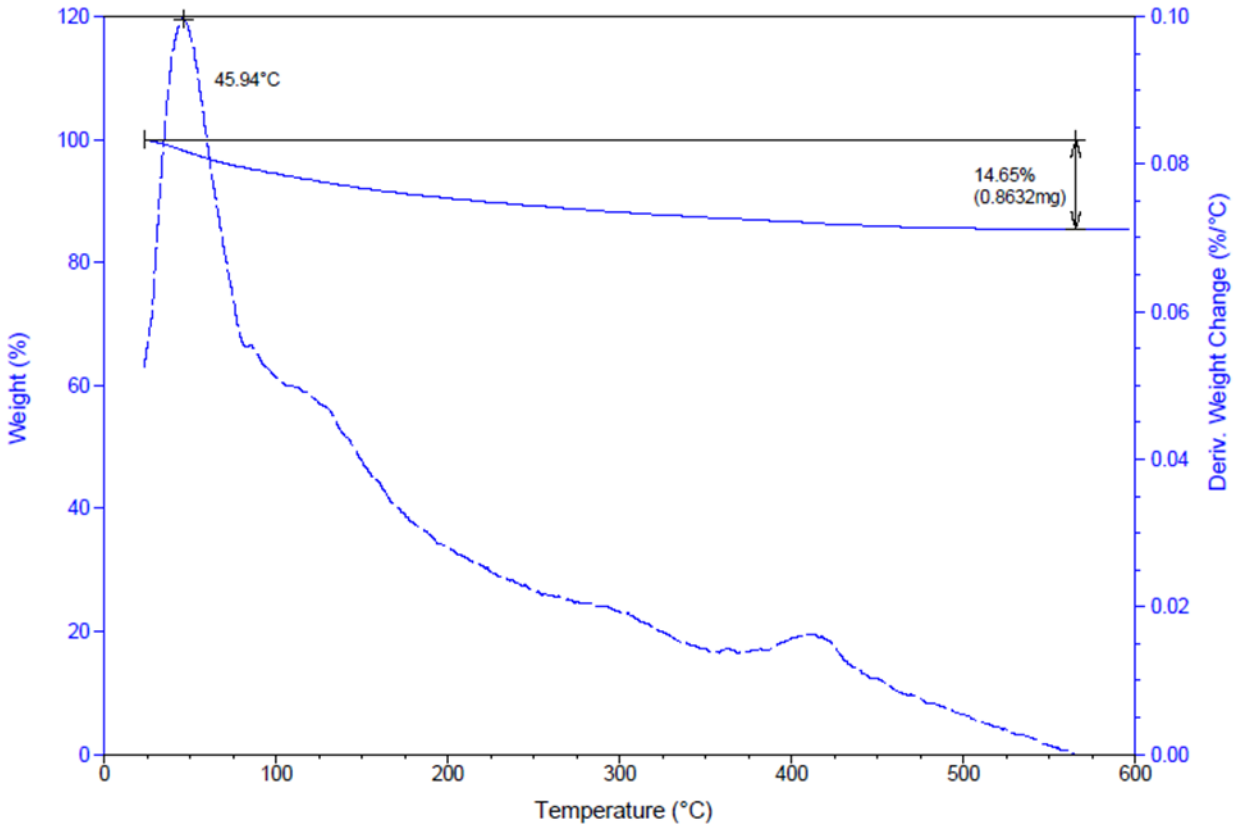

Figure 4a. Weight loss (% and mg) and derivative weight change of TiO_2 by increasing temperature of 10℃/min under nitrogen atmosphere.

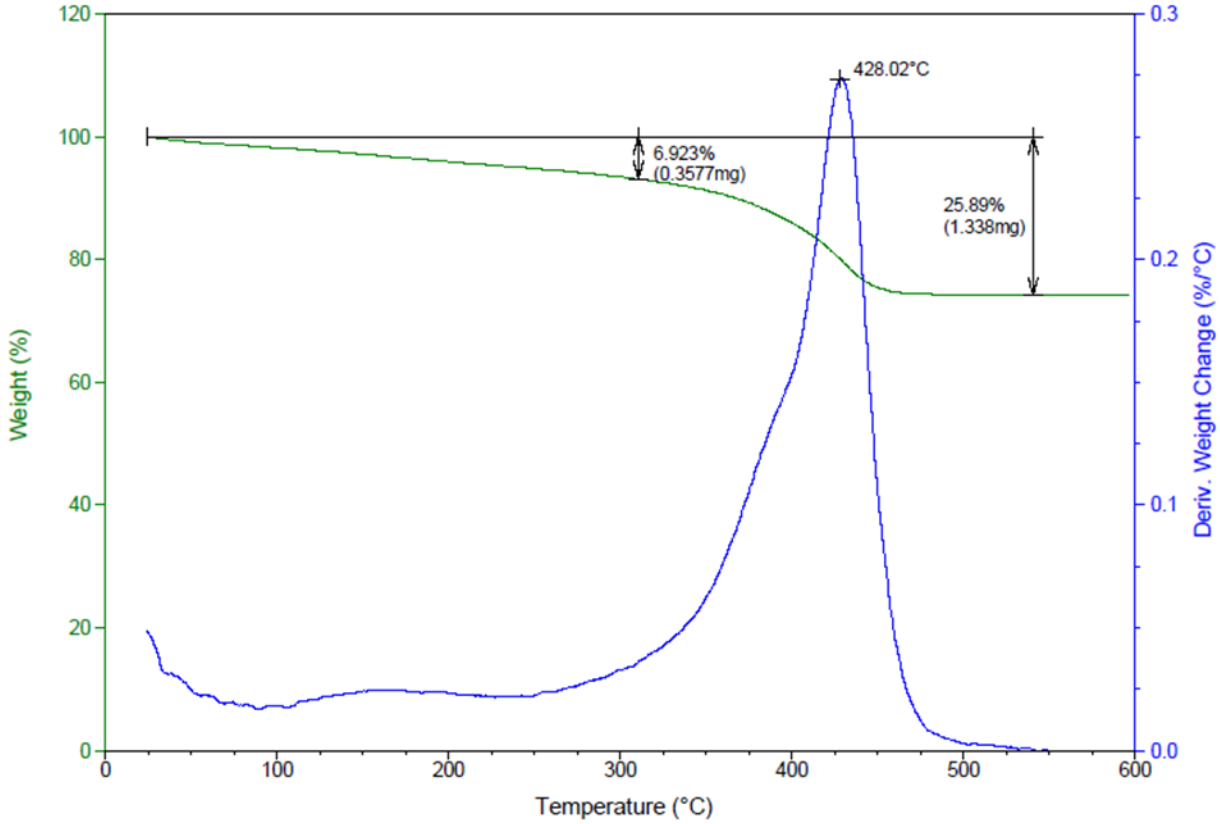

Figure 4b. Weight loss (% and mg) and derivative weight change of OA_TiO_2 by increasing temperature of 10℃/min under nitrogen atmosphere.

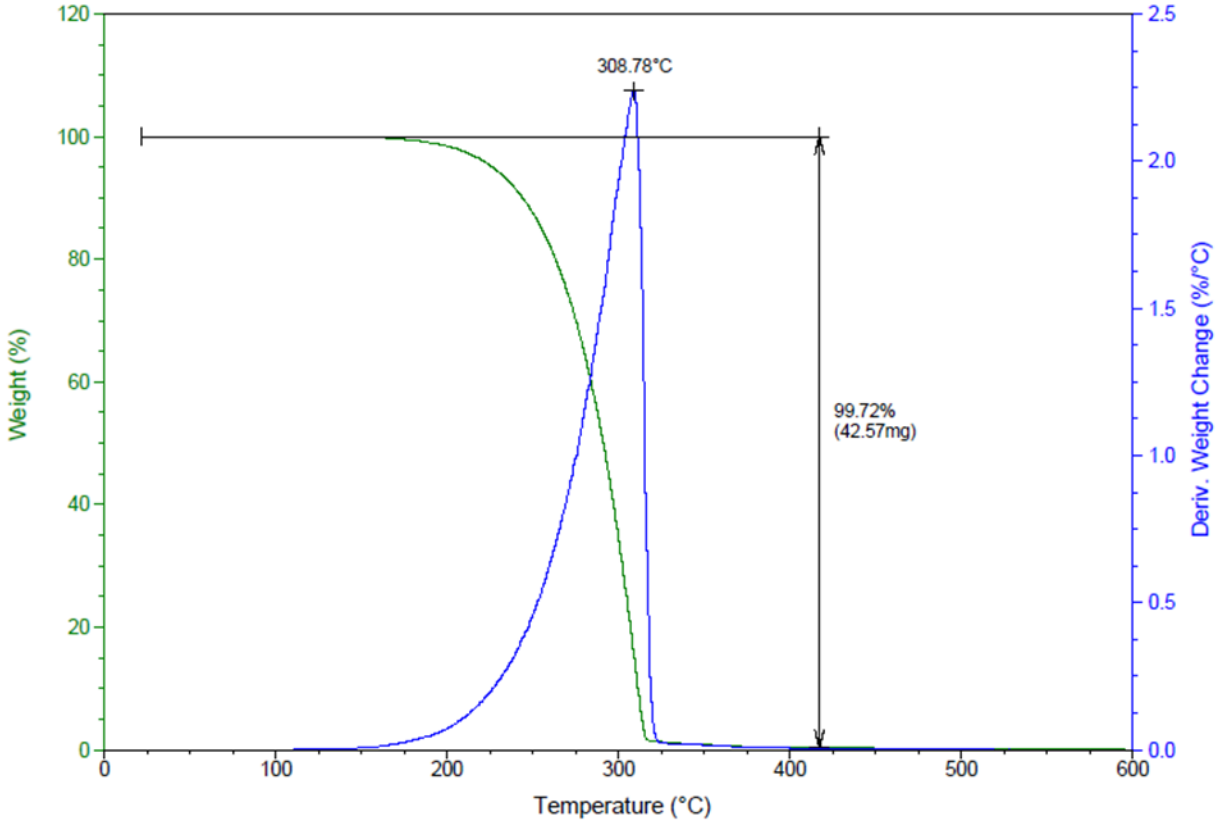

Figure 4c. Weight loss (% and mg) and derivative weight change of oleic acid by increasing temperature of 10℃/min under nitrogen atmosphere.

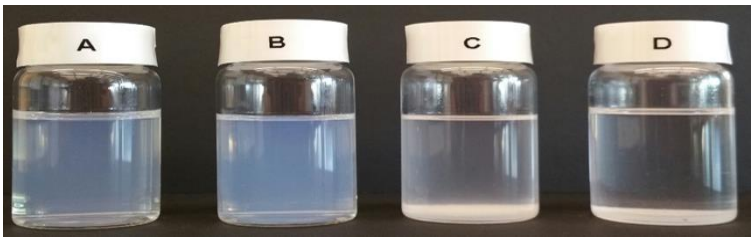

Figure 5a. Dispersion state of 0.1 % (W/V) of TiO_2 in water suspension (A), TiO_2 in methanol suspension (B), TiO_2 in chloroform suspension (C) and TiO_2 in toluene suspension (D) after one day.

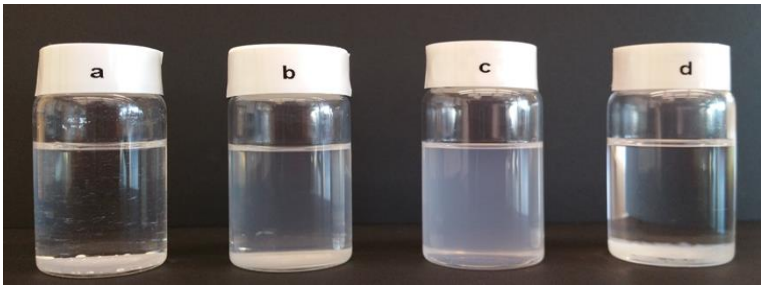

Figure 5b. Dispersion state of 0.1 % (W/V) of OA_TiO_2 in water suspension (a), OA_TiO_2 in methanol suspension (b), OA_TiO_2 in chloroform suspension (c) and OA_TiO_2 in toluene suspension (d) after one day.

Table 1. Dispersion stability of TiO_2 and OA_TiO_2 in water, methanol, chloroform and toluene.

Sample	**Solvents**			
	Water	Methanol	Chloroform	Toluene
TiO_2	Dispersible	Dispersible	Non-dispersible	Non-Dispersible
OA_TiO_2	Non-dispersible	Partially dispersible	Dispersible	Partially dispersible

REFERENCES

1. Bogdan, J., Jackowska-Tracz, A., Zarzyńska, J., & Pławińska-Czarnak, J. (2015). Chances and limitations of nanosized titanium dioxide practical application in view of its physicochemical properties. *Nanoscale Research Letters,10*(C.J Moorea), 1-10. doi: 10.1186/s11671-015-0753-2.

2. Cargnello, M., Gordon, T. R., & Murray, C. B. (2014). Solution-phase synthesis of titanium dioxide nanoparticles and nanocrystals. *Chemical Reviews*, 114(19), 9319-9345. doi: 10.1021/cr500170p.

3. Iijima, M., & Kamiya, H. (2009). Surface modification for improving the stability of nanoparticles in liquid media. *KONA Powder and Particle Journal,27*(0), 119-129.

4. Macwan, D. P., Dave, P. N., & Chaturvedi, S. (2011). A review on nano-TiO2 sol–gel type syntheses and its applications. *Journal of Materials Science*, *46*(11), 3669-3686.

5. Pan, H., Wang, X., Xiao, S., Yu, L., & Zhang, Z. (2013). Preparation and characterization of TiO_2 nanoparticles surface-modified by octadecyltrimethoxysilane. *Indian Journal of Engineering Mater Sciences*, *20*, 561-567.

6. Molina, J., Sanchez-Salas, J. L., Zuniga, C., Mendoza, E., Cuahtecontzi, R., Garcia-Perez, G., ... & Bandala, E. R. (2014). Low-temperature processing of thin films based on rutile TiO_2 nanoparticles for UV photocatalysis and bacteria inactivation. *Journal of Materials Science*, *49*(2), 786-793.

7. Chen, H. J., Wang, L., & Chiu, W. Y. (2007). Chelation and solvent effect on the preparation of titania colloids. *Materials Chemistry and Physics*, *101*(1), 12-19.

8. Seentrakoon, B., Junhasavasdikul, B., & Chavasiri, W. (2013). Enhanced UV-protection and antibacterial properties of natural rubber/rutile-TiO_2 nanocomposites. *Polymer Degradation and Stability*, *98*(2), 566-578. doi: http://dx.doi.org/10.1016/j.polymdegradstab.2012.11.018

9. Althues, H., Henle, J., & Kaskel, S. (2007). Functional inorganic nanofillers for transparent polymers. *Chemical Society Reviews*, 36(9), 1454-1465.

10. Iijima, M., Kobayakawa, M., Yamazaki, M., Ohta, Y., & Kamiya, H. (2009). Anionic surfactant with hydrophobic and hydrophilic chains for nanoparticle dispersion and shape mmory polymer nanocomposites. *Journal of the American Chemical Society*, 131(45), 16342-16343. doi: 10.1021/ja906655r

11. Cheyne, R. W., Smith, T. A., Trembleau, L., & Mclaughlin, A. C. (2011). Synthesis and characterisation of biologically compatible TiO_2 nanoparticles. *Nanoscale Research Letters*, *6*(1), 1-6.

12. Zhang, L., Chen, L., Wan, H., Chen, J., & Zhou, H. (2011). Synthesis and tribological properties of stearic acid-modified anatase (TiO_2) nanoparticles. *Tribology Letters*, *41*(2), 409-416.

13. Arita, T., Moriya, K. I., Yoshimura, T., Minami, K., Naka, T., & Adschiri, T. (2010). Dispersion of phosphonic acids surface-modified titania nanocrystals in various organic solvents. *Industrial & Engineering Chemistry Research*, *49*(20), 9815-9821.

14. Arita, T., Ueda, Y., Minami, K., Naka, T., & Adschiri, T. (2009). Dispersion of fatty acid surface modified ceria nanocrystals in various organic solvents. *Industrial & Engineering Chemistry Research*, *49(*4), 1947-1952.

15. Wang, X., Wang, H., Zhou, Y., Liu, Y., Li, B., Zhou, X., & Shen, H. (2015). Confined-space synthesis of single crystal TiO_2 nanowires in atmospheric vessel at low temperature: a generalized approach. *Scientific Reports*, 5.

16. Nakayama, N., & Hayashi, T. (2008). Preparation of TiO2 nanoparticles surface-modified by both carboxylic acid and amine: Dispersibility and stabilization in organic solvents. *Colloids and Surfaces A: Physicochemical and Engineering Aspects*, 317(1), 543-550.

17. Cozzoli, P. D., Kornowski, A., & Weller, H. (2003). Low-temperature synthesis of soluble and processable organic-capped anatase TiO_2 nanorods. *Journal of the American Chemical Society*, 125(47), 14539-14548. doi: 10.1021/ja036505h.

18. Qian, J., Yin, X., Wang, N., Liu, L., & Xing, J. (2012). Preparation and tribological properties of stearic acid-modified hierarchical anatase TiO_2 microcrystals. *Applied Surface Science*, *258*(7), 2778-2782.

19. Castro, A. L., Nunes, M. R., Carvalho, A. P., Costa, F. M., & Florêncio, M. H. (2008). Synthesis of anatase TiO2 nanoparticles with high temperature stability and photocatalytic activity. *Solid State Sciences*, 10(5), 602-606. doi: http://dx.doi.org/10.1016/j.solidstatesciences.2007.10.012

20. Jiang, G., & Zeng, J. (2010). Preparation of nano-TiO_2/polystyrene hybride microspheres and their antibacterial properties. *Journal of Applied Polymer Science*, 116(2), 779-784.

21. Polarity Index. Retrieved from http://macro.lsu.edu/howto/solvents/Polarity%20index.htm

22. Baek, S. Y., Chai, S. Y., Hur, K. S., & Lee, W. I. (2005). Synthesis of highly soluble TiO_2 nanoparticle with narrow size distribution. *Bulletin-Korean Chemical Society*, 26(9), 1333.

23. Yin, M., Willis, A., Redl, F., Turro, N. J., & O'Brien, S. P. (2004). Influence of capping groups on the synthesis of γ-Fe_2O_3 nanocrystals. *Journal of Materials Research*, *19*(04), 1208-1215.

24. Nickel, C., Angelstorf, J., Bienert, R., Burkart, C., Gabsch, S., Giebner, S., . . . Kuhlbusch, T. J. (2014). Dynamic light-scattering measurement comparability of nanomaterial suspensions. *Journal of Nanoparticle Research*, *16*(2), 1-12. doi: 10.1007/s11051-014-2260-2

25. Malvern Instruments Ltd. (2011). Dynamic light scattering common terms defined. Inform White Paper. Retrieved from http://www.biophysics.bioc.cam.ac.uk/wp-content/uploads/2011/02/DLS_Terms_defined_Malvern.pdf

26. Malvern Instruments Ltd. Frequently asked questions, how different are the z average and TEM Sizes? [PDF document] Retrieved from https://scholar.vt.edu/access/content/group/c9ba3a24-bc88-481a-ae5f45480ce8fc64/2DLS%20Intro/DLS%20Theoretical%20Material/10FAQ%20-%20How%20different%20are%20the%20Z%20average%20_%20TEM%20sizes.pdf

CHAPTER 4. Characterization of Hydrophobically Modified TiO_2PLA Nanocomposite Films for Food Packaging

ABSTRACT

When TiO_2 polymer nanocomposites are created, they improve toughness and barrier properties as well as provide color, antibacterial effects and UV light protection. However, low compatibility between hydrophilic TiO_2 nanoparticles and hydrophobic polymers such as polylactic acid (PLA) is problematic because TiO_2 nanoparticles tend to agglomerate and form larger clusters, resulting in decrease efficiency. A modification of TiO_2 surface with long chain fatty acid may improve compatibility between PLA and TiO_2. The goal of this study was to characterize properties of oleic acid-modified TiO_2 PLA nanocomposite films (OT-PLA) and unmodified TiO_2 PLA nanocomposite films (T-PLA) for food packaging. OT-PLA, T-PLA and PLA films were prepared by a solvent casting method. The films' morphology, mechanical strength, UV-Vis absorbance, and barrier properties of oxygen and water vapor were investigated. The images of scanning electron microscopy showed aggregation of TiO_2 in the T-PLA, but not in the OT-PLA. Barrier properties of oxygen and water vapor of the OT-PLA were improved more effectively than the PLA and the T-PLA. Oxygen permeability and water vapor permeability of 1% OT-PLA were reduced by 29 % and 26 % respectively. The flexibilities of the OT-PLA were higher than the T-PLA, but toughness of the films based on Young's modulus of OT-PLA were lower than the T-PLA and the PLA. It is obvious that oleic acid improved dispersion of TiO_2 in the PLA matrices. The OT-PLA may have a potential to be used as transparent, functional and environmentally friendly packaging films.

KEY WORDS

Polylactic acid, TiO_2, polymer nanocomposites, long chain fatty acid surface modification

INTRODUCTION

When it comes to food packaging, biobased and biodegradable polymers have recently received attention as an environmentally friendly alternatives to non-degradable petroleum based polymers [1]. The biobased and biodegradable polymers show potential of reducing environmental concerns induced by accumulations of plastic wastes [1, 2]. Polylactic acid (PLA), which is produced from 100% renewable natural resources such as corn and other agricultural products, is commercially available in biobased and biodegradable polymers [3, 4]. PLA retains good biocompatibility, rigidity, excellent clarity, high gloss, good thermal processability, convenience and safety for food packaging applications [3, 4]. PLA currently is used for short-term shelf life packaging such as drinking cups, disposable food trays, portable containers, overwrap, lamination films and blister packages [5, 6]. Although PLA provides beneficial properties for food packaging, drawbacks of PLA are recognized as brittleness and poor barrier properties of oxygen and moisture compared to non-degradable petroleum based polymers which limited applications in a wider range of food packaging [2, 3].

Polymer nanotechnology has been extensive interdisciplinary areas of research in various applications of chemistry, biology, physics and engineering for development of innovative and high performance materials [7, 8]. When nanocomposites are created by incorporation of nanomaterial into compatible polymers, they play important roles in enhancing physical properties of polymers such as mechanical strengths, thermal stability and barrier properties of oxygen and moisture as a result of reinforcement effects of nanomaterial with high surface area to volume ratio [8, 9]. Besides improving physical properties, nanomaterials provide unique functions to increase shelf life of foods in active packaging systems and add communication

functions by creating sensors and indicators for consumers, producers and retailers in intelligent packaging systems [8, 9, 11].

TiO_2, a non-toxic, abundant, inexpensive inorganic nanostructured material, has unique physical and chemical properties that can be used in a wide range of applications [12, 13]. In addition, TiO_2 is one of the most well known nanofillers for polymer applications in food packaging, enhancing toughness and the barrier properties as well as providing color, antibacterial effects and UV light protection [12, 14].

However, low compatibility between hydrophilic TiO_2 nanoparticles and hydrophobic polymer such as PLA has been problematic due to aggregations of TiO_2 nanoparticles in PLA matrices by a repulsive force between TiO_2 nanoparticles and the polymer matrices. This causes reduced effectiveness of TiO_2 nanoparticles in PLA matrices and reduces transparency of PLA nanocomposites [15].

Stable dispersion TiO_2 nanoparticles is essential to obtain desired properties with PLA. It was suggested in other studies that surface modification of TiO_2 particles using an appropriate surface modifier and dispersant can be one of the solutions to improve dispersion stability of TiO_2 nanoparticles in hydrophobic polymer matrices [16, 17]. In this study, chloroform was used as a dispersant to enhance dispersion of TiO_2 nanoparticles in PLA. The surface of TiO_2 nanoparticles was modified with oleic acid in order to change hydrophilic surface of TiO_2 to hydrophobic surface as PLA and oleic acid are highly soluble in chloroform. In addition, oleic acid is commonly used as long chain fatty acid in polymers as a plasticizer and functional modifier to improve water barrier properties using hydrophobicity and enhancing flexibility [18-20, 21].

Unmodified TiO_2 and oleic acid-modified TiO_2 (OA_TiO_2) nanoparticles, which we produced in the previous study, were incorporated into PLA solution with different weight percentage loadings to prepare OA_TiO_2 PLA nanocomposite films (OT-PLA) and TiO_2 PLA nanocomposites (T-PLA) in this study. As seen in Figure 1, our hypothesis was that oleic acid modified TiO_2 will be dispersed better in PLA matrices than unmodified TiO_2. The purpose of this study was to characterize properties of T-PLA and OT-PLA for food packaging applications. The objective of this study was to investigate dispersion of TiO_2 and OA_TiO_2 in PLA matrices, evaluate barrier properties of oxygen and water vapor, mechanical and thermal properties and light absorption of neat PLA films and PLA nanocomposite films with different weight loading of TiO_2 and OA_TiO_2.

MATERIALS AND METHODS

Materials

Polylactic acid 7000 D (PLA) (Molecular weight (Mw: 210 kDa), polydispersity index (Mw/Mn: 1.78) was obtained from the NatureWorks LLC (Minnetonka, MN). PLA was completely dried in vacuum oven at 40℃ to remove moisture for at least 48 hours prior to use. Chloroform (HPLC) grade was purchased from Fisher Scientific (Pittsburgh, PA).

Synthesis of TiO_2 and Oleic acid modified TiO_2 nanoparticles

Synthesis of TiO_2 and the surface modification of TiO_2 with oleic acid was conducted according to the method described in the previous research chapter. Each of the TiO_2 and OA_TiO_2 preparations was dispersed in a dispersant solvent in order to obtain good dispersion of the particles in PLA solution, because PLA is highly soluble in chloroform.

Preparation of TiO_2 PLA nanocomposite films (T-PLA), OA_TiO_2PLA nanocomposite films (OT-PLA) and PLA films

PLA films, TiO_2 (0.5, 1, and 3 wt % with respect to the weight of PLA) PLA nanocomposite films and OA_TiO_2 (0.5, 1 and 3 wt % with respect to the weight of PLA) PLA nanocomposite films were prepared by a solvent casting method described by Rhim, Hong & Ha (2009) and Nakayama & Hayashi (2007) [22, 23].

Five g of PLA resin was first dissolved in 125 ml of chloroform. TiO_2 solution and OA_TiO_2 solution (0.5, 1, 3 wt. % with respect to PLA) were added into the PLA solutions separately. Each PLA solution containing the different weight ratios of TiO_2 or OA_TiO_2 was sonicated for 15 minutes in the sonication bath and vigorously stirred for 24 hours to obtain well mixed TiO_2 or OA_TiO_2 PLA solutions. Each of mixtures of the different wt. % of TiO_2 or OA_TiO_2 loading and PLA solutions was cast on glass plates covered with a polytetrafluoroethylene coated film (25.4 x 25.4 cm^2). The casted films were dried for 24 hours in the fume hood at room temperature. Once dried in the hood, the films were peeled off and dried in the vacuum oven at 40 ℃ for one week to completely remove remaining chloroform. All films (0.5% T-PLA, 1% T-PLA, 3% T-PLA, 0.5% OT-PLA, 1% OT-PLA, 3% OT-PLA and PLA films) were stored in a desiccator prior to characterization.

Characterizations of T-PLA, OT-PLA and PLA films

Morphology of T-PLA, OT-PLA and PLA films was observed by Field Emission Scanning Electron Microscopy (LEO Zeiss1550 Field Emission Scanning Electron Microscopy, Germany) operated at 2.00 kV with the inlens detector. Cross-sections of the T-PLA, OT-PLA and PLA films were observed. The samples were deposited with 5 nm of iridium by a Leica EM ACE 600 sputter coating instrument (Buffalo Grove, IL). Oxford INCA Energy E2H X-ray Energy Dispersive Spectrometer (EDS) system (Abingdon, United Kingdom) with a silicon drifted detector at 10 kV with the inlens detector was used to identify elements in the films.

Oxygen permeability coefficients (OP, ml · mm / m^2 day) of the T-PLA, OT-PLA and PLA films were measured by using an Oxysense 5250i (Las Vegas, NE) based on an ASTM method (F3136-15) [24]. Each film was cut into 7 cm x 7 cm pieces, and thicknesses of each sample were averaged after measuring three sections on the films using a digital micrometer (Mitutoyo 700-118-20 Digital Thickness Gage, Japan). Each film was attached inside the chamber using vacuum grease (Dow corning, Auburn, MI). Nitrogen and highly pure oxygen (99.99%) were purged into the sensing well and the driving well for one and four minutes respectively. An oxygen reading in the sensing well was collected at 5 minutes increments. The data of oxygen concentration vs. time was recorded at every 5 min interval until steady state was reached.

Water vapor permeability coefficients (WVP, g · cm / cm^2 s ·pa) of the films were measured with i-Hydro 7500 Water Vapor Transmission Rate Testing System (Labthink Instruments Co., Ltd., China) according to an internal standard ISO 15106-3 with the electrolytic detection sensor method [25]. The thicknesses of the three parts of each film were measured by the micrometer then averaged thickness of each film. The WVP coefficient of each film was calculated using as an equation: WVP coefficient (g·cm / cm^2 s·pa) = wvtr x l / Δp where wvtr is water vapor transmission rate (g / m^2·24 hr) through the film and l indicates the mean thickness of each films (μm). Δp (Pa) is the difference in water vapor partial pressure between the two sides (a dry chamber and controlled humidity chamber) of the film. Each film (7 cm x 7 cm) was attached between two sides of the punched aluminum plates. The diameter of the punched area on the plates was 5.08 cm. The actual test area of WVP was 3.5 cm x 3.5 cm based on the exposed punched area of the plates. The aluminum plate containing the film was inserted in the cell chamber and closed it tight. The flow rate was adjusted to 100 ml/min, and the test relative

humanity and temperature was controlled at 50 ± 2% and at 23.5℃ receptively. The standard testing mode was programmed with four cycles testing mode for each cell chamber. Each test time interval per a cycle was 30 minutes. Before four cycles of each test was started, the zero purging for 60 minutes was conducted. WVP coefficient vs. time interval (30 minutes) per a cycle was recorded. The steady value of WVP coefficient was obtained with the standard testing mode.

Mechanical properties of tensile strength (MPa), elongation at break (%) and Young's modulus (MPa) of each film were evaluated using ASTM method D882-12 using a MTS testing machine (Eden Prairie, MN) [26]. The grip distance was set at 50 mm with cross-head speed at 5 mm/min. The size of each sample was cut into width 1.27 cm and height 10 cm. The thicknesses of three parts on each sample were measured by the digital micrometer then averaged the thickness of each sample. The results were obtained from five replications within each sample within triplicate samples (n=15). The samples were conditioned in RH 50% chamber at 23 ℃ for 48 hours prior to the test.

Thermal properties of glass transition temperatures (Tg, ℃), melting temperatures (Tm, ℃) and crystallinity (Xc, %) were determined by using TA Discovery Differential scanning calorimetry (DSC) (New Castle, DE). The samples were conditioned at 40℃ in the vacuum oven for 48 hours. The heating cycle was operated under nitrogen atmosphere; each sample was heated from 30 ℃ to 200 ℃ with a scanning rate 5℃/min for the first heating cycle. After the first heating cycle, the films were cooled by 10℃/min. The second heating cycle was operated at 30 ℃ to 200 ℃ with scanning rate of 5℃/min. The Tg (℃), Xc (%), and Tm (℃) of the samples were determined using the second heating cycle by Trios data analysis program (New Castle, DE). Crystallinity, Xc (%), of the films was calculated based on an equation following

with a heat fusion enthalpy for 100 % crystalline PLA (93.1 j/g), melting enthalpy ($\Delta Hm, j/g$) and cold crystallization enthalpy($\Delta Hc, j/g$) [27].

$$Xc(\%) = \frac{\Delta Hm - \Delta Hc}{93.1(j/g)}$$

UV-absorbance of the films was measured by the UV/Vis spectrometer (Shimadzu 2550 UV-Vis spectrometer spectrum, Kyoto, Japan) with wavelength ranging of 200-800 nm.

STATISTICAL ANALYSIS

Results in triplicate were reported as means ± standard deviations. Significant differences between the films were evaluated by one-way ANOVA and Tukey's HSD test at a level of $p < 0.05$ using JMP Pro 12 (Cary, NC).

RESULTS

Morphology

The films were embedded with epoxy glues in a mold to break the thin films into two parts easily. The films were broken into two parts by liquid nitrogen in order to observe morphology of cross-sections of each film. Each cross-section of the films was observed by FESEM to compare dispersion of unmodified TiO_2 and OA_TiO_2 in PLA matrices. Figure 2b-f shows SEM images of cross-section PLA films incorporated with TiO_2 or OA_TiO_2 of different weight loadings. As seen in the Figure 2b, 2d and 2e, it was obvious that heavy agglomerations of TiO_2 without the surface modification in PLA matrices were seen. More spots of white TiO_2 clusters in various sizes were seen with higher concentrations of TiO_2 while evident agglomerations and clusters of OA_TiO_2 were not exhibited in the Figure 2b, 2d and 2f. With 5000 magnification, it was difficult to see any OA_TiO_2 in PLA matrices because the FESEM may not be able to detect well distributed small sizes of OA_TiO_2 with 5000 magnification or even higher magnifications. Although OA_TiO_2 were not visibly shown, the Energy Dispersive

Spectrometer (EDS) supported existence of Ti in the OT-PLA. The images of OT-PLA supported that dispersion of TiO_2 are greatly improved by the oleic acid surface modification.

Oxygen Barrier Properties

Figure 4 shows OP of PLA nanocomposite films incorporated with TiO_2 and OA_TiO_2 for different loadings. OP of 1% OT-PLA was 17.1 ml·mm / m^2 day of the lowest value in T-PLA and OT-PLA. The OP of 1% OT-PLA, 0.5% OT-PLA and 3% OT-PLA were decreased by 28.8%, 19.2 % and 11.7 % respectably compared to neat PLA film. 0.5% T-PLA and 3% T-PLA shows 9.59 % and 3.33 % of reduction in OP while 1%T-PLA were increased by 3.33 % against the neat PLA film. Well-dispersed 0.5 % and 1 % OA_TiO_2 in PLA matrices indicated significant reductions in OP ($p < 0.05$) whereas PLA nanocomposites incorporated with unmodified TiO_2 did not significantly reduce oxygen permeability coefficients of the films. The results indicated the surface modification of TiO_2 with oleic acid influence reduction of OPs and increase of oxygen barrier property of PLA films because well dispersion of OA_TiO_2 in PLA matrices may restrict diffusion path and free volumes than TiO_2 without the modification. Fortunati and others (2012) reported that surface modified cellulose nanocrystals attributed to more effective reduction in oxygen transmission rate of PLA than unmodified cellulose nanocrystals [17]. Transporting oxygen across PLA films was significantly affected by tortuosity of their paths through the films. Stable dispersion of nanofillers created irregular tortuous paths that may help slow oxygen flow rate and retarding transporting oxygen through PLA film [17, 28, 29].

Water vapor barrier property

The water vapor permeability (WVP) coefficients of PLA nanocomposites films with different amounts of TiO_2 or OA_TiO_2 loading are seen in the Figure 5. Addition of TiO_2 and

OA_TiO_2 into PLA films shows improvements in barrier property against water vapor. Especially, the results showed significant reduction in WVP coefficients of higher amounts of OA_TiO_2 loading into PLA nanocomposite films such as 1% OT-PLA and 3% OT-PLA. The WVP decreasing rate of 1% OT-PLA and 3% OT-PLA were both 26 % when compared to neat PLA film. PLA nanocomposite films reinforced with unmodified TiO_2 and OA_TiO_2 exhibited OT-PLA had lower WVP coefficients than T-PLA. These results agree with previous reports with improved water vapor properties of biopolymers with long chain fatty acid treatment. Although small amounts of oleic acid were attached to TiO_2, it still provided efficient barrier effects. Other studies reported that lipid treatments with hydrophobic components and long chain fatty acids with alcohols and alkanes are effective means of reducing WVP and improving water vapor barrier properties of biopolymers [18-20]. High hydrophobic long chain fatty acid groups were not compatible with water and hinder water vapor permeating through polymer matrices as seen by reduced WVP coefficients.

Mechanical properties

Mechanical properties of tensile strength, Young's modulus and elongation break (%) were measured to investigate PLA reinforcing effects by TiO_2 and OA_TiO_2 loading. Tensile strength measures strengths of the materials by force per unit of area that require to break the material. Tensile strengths of the T-PLA and OT-PLA are displayed in the Figure 6a. The tensile strengths of the PLA were not significantly different between the PLA nanocomposite films incorporated with TiO_2 or OA_TiO_2 ($p>0.05$). Zhu and others (2011) reported that the highest tensile strength of PLA was obtained with 2% TiO_2 loading among 4, 6, 8 and 10 % TiO_2 loadings produced by compression molding and a twin screw melt extrusion method [28]. The

film producing method influence tensile strengths of PLA significantly because PLA can be affected by the thermal processing of film preparation [28].

Young's modulus measures ratio of stress required to elastic stain in tension. Young's modulus versus PLA and PLA nancomposite films with addition of TiO_2 and OA_TiO_2 are shown in the Figure 6b. Higher Young's modulus of the material indicated stiffer and tougher materials. One % T-PLA and 3% T-PLA significantly increased the modulus compared to PLA, whereas addition of OA_TiO_2 did not have significant effects in enhancing the modulus of PLA. The results conveyed high Young's modulus of 1%T-PLA and 3% T-PLA reinforced stiffness and toughness of PLA by addition of TiO_2 nanoparticles as nanofillers, but it might increase brittleness of PLA [2]. This result of Young's modulus agreed well with a previous study that reported higher loading of TiO_2 in PLA showed increasing values of Young's modulus [29].

Figure 6c represents the elongation at break (%) of PLA and PLA nancomposite films with addition of the TiO_2 and OA_TiO_2. The elongation break (%) measures flexibilities and stretching abilities of materials by percentage of increase in length by original length before it breaks under tension. The elongation at break (%) of 1% OT-PLA and 3% OT-PLA had significantly higher values than T-PLA. This result shows increasing patterns of elongation at break (%) of PLA nanocomposite films with incorporation of OA_TiO_2 whereas the elongation at break (%) of T-PLA was significantly decreased. As previous studies reported, addition of long chain fatty acids and lipid treatments showed increasing flexibility as well as reducing brittleness of polymers [18, 19]

Thermal stability

Glass transition temperature (Tg °C), melting temperature (Tm °C) and cystallinity (Xc %) of the T-PLA and OT-PLA are shown in the Table 4. Tg (°C) and Tm (°C) of the T-PLA and OT-PLA showed slight changes compared to PLA films, with no significant difference ($p > 0.05$).The PLA nanocomposites films loaded with TiO_2 and OA_TiO_2 nanoparticles had higher crystallinity (Xc %) than the crystallinity (Xc %) of PLA. Increase of crystallinity (Xc %) by addition of TiO_2 nanoparticles in PLA were similar patterns with previous reports [16, 19, 28]. PLA nanocomposites with the OA_TiO_2 loadings also showed increasing patterns of crystallinity (Xc %). Three % OT-PLA had the most effect in increase of the crystallinity (Xc %). Oleic acid might work as plasticizer and help chain mobility as well as improve packing of the segments in PLA matrix [18, 20].

UV-Vis light absorbance property.

Figure 7 illustrates the light absorbance of the T-PLA and OT-PLA films were scanned by in UV-Vis range of 200 nm – 800 nm. PLA is a highly transparent and light sensitive film. Figure 7 indicates that UV-light absorption of PLA nanocomposite films with TiO_2 and OA_TiO_2 are higher than PLA films. TiO_2 is well known as UV-light blocker and protects deterioration by UV-light [30]. These T-PLA and OT-PLA showed high efficiency of UV-light shielding effects because light absorption of PLA film was improved significantly in the UV region after addition of TiO_2 and OA_TiO_2. In addition, higher loadings of TiO_2 and OA_TiO_2 were more effective in UV-light absorption. PLA nanocompostie with addition of OA_TiO_2 showed highly increasing patterns of UV-light absorption in the UVB region (280-320 nm) because good distribution of OA_TiO_2 in PLA nanocomposite films possess larger surface area of TiO_2 for UV light absorption and completely shields UVB light [30]. The light absorptions of 0.5% OT-PLA and 1% OT-PLA in the UVB region were higher than 0.5% T-PLA and 1% T-

PLA. The 0.5% OT-PLA and 1% OT-PLA attributed to higher light scattering effect and protection in the UVB region. The T-PLA has higher UVA and visible absorbance than the OT-PLA which exhibits high light protection effects in the UVA and visible regions. Transparent OT-PLA improved UV light absorption of PLA films and had higher light protecting efficiency in UVB region, but the OT-PLA shows less effective light absorption in the UVA region and visible region than T-PLA. The results suggest that PLA incorporated with TiO_2 may provide an effective light protecting property although it can decrease transparency of PLA films.

CONCLUSIONS

In this study, the PLA nanocomposites films were prepared by incorporation of the TiO_2 and OA_TiO_2. The surface modified TiO_2 with oleic acid improved dispersion in PLA matrices than unmodified TiO_2. There was no severe agglomeration found on the cross-sections of OT-PLA by FESEM. Addition of OA_TiO_2 into PLA films showed more effective improvements in oxygen and water vapor barrier properties than addition of TiO_2 into PLA. Ops of 0.5% T-PLA and 1% T-PLA were reduced by 29 % and 19% respectively. WVP of 1% OT-PLA and 3% OT-PLA were 26 % lower than PLA film. In addition, increase of flexibility and reduction of brittleness of PLA films were shown with OT-PLA. However, incorporations of OA_TiO_2 into PLA decreased Young's modulus of the PLA films compared to T-PLA. The OT-PLA were transparent and had low light absorption in the visible and UVA ranges, but the light absorptions of the OT-PLA were particularly increased in the UVB regions due to UV-light protecting properties of TiO_2. As the concentration of TiO_2 increased in PLA films, PLA nanocomposites films with higher loadings of TiO_2 became more opaque and had higher light absorption in the visible and UVA regions. Although light barrier properties of OT-PLA in visible region and Young's modulus of OT-PLA still needs an improvement for wider and more effective

applications for food packaging, enhancing the barrier properties of PLA films and dispersion of TiO_2 in PLA nanocomposite films by the surface modification may add great values and potentials of wider uses of PLA as biobased and biodegradable sustainable films in food packaging.

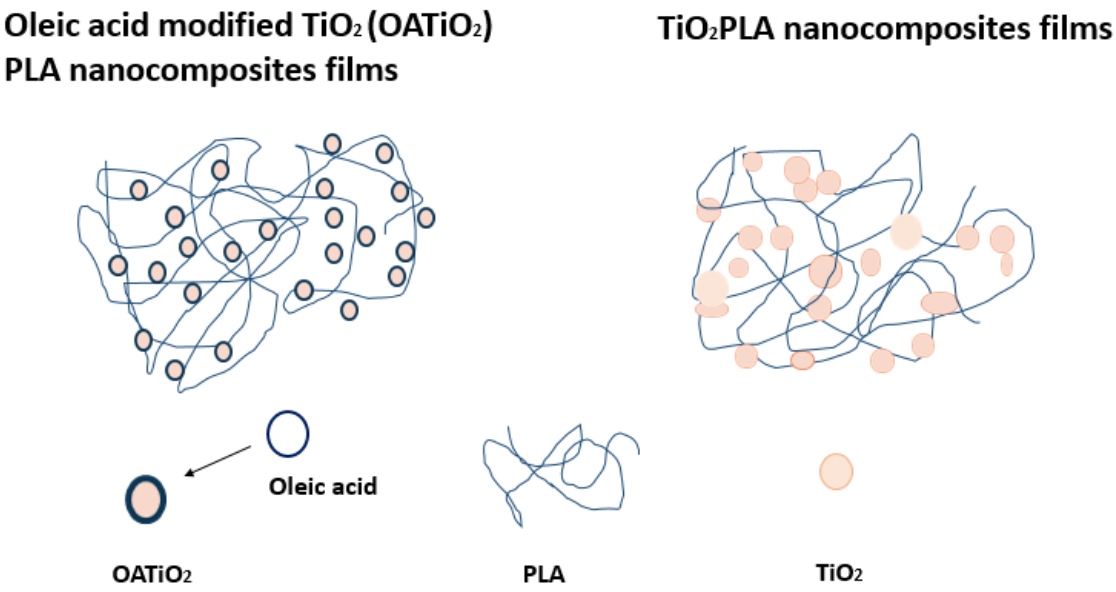

Figure1. Hypothesized schematic illustrations of oleic acid modified TiO_2 PLA nanocomposites and unmodified TiO_2 PLA nanocomposites. The blue around the pink circle of OA_TiO_2 is oleic acid on TiO_2.

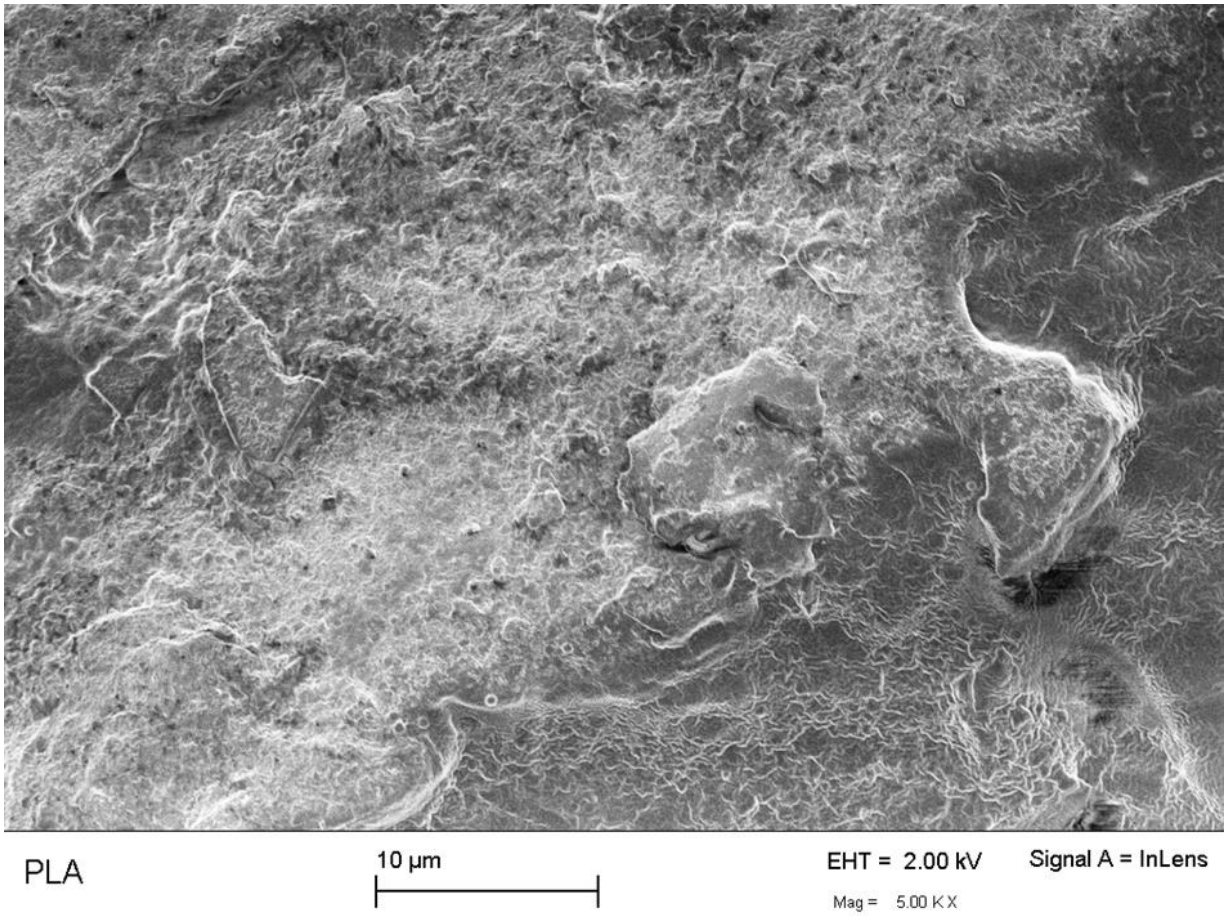

Figure 2a. Field emission scanning electron microscopy images of the cross section of PLA film was taken at 2.00 kV with 5000 X magnification.

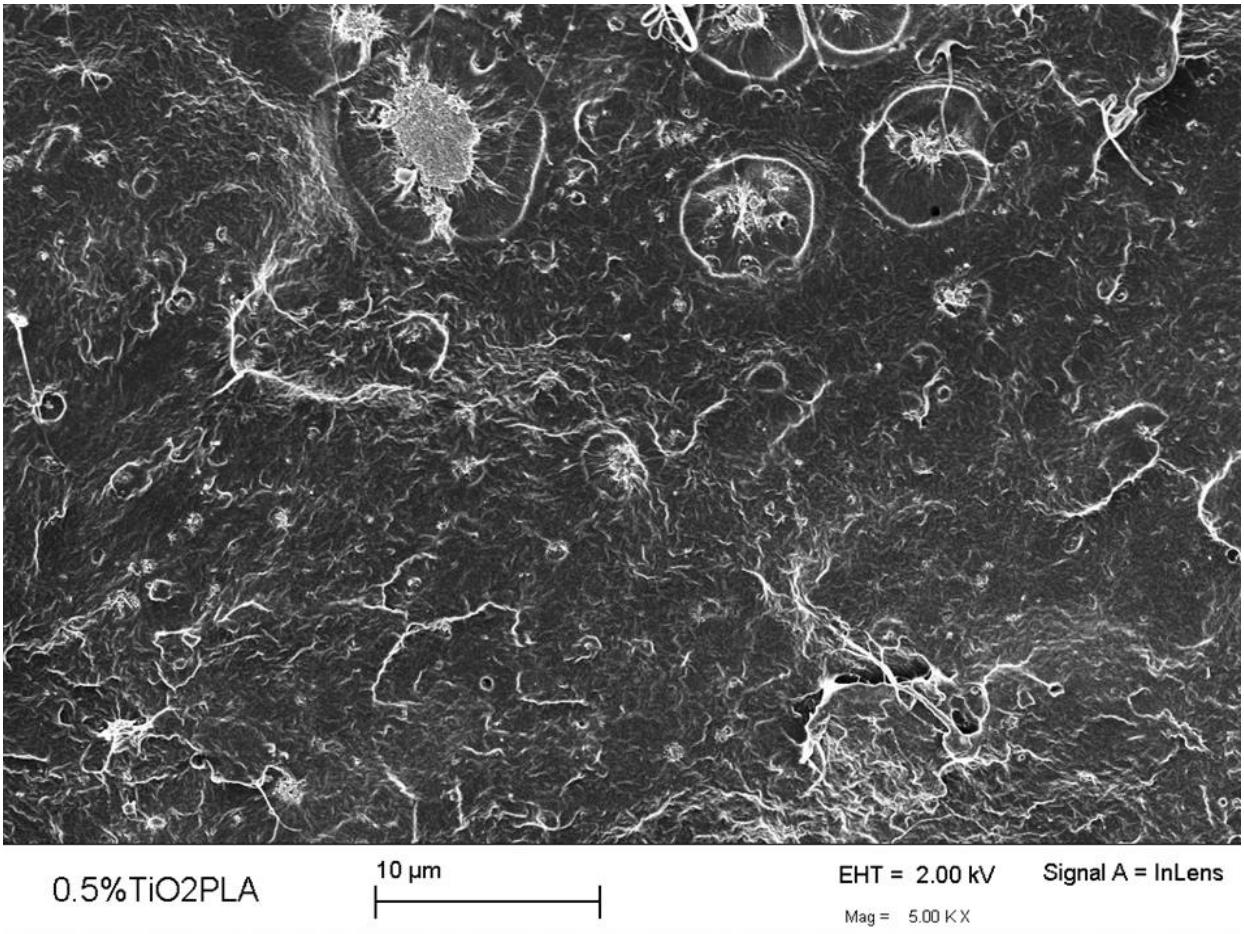

Figure 2b. . Field emission scanning electron microscopy images of the cross section of 0.5% TiO_2 PLA nanocomposite film was taken at 2.00 kV with 5000 X magnification.

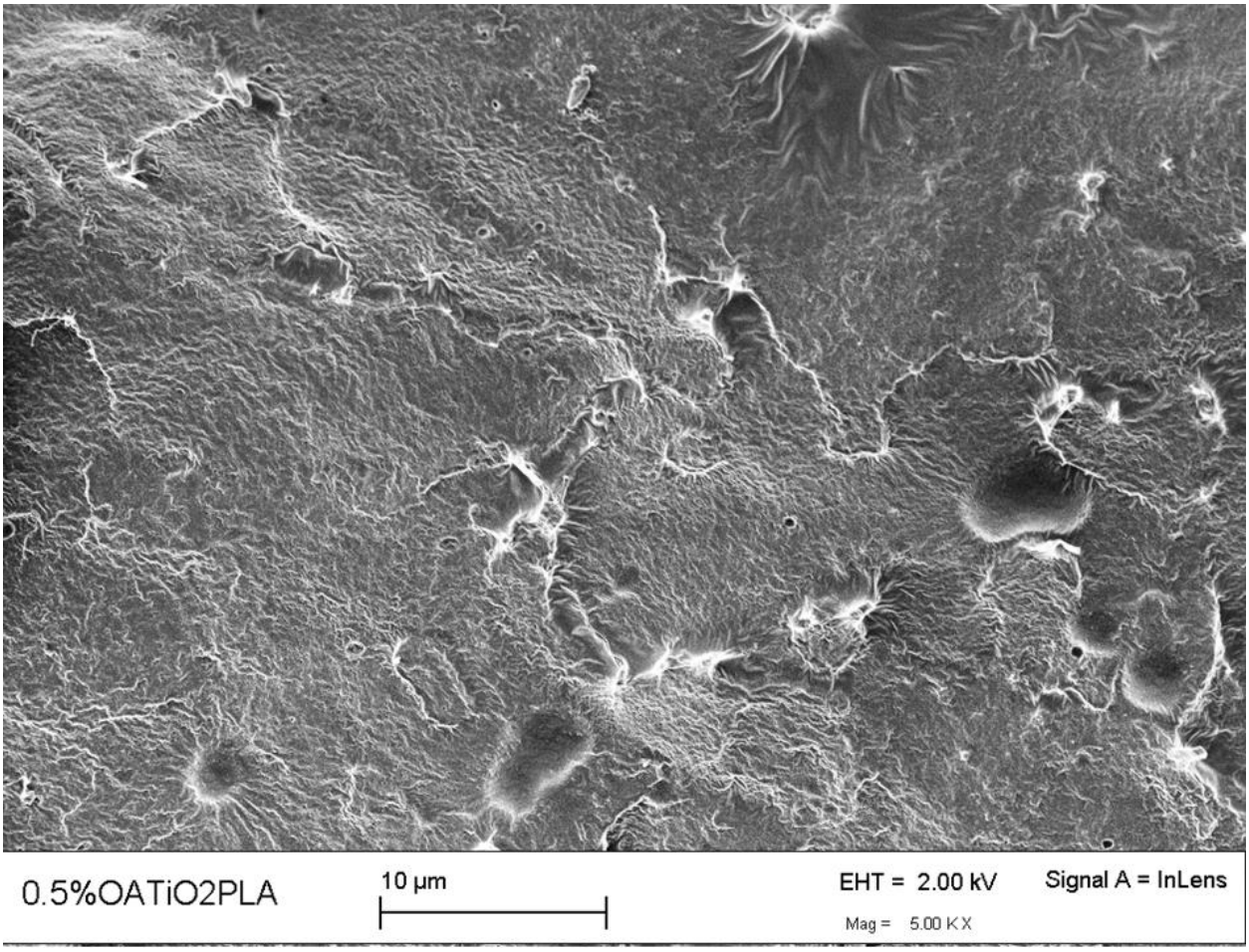

Figure 2c. Field emission scanning electron microscopy images of the cross section of 0.5% OA_TiO_2 PLA nanocomposite film was taken at 2.00 kV with 5000 X magnification.

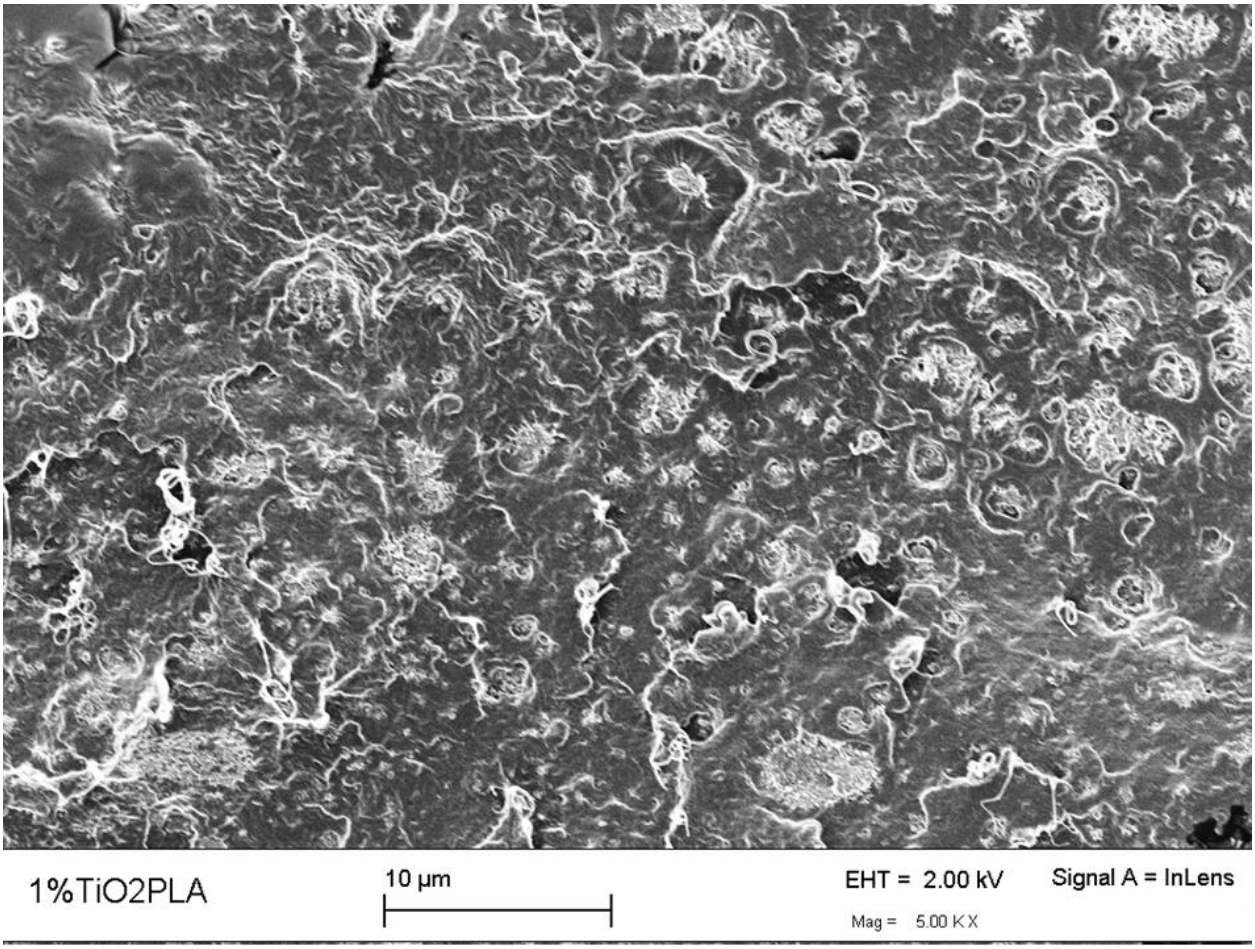

Figure 2d. Field emission scanning electron microscopy images of the cross section of 1% TiO_2 PLA nanocomposite film was taken at 2.00 kV with 5000 X magnification.

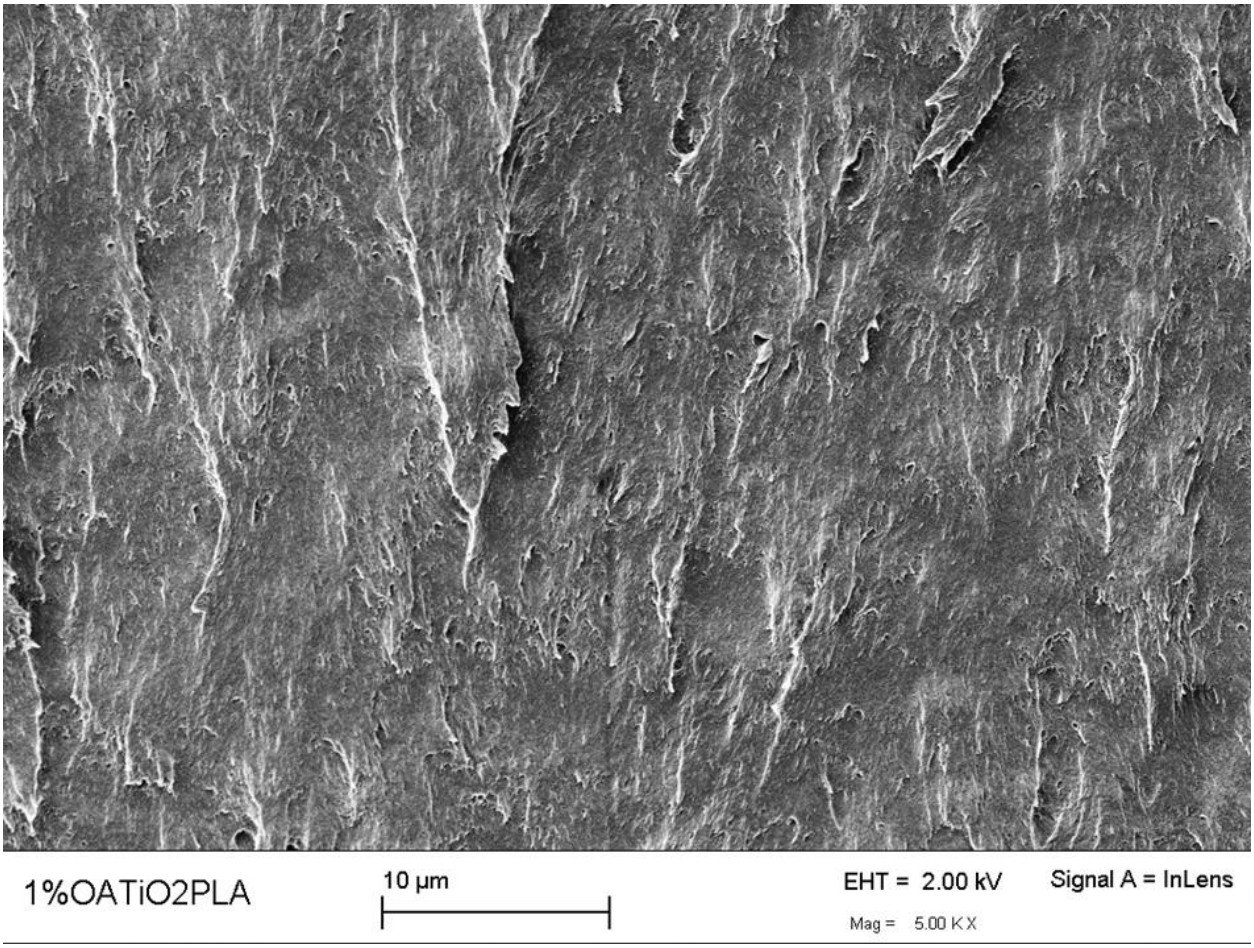

Figure 2e. Field emission scanning electron microscopy images of the cross section of 1% OA_TiO_2 PLA nanocomposite film was taken at 2.00 kV with 5000 X magnification.

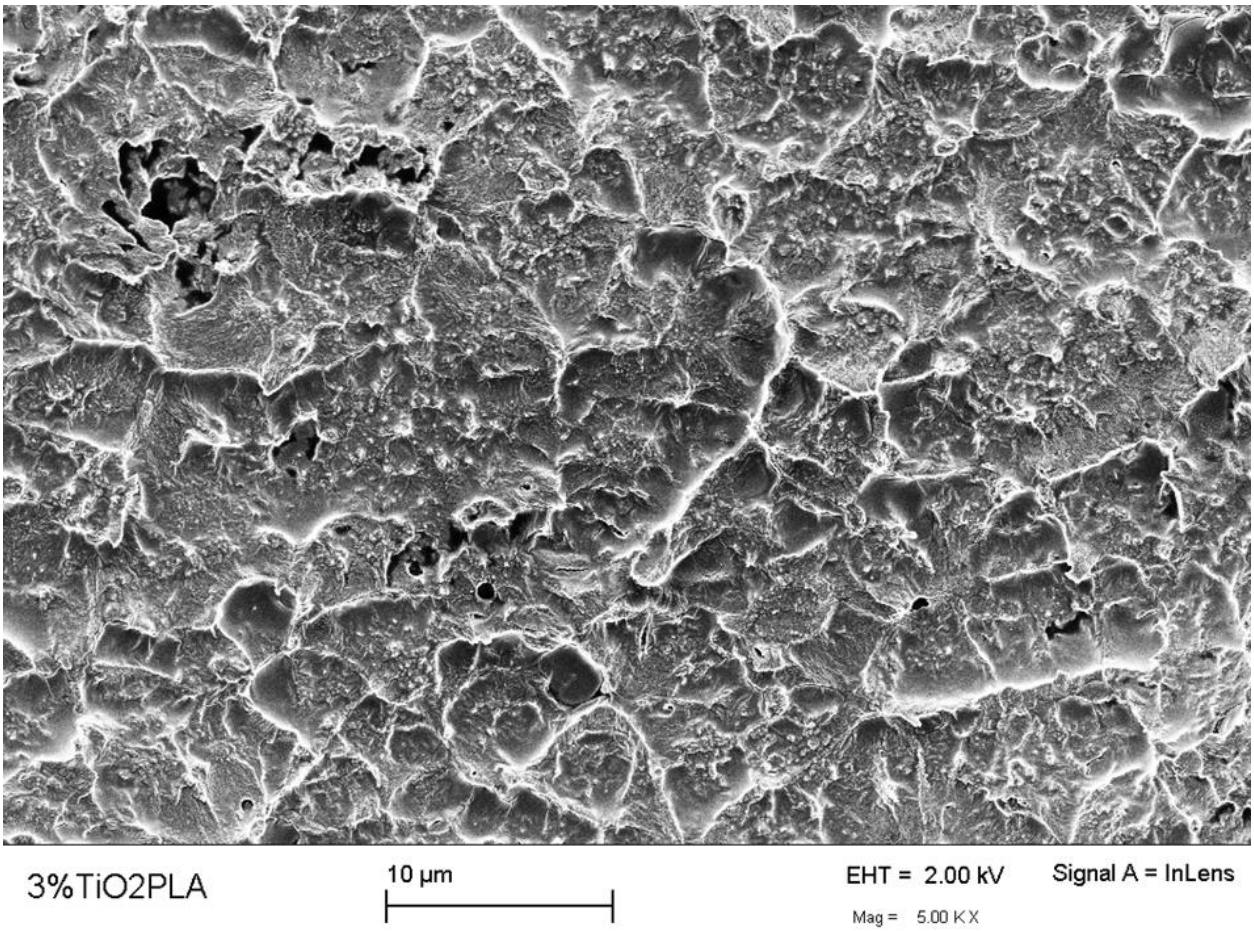

Figure 2f. Field emission scanning electron microscopy images of the cross section of 3%TiO_2 PLA nanocomposite film was taken at 2.00 kV with 5000 X magnification.

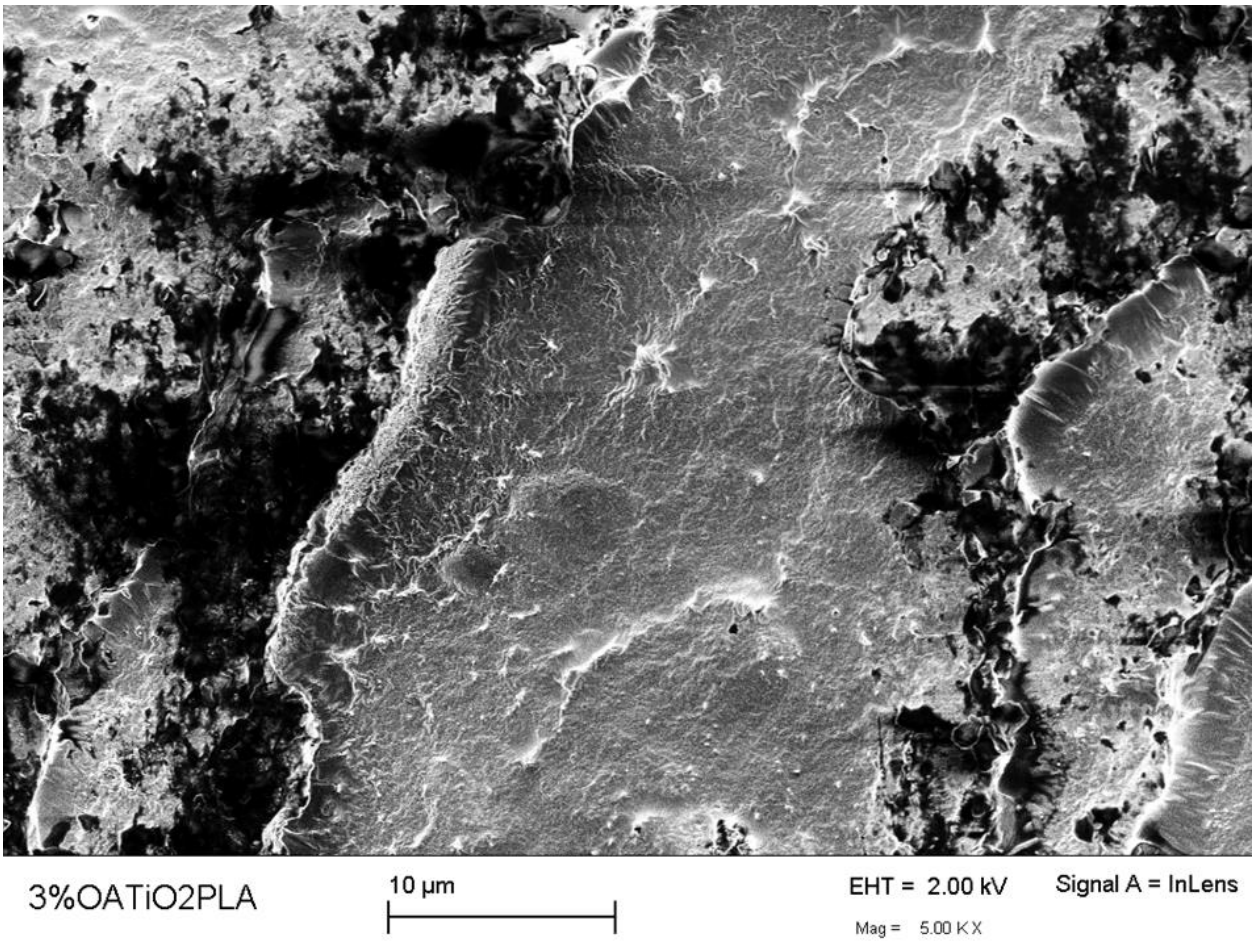

Figure 2g. Field emission scanning electron microscopy images of the cross section of 3%TiO_2 PLA nanocomposite film was taken at 2.00 kV with 5000 X magnification.

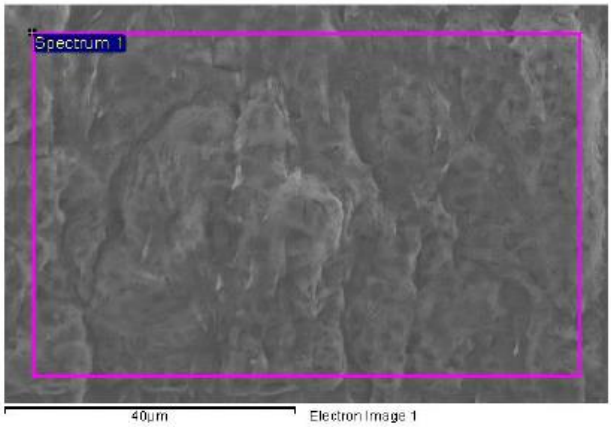

Element	Weight%	Atomic %
C K	60.34	67.51
O K	37.89	31.82
Cl K	1.77	0.67
Totals	100.00	

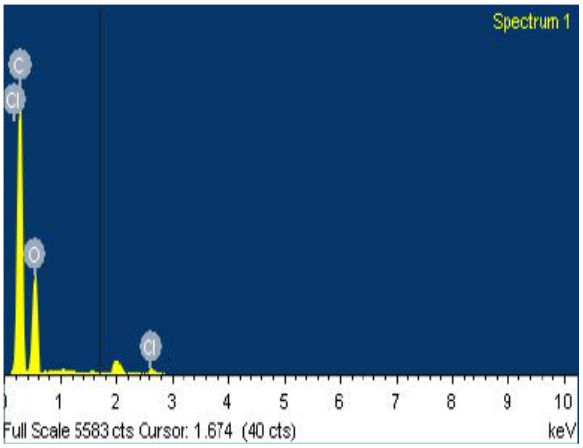

Figure 3a. Element compositions and spectrum of PLA in the top image of the assigned spot were analyzed by the FESEM equipped with X-ray Energy Dispersive Spectrometer (EDS) system operated at 10 Kv with the inlens detection.

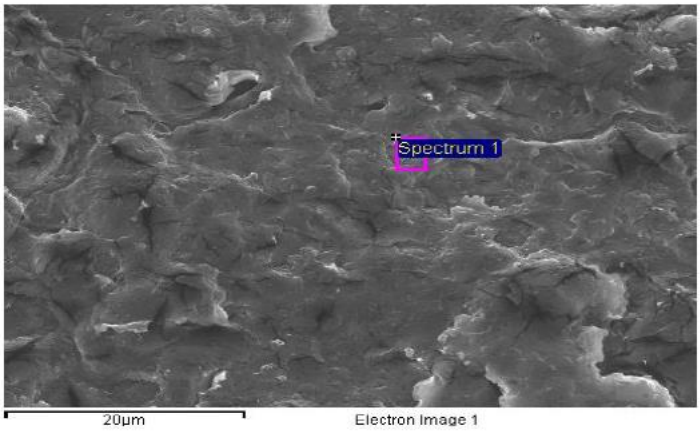

Element	Weight%	Atomic%
C K	69.82	78.74
O K	22.13	18.74
Cl K	2.47	0.95
Ti K	5.58	1.58
Totals	100.00	

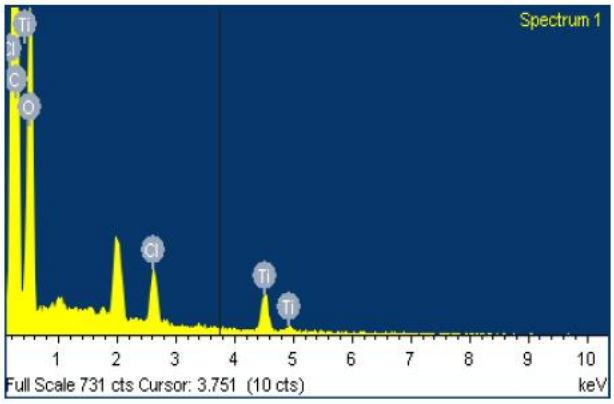

Figure 3b. Element compositions and spectrum of 1%TiO_2 PLA in the top image of the assigned spot were analyzed by the FESEM equipped with X-ray Energy Dispersive Spectrometer (EDS) system operated at 10 Kv with the inlens detection.

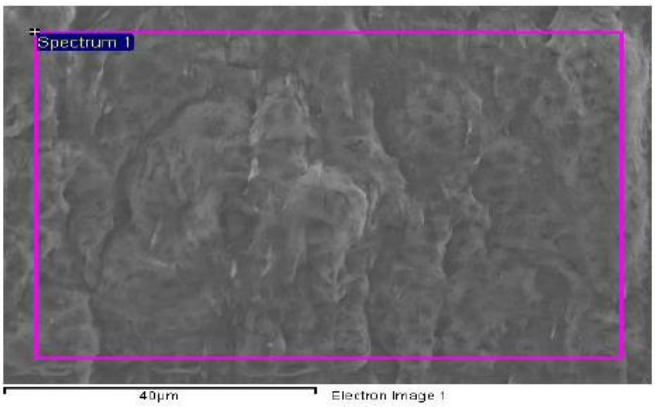

Element	Weight%	Atomic%
C K	65.48	72.39
O K	32.44	26.93
Cl K	1.08	0.41
Ti K	0.99	0.28
Totals	100.00	

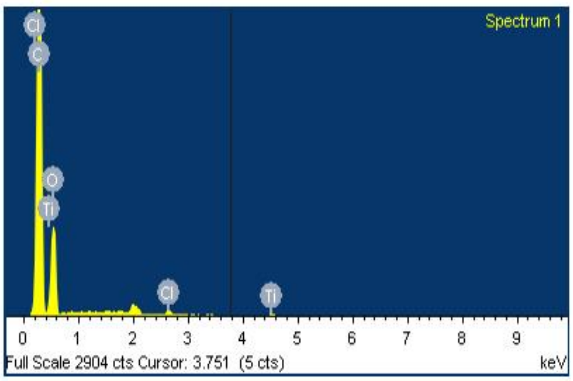

Figure 3c. Element compositions and spectrum of 1% OA_TiO_2 PLA in the top image of the assigned spot were analyzed by the FESEM equipped with X-ray Energy Dispersive Spectrometer (EDS) system operated at 10 Kv with the inlens detection.

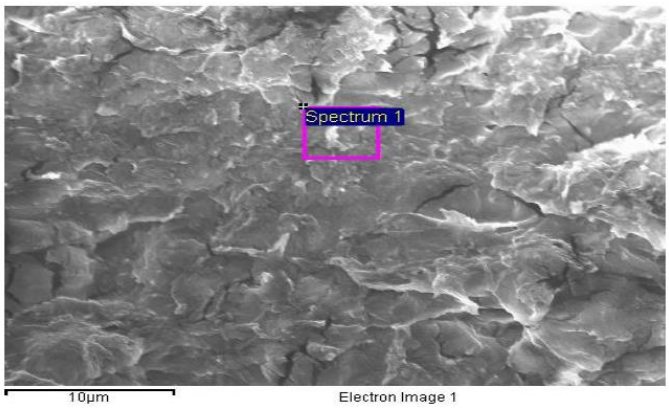

Element	Weight%	Atomic%
C K	72.92	82.05
O K	17.80	15.04
Cl K	2.98	1.13
Ti K	6.31	1.78
Totals	100.00	

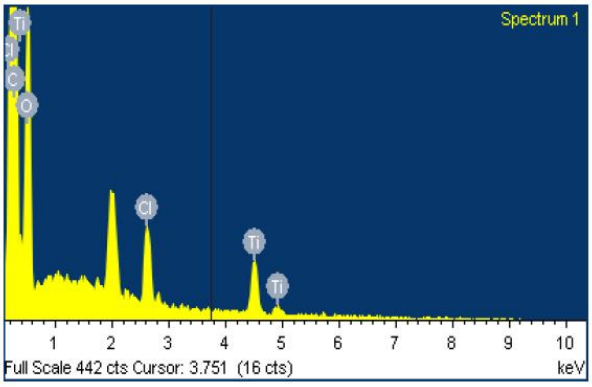

Figure 3d. Element compositions and spectrum of 3% TiO_2 PLA in the top image of the assigned spot were analyzed by the FESEM equipped with X-ray Energy Dispersive Spectrometer (EDS) system operated at 10 Kv with the inlens detection.

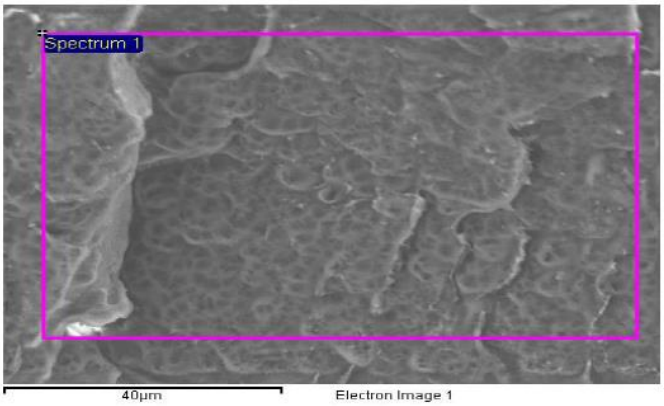

Element	Weight%	Atomic%
C K	60.19	68.93
O K	33.80	29.06
Cl K	2.82	1.09
Ti K	3.19	0.92
Totals	100.00	

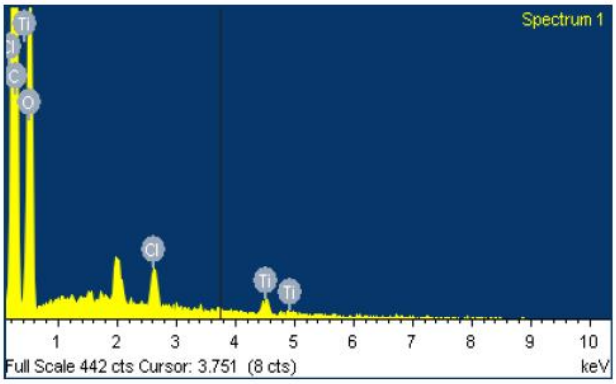

Figure 3e. Element compositions and spectrum of 3% OA_TiO_2PLA in the top image of the assigned spot were analyzed by the FESEM equipped with X-ray Energy Dispersive Spectrometer (EDS) system operated at 10 Kv with the inlens detection.

Table 1. Thickness (Mean ± Standard deviation) of PLA, 0.5%TiO_2 PLA, 1%TiO_2 PLA, 3%TiO_2 PLA, 0.5%OA_TiO_2 PLA, 1%OA_TiO_2 PLA and 3% OA_TiO_2 PLA nanocomposite films were shown.

Sample (n=6)	Mean (μm) ± Std Dev
PLA	61.7 ± 12.1
0.5%TiO_2PLA	59.2 ± 6.65
1%TiO_2PLA	63.3 ± 8.76
3%TiO_2PLA	66.7 ± 10.3
0.5%OA_TiO_2PLA	61.7 ± 9.83
1%OA_TiO_2PLA	68.3 ± 7.53
3%OA_TiO_2PLA	63.3 ± 12.1

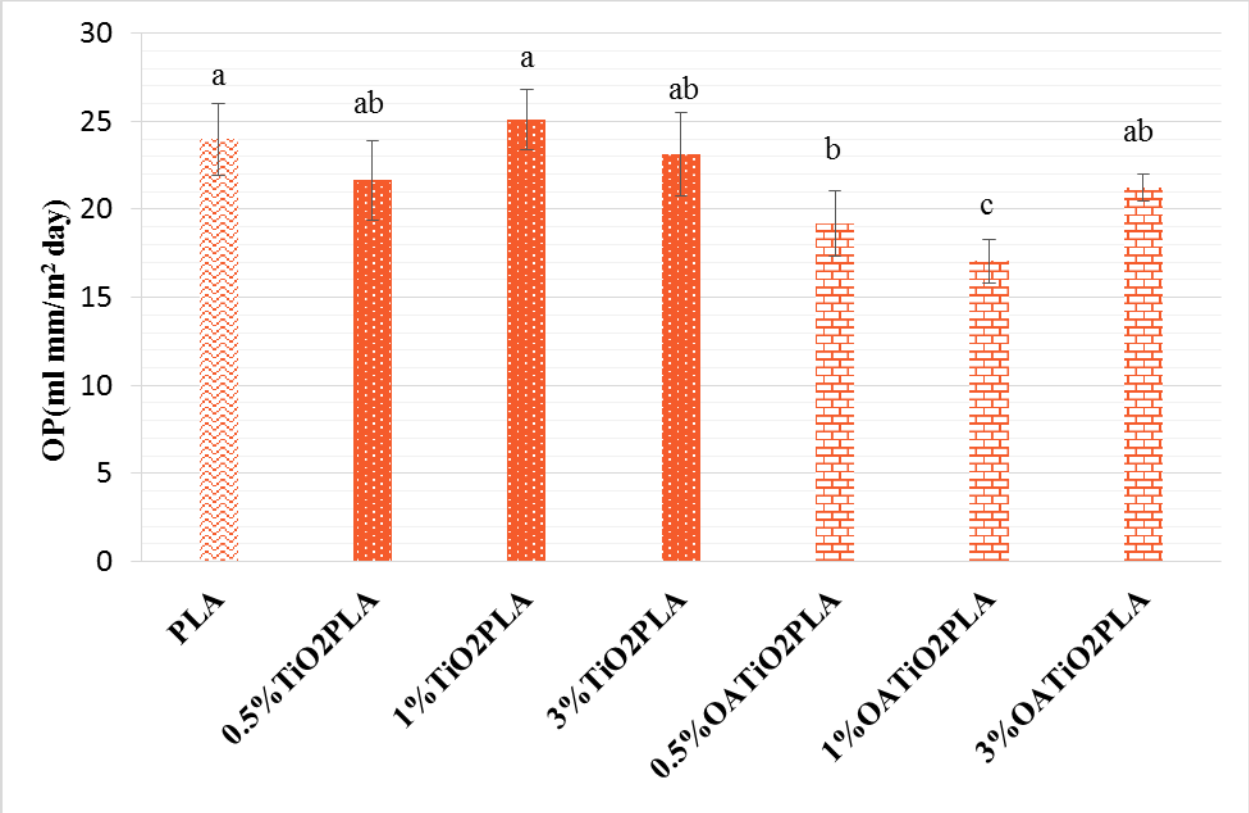

Figure 4. Oxygen permeation rate of PLA, 0.5%, 1% and 3% TiO_2 PLA, 0.5%, 1% and 3% OA_TiO_2 PLA nanocomposite films were shown. The significant differences of mean values between the samples were indicated using different letters by the Tukey's test with p-value ($p < 0.05$).

Table 2. Thickness (Mean ± Standard deviation) of PLA, 0.5%TiO_2PLA, 1%TiO_2 PLA, 3%TiO_2 PLA, 0.5%OA_TiO_2 PLA, 1%OA_TiO_2 PLA and 3% OA_TiO_2 PLA nanocomposite films used for wvp coefficient measurement.

Sample (n=6)	Mean (μm) ± Std Dev
PLA	51 ± 9.5
0.5%TiO_2PLA	49.3 ± 3.8
1%TiO_2PLA	59.8 ± 59.8
3%TiO_2PLA	59.8 ± 12.5
0.5%OA_TiO_2PLA	46.7 ± 46.7
1%OA_TiO_2PLA	58.3 ± 10.8
3%OA_TiO_2PLA	61.2 ±10.9

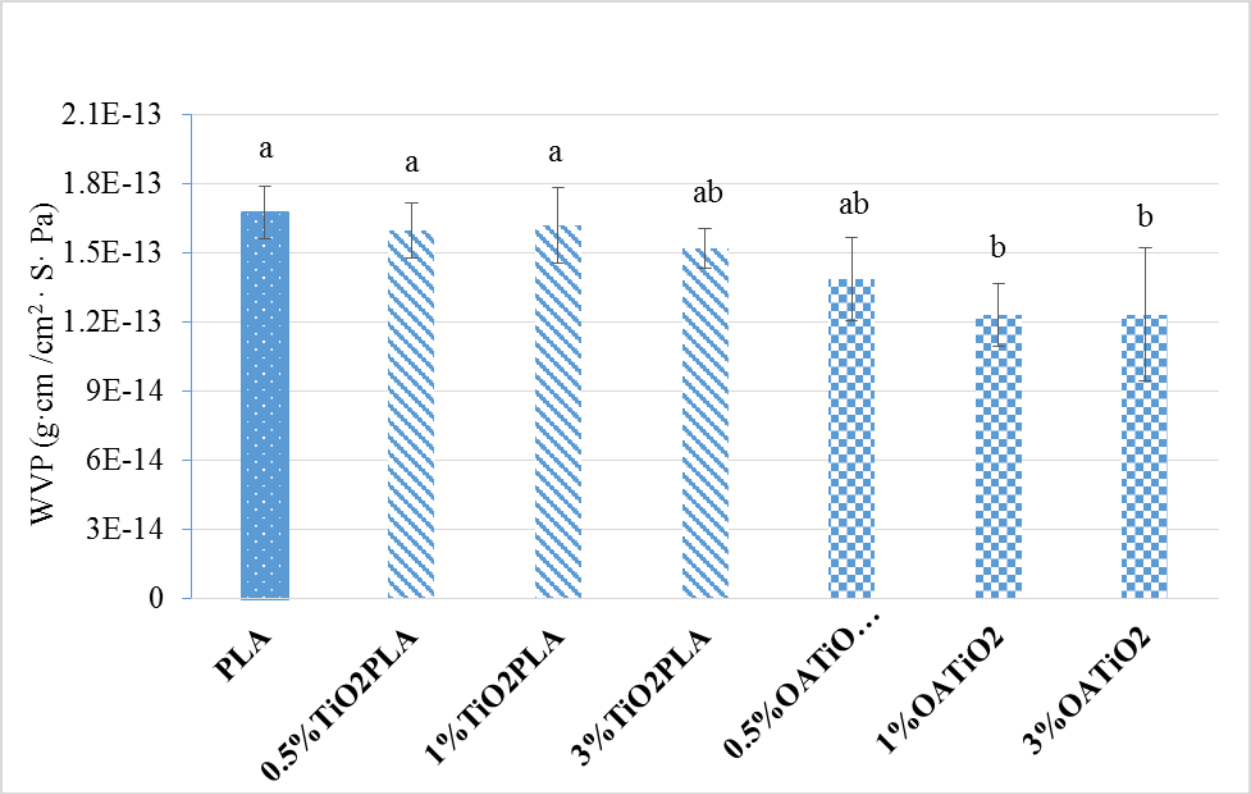

Figure 5. Water vapor permeability coefficient (g·cm /cm^2·S·Pa) of PLA, 0.5%, 1% and 3% TiO_2 PLA, 0.5%, 1% and 3% OA_TiO_2 PLA nanocomposite films were shown. The significant differences of mean values between the samples were indicated using different letters by the Tukey test with p-value ($p < 0.05$).

Table 3. Thickness (Mean ± Standard deviation) of PLA, 0.5%TiO_2 PLA, 1%TiO_2 PLA, 3%TiO_2 PLA, 0.5%OA_TiO_2 PLA, 1%OA_TiO_2 PLA and 3% OA_TiO_2 PLA nanocomposite films used for mechanical properties

Sample (n=15)	Mean (μm) ± Std Dev
PLA	48.7 ± 9.54
0.5%TiO_2PLA	54.8 ± 9.03
1%TiO_2PLA	50 ± 9.03
3%TiO_2PLA	59.2 ± 11.6
0.5%OA_TiO_2PLA	48 ± 8.49
1%OA_TiO_2PLA	51.3 ± 10.4
3%OA_TiO_2PLA	52 ± 8

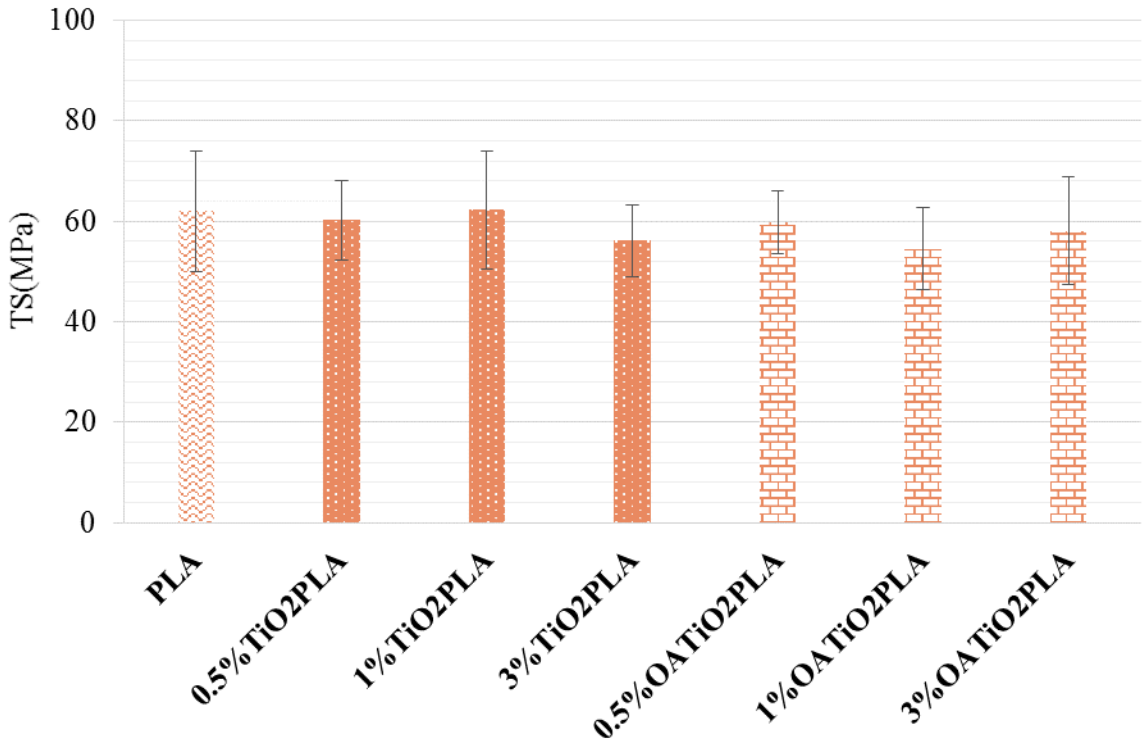

Figure 6a. Tensile strengths (TS) of PLA, 0.5%TiO $_2$PLA, 1%TiO_2 PLA, 3%TiO_2 PLA, 0.5%OA_TiO_2 PLA, 1%OA_TiO_2 PLA and 3% OA_TiO_2 PLA nanocomposite films.

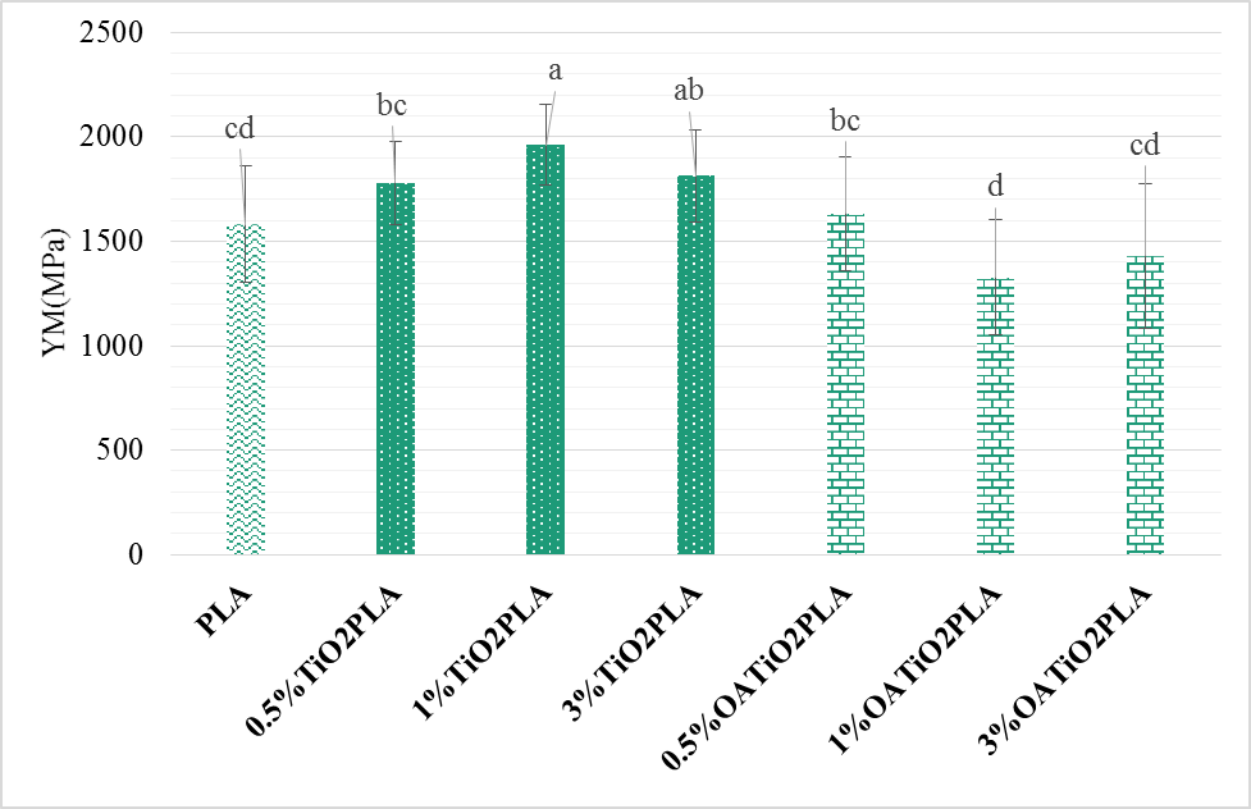

Figure 5b. Young's modules (YM) of PLA, 0.5%TiO_2 PLA, 1%TiO_2 PLA, 3%TiO_2 PLA, 0.5%OA_TiO_2 PLA, 1%OA_TiO_2 PLA and 3% OA_TiO_2 PLA nanocomposite films. Significant different mean values were shown with different letter by the Tukey's analysis when p-value is smaller than 0.05.

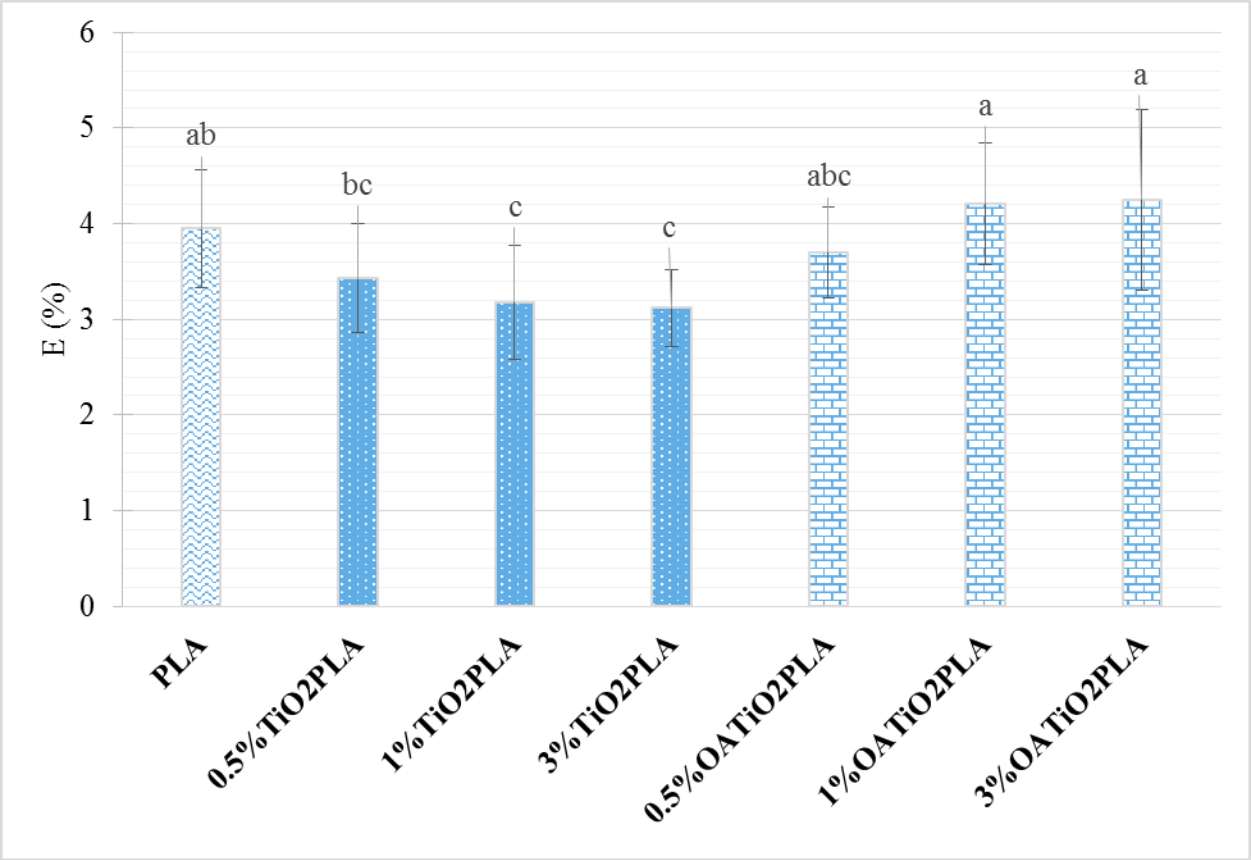

Figure 5c. Elongation at break (%) of PLA, 0.5%TiO_2 PLA, 1%TiO_2 PLA, 3%TiO_2 PLA, 0.5%OA_TiO_2 PLA, 1%OA_TiO_2 PLA and 3% OA_TiO_2 PLA nanocomposite films. Significant different mean values were shown with different letter by the Tukey's analysis when p-value is smaller than 0.05.

Table 4. Glass transition temperature (Tg,℃), melting temperature (Tm,℃) and cystallinity (Xc %) was indicated mean values ± standard deviation by temperature increase from 30 ℃ to 200 ℃ with 5℃ /min using the second heating cycle. The significant differences between samples were indicated with different letters by the Tukey analysis with p-value smaller than 0.05.

Sample (n=3)	Tg ℃ ± Std Dev	Tm ℃ ± Std Dev	Xc % ± Std Dev
PLA	55.64±0.76	149.68±0.41	1.42±0.05 [a]
0.5%TiO_2PLA	53.73± 2.2	148.74±1.68	1.68±0.57 [ab]
1%TiO_2PLA	55.51±2.54	149.84±0.58	1.61±0.41 [ab]
3%TiO_2PLA	52.73±3.25	148.47±1.04	2.63±0.55 [ab]
0.5%OA_TiO_2PLA	55.51±2.54	149.84±0.58	1.61±0.41 [ab]
1%OA_TiO_2PLA	53.55±2.89	148.86±1.55	2.63±0.55 [ab]
3%OA_TiO_2PLA	54.74±1.28	149.47±0.31	3.34±0.77 [b]

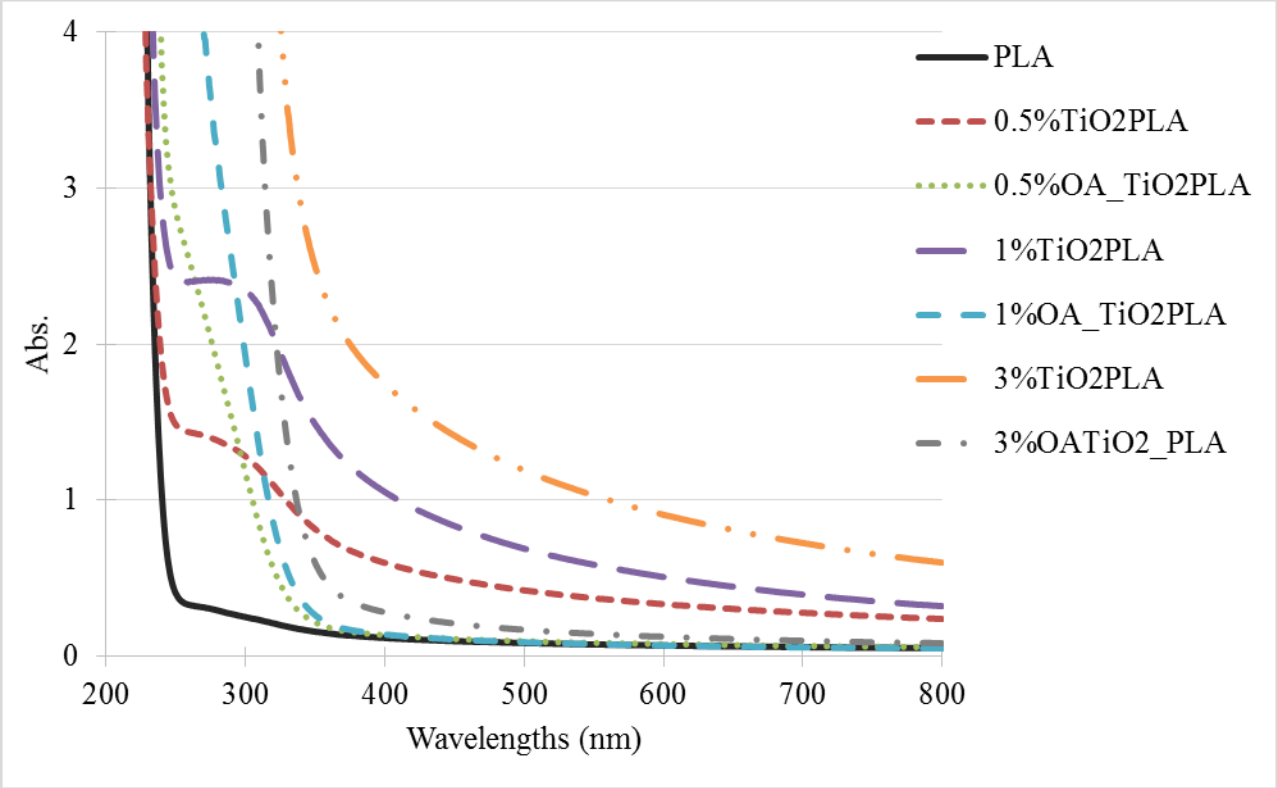

Figure 7. UV-Vis absorbance spectra of PLA, 0.5% TiO_2 PLA, 1% TiO_2 PLA, 3% TiO_2 PLA, 0.5% OA_TiO_2 PLA, 1% OA_TiO_2 PLA and 3% OA_TiO_2 PLA nanocomposite films in the wavelength range of 200-800 nm.

REFERENCES

1. Rhim, J. W., Park, H. M., & Ha, C. S. (2013). Bio-nanocomposites for food packaging applications. *Progress in Polymer Science, 38(10)*, 1629-1652.

2. Balakrishnan, H., Hassan, A., Imran, M., & Wahit, M. U. (2012). Toughening of polylactic acid nanocomposites: A short review. *Polymer-Plastics Technology and Engineering, 51(2)*, 175-192.

3. Jamshidian, M., Tehrany, E. A., Imran, M., Jacquot, M., & Desobry, S. (2010). Poly-Lactic Acid: production, applications, nanocomposites, and release studies. *Comprehensive Reviews in Food Science and Food Safety, 9*(5), 552-571.

4. Hartmann, M. H. (1998). High molecular weight polylactic acid polymers. In biopolymers from renewable resources (pp. 367-411). Berlin, Heidelberg: Springer.

5. Shah, A. A., Hasan, F., Hameed, A., & Ahmed, S. (2008). Biological degradation of plastics: a comprehensive review. *Biotechnology Advances, 26(3)*, 246-265.

6. Auras, R., Harte, B., & Selke, S. (2004). An overview of polylactides as packaging materials. *Macromolecular bioscience, 4(9)*, 835-864.

7. Silvestre, C., Duraccio, D., & Cimmino, S. (2011). Food packaging based on polymer nanomaterials. *Progress in Polymer Science, 36(12)*, 1766-1782.

8. Mihindukulasuriya, S. D. F., & Lim, L. T. (2014). Nanotechnology development in food packaging: A review. *Trends in Food Science & Technology, 40(2)*, 149-167.

9. Duncan, T. V. (2011). Applications of nanotechnology in food packaging and food safety: Barrier materials, antimicrobials and sensors. *Journal of colloid and interface science, 363(1)*, 1-24.

10. Robertson, G. L. (2012). Food packaging: principles and practice. CRC press.

11. De Azeredo, H. M. (2009). Nanocomposites for food packaging applications. *Food Research International, 42(9)*, 1240-1253.

12. Llorens, A., Lloret, E., Picouet, P. A., Trbojevich, R., & Fernandez, A. (2012). Metallic-based micro and nanocomposites in food contact materials and active food packaging. *Trends in Food Science & Technology, 24(1)*, 19-29.

13. Smijs, T. G., & Pavel, S. (2011). Titanium dioxide and zinc oxide nanoparticles in sunscreens: focus on their safety and effectiveness. *Nanotechnology,Sscience and Applications, 4*, 95.

14. Gumiero, M., Peressini, D., Pizzariello, A., Sensidoni, A., Iacumin, L., Comi, G., & Toniolo, R. (2013). Effect of TiO_2 photocatalytic activity in a HDPE-based food packaging on the structural and microbiological stability of a short-ripened cheese. *Food Chemistry, 138(2)*, 1633-1640.

15. Chau, J. L. H., Lin, Y. M., Li, A. K., Su, W. F., Chang, K. S., Hsu, S. L. C., & Li, T. L. (2007). Transparent high refractive index nanocomposite thin films. *Materials Letters, 61(14)*, 2908-2910.

16. Buzarovska, A. (2013). PLA nanocomposites with functionalized TiO2 nanoparticles. *Polymer-Plastics Technology and Engineering, 52(3)*, 280-286.

17. Fortunati, E., Peltzer, M., Armentano, I., Torre, L., Jiménez, A., & Kenny, J. M. (2012). Effects of modified cellulose nanocrystals on the barrier and migration properties of PLA nano-biocomposites. *Carbohydrate Polymers, 90(2)*, 948-956.

18. Lim, J. H., Kim, J., Ko, J. A., & Park, H. J. (2015). Preparation and Characterization of Composites Based on Polylactic Acid and Beeswax with Improved Water Vapor Barrier Properties. *Journal of Food Science, 80(11)*, E2471-E2477.

19. Khanzadi, M., Jafari, S. M., Mirzaei, H., Chegini, F. K., Maghsoudlou, Y., & Dehnad, D. (2015). Physical and mechanical properties in biodegradable films of whey protein concentrate–pullulan by application of beeswax. *Carbohydrate Polymers, 118*, 24-29.

20. He, M., Xu, M., & Zhang, L. (2013). Controllable stearic acid crystal induced high hydrophobicity on cellulose film surface. *ACS Applied Materials & Interfaces, 5(3*), 585-591.

21. Lai, H. M., & Padua, G. W. (1998). Water vapor barrier properties of zein films plasticized with oleic acid. *Cereal Chemistry, 75(2)*, 194-199.

22. Rhim, J. W., Hong, S. I., & Ha, C. S. (2009). Tensile, water vapor barrier and antimicrobial properties of PLA/nanoclay composite films. *LWT-Food Science and Technology, 42(2)*, 612-617.

23. Nakayama, N., & Hayashi, T. (2007). Preparation and characterization of poly (l-lactic acid)/TiO_2 nanoparticle nanocomposite films with high transparency and efficient photodegradability. *Polymer Degradation and Stability, 92(7)*, 1255-1264.

24. ASTM F3136-15. (2015) Standard test method for oxygen gas transmission rate through plastic film and sheeting using a dynamic accumulation method. ASTM International.

25. EN ISO 15106-3. (2003) Plastics- Film and sheeting- Determination of water vapour transmission rate- Part 3: Electrolytic detection sensor method (1th ed.), International Organization for Standardization (ISO).

26. ASTM–D882-12. (2012). Standard test method for tensile properties of thin plastic sheeting. ASTM International.

27. Duan, Z., Thomas, N. L., & Huang, W. (2013). Water vapour permeability of poly (lactic acid) nanocomposites. *Journal of Membrane Science, 445*, 112-118.

28. Zhu, Y., Buonocore, G. G., Lavorgna, M., & Ambrosio, L. (2011). Poly (lactic acid)/titanium dioxide nanocomposite films: influence of processing procedure on dispersion of titanium dioxide and photocatalytic activity. *Polymer Composites, 32(4)*, 519-528.

29. Ali, N. A., & Noori, F. T. M. (2014). Gas barrier properties of biodegradable polymer nanocomposites films. *Chemistry and Materials Research, 6(1)*, 44-51.

30. Díaz-Visurraga, J., Melendrez, M. F., Garcia, A., Paulraj, M., & Cardenas, G. (2010). Semitransparent chitosan-TiO2 nanotubes composite film for food package applications. *Journal of Applied Polymer Science, 116(6)*, 3503-3515.

CHAPTER 5. (-)-Epigallocatechin Gallate Stability in Ready to Drink Green Tea Infusion in TiO_2 and OA_TiO_2 PLA Film Packaging model under Fluorescent Lightening during Refrigerated Storage at 4 °C

ABSTRACT

The light protective effectiveness of TiO_2 PLA nanocomposite films (T-PLA) and OA_TiO_2PLA nanocomposite films (OT-PLA) were investigated in RTD green tea infusion in oxygen impermeable glass packaging. Particularly, stability of the most abundant polyphenolic compound (-)-Epigallocatechin gallate (EGCG), which is an indicator of green tea quality, was evaluated in RTD green tea in the glass packaging covered by foil, PLA, 1% T-PLA, 3%T-PLA, 1% OT-PLA and 3% OT-PLA under a fluorescent light during 20 days of storage at 4 ℃. Levels of EGCG in RTD green tea infusion and color change of RTD green tea infusion were determined by a HPLC analysis and a colorimeter. In addition, fluorescent light effect on sensory perception of RTD green tea infusion in glass packaging without and with a complete light protection (foil wrap) during 10 days of storage at 4 ℃ was evaluated. Sixty % of the panelists noticed sensory difference in the RTD green tea infusion in two different packaging condition during 10 days of the storage under fluorescent light by a triangle test (n=58). During 20 days of the storage, level of EGCG was the most stable in the glass packaging with complete light protection among the films. Level of EGCG was decreased by 10.8 % (0.73 mg/ml) whereas 42.2% loss of EGCG (0.48 mg/ml) was found in RTD green tea infusion in the glass packaging covered by PLA from the initial concentration of EGCG (0.83mg/ml) in RTD green tea infusion before the storage. 3% T-PLA preserved higher levels of EGCG in RTD green tea infusion compared to 1% T-PLA and OT-PLA.

KEY WORDS

TiO_2, RTD green tea infusion, EGCG, light protection, fluorescent light

INTRODUCTION

There has been growing consumption of green tea (*Cameilla sinesis*) due to potential health benefits associated with tea catechins; they may reduce risk of cardiovascular diseases, strokes and cancers [1, 2]. Green tea is non-fermented tea containing higher amounts of tea catechins than any other major types of tea such as oolong tea (semi-fermented tea) or black tea (fermented) tea [3]. Green tea contains polyphenol compounds such as (+)-catechin (C), (-)-epicatechin (EC), (-)-epicatechin gallate(ECG), (-)-epigallocatechin (ECG), (-)-epigallocatechin gallate(EGCG), (-)-gallocatechin gallate (GCG), and (-)-gallocatechin (GC). (-)-Epigallocatechin gallate (EGCG) is not only the most abundant catechin, it is also a potent antioxidant and a green tea quality indicator [4].

Ready to drink (RTD) green tea infusions are widely available in various packaging such as glass, plastic and aluminum containers because consumers have been looking for healthier drinks than soft drinks [5]. However, EGCG, which is a major bioactive compound, is found in lower amounts in the commercial RTD than in prepared green tea using traditional brewing methods [6]. EGCG is easily susceptible to epimerization and oxidation by light, oxygen, brewing methods, storage conditions and packaging materials [6-9].

Kim, Welt and Talcott (2011) reported stability of tea catechin was influenced significantly by oxygen contact [5]. Green tea infusion in glass bottles, which have the lowest oxygen permeation rates, retained the most tea catechins compared to green tea stored in polyethylene terephthalate (PET) bottles and retortable pouches [5]. In addition, degradation of EGCG and EGC influences sensory quality of green tea infusions. EGCG and other tea catechins in green tea infusion drinks should be maintained at highest levels possible before consumption to provide healthful bioactive compounds and the delicate green tea sensory quality [10].

Green tea leaves contain photosensitized pigments such as chlorophylls (0.2 ~0.6 % dry weight (%)) and carotenoids [11]. Major light absorption of chlorophylls reported at the wavelengths of 430 nm and 660 nm [16]. Others have reported that light has a detrimental effect on green tea flavor [11]. When green tea was exposed under 2000 lux light for one month, the green tea infusion had unacceptable off-flavors [12].

The stability of EGCG and other tea catechins in green tea infusion have been extensively studied. However, studies related to light influence on photochemical stability of EGCG in green tea infusion has been scarce [6, 8, 14]. Investigating photochemical behavior of EGCG level in green tea infusion by light exposure is important to prevent decomposition of EGCG level and keep major antioxidant as well as delicate green tea taste in suitable packaging during retail display.

TiO_2 is well known nanostructured fillers for polymer nanocomposites in food packaging applications due to enhancing barrier properties as well as providing color, UV-light protector and antibacterial effects under UV-light illumination [18, 19].

In the previous study, TiO_2 PLA and OA_TiO_2 PLA nanocomposites films were prepared. Our hypothesis was PLA nanocomposite films incorporated with TiO_2 and OA_TiO_2 might reduce degradation of EGCG in RTD green tea infusion under fluorescent light illumination.

The goal of the first study was to determine if fluorescent light exposure was changed EGCG and taste of RTD green tea infusion retained in clear glass packaging for 10 days at 4 °C. The objectives of this study were 1) to evaluate stability of EGCG in RTD green tea infusion stored in clear glass packaging exposed to fluorescent light and 2) to determine if consumers can

detect overall sensory differences of RTD green tea infusion in clear glass packaging using a triangle test during 10 days of storage at 4 ℃ under fluorescent light.

The purpose of the second study was to investigate effectiveness of T-PLA and OT-PLA films for preservation of EGCG in a RTD green tea infusion model under fluorescent light. The objective of this study was to determine level of EGCG in RTD green tea retained in glass bottles overwrapped by PLA (light exposed packaging), foil (light blocking), 1% and 3% T-PLA and 1% and 3% OT-PLA during 20 days of storage at 4 ℃ under fluorescent light.

MATERIALS AND METHODS

Materials

Dragon Well Green Tea bush (4 ounce) was purchased from an established online tea merchant (enjoyingtea.com). Spring water (6L) and granulated sugar were obtained from a local super market (Kroger, Blacksburg, VA). Food grade anhydrous fine granular citric acid was received from ADM (Decatur, IL). (-)-Epigallocatechin gallate (EGCG) as analytical standard was obtained from Sigma-Aldrich Chemical Co (St. Louis, MO). Methanol, phosphoric acid and acetonitrile (HPLC grade) were purchased from Fisher scientific company (Pittsburgh, PA). Food grade Star San ™ (32 ounce) was purchased as sanitizer for glass bottles used for green tea drink samples.

Methods

Study 1. Light effects on sensory differences and degradation of (-)-Epigallocatechin gallate (EGCG) of Ready to Drink Green Tea Infusion during Refrigerated Storage at 4 ℃

Ready to drink (RTD) green tea infusion preparation

First of all, fourteen clean glass bottles (340ml each) that were washed and air-dried then sanitized following Star San™ instruction [.

Dragon Well green tea bush of 60g was brewed in 6L of spring water at 90℃ for five

minutes then sugar (216g) was added into the RTD green tea infusion. Citric acid (6g) was added to the green tea infusion to create pH less than 4. The RTD green tea infusion was filled into sanitized glass bottles and then the bottles were placed upside down for two minutes. The green tea was cooled down in ice water bath.

Storage conditions

RTD green tea infusion stored in two different packaging such as light blocked and exposed glass packaging. Control samples of RTD green tea infusion was contained in light blocked glass bottles (7 bottles) covered by aluminum foil. Treatment samples of RTD green tea samples did not have the aluminum foil wrap (7 bottles). Approximately 2000-2500lux of florescent light produced by Sylvania (Designer cool white 30W, F30T12/DCW/RS, Ontario, Canada) was exposed to fourteen glasses bottles containing RTD green tea infusion in walk-in cooler at 4℃ during 10 days of storage. The positions of the glass bottles were rotated every 24 hours for even light exposure. All glass bottles were removed from florescent light after 10 days of storage at 4℃ before three hours conducting sensory triangle test and HPLC analysis. RTD green tea infusion in the light blocked glasses overwrapped foil was transferred into 3L of plastic bottle to blend. Also, other RTD green tea infusion in seven bottles without the aluminum foil was transferred into 3L of plastic water bottle to blend as well. One ounce of RTD green tea infusion was filled in two ounce cups codded with randomly assigned 3 digit numbers two hours prior to the sensory triangle test, then capped and stored at 4℃ of refrigerator in sensory preparation lab until the samples were served to panelists.

HPLC analysis

Level of EGCG was determined using an Agilent Technologies model 1200 series HPLC system (Santa Clara, CA) following procedure described by Yoshida and others (1999) [13]. C-

18 Luna 5µm (25cm x 4.9mm) column fitted with a guard column, which was obtained from Phenomenex (Torrence, CA), was used for the analysis. Two mobile phase systems were consisted of mobile phase A (95.45% distilled water, 4.5% acetonitrile and 0.05% O-phosphoric acid) and mobile phase B (49.95% distilled water, 50% acetonitrile and 0.05% O-phosphoric acid). The flow rate set to 1.0ml/min, and the system temperature was maintained at 40℃.

Sensory analysis

A triangle test for differences was determined if light influenced sensory perception of RTD green tea infusion stored in two different packaging for 10 days of storage at 4℃ was differentiated. The sensory triangle test for differences was conducted in room number 204 in the sensory lab of HABBI1. The number of panelists we need for the triangle test was at least 53 according to in Table 17.8 of critical number of correct response in a triangle test [21]. Training was not required, but the panelists should be familiar with the triangle test method. Panelists were recruited from undergraduates and graduates students, faculty and staff from Department of Food Science and Technology and Biological System Engineering at Virginia Tech. Panelists were seated in individual booths and evaluated samples under red light in order to mask colors of RTD green tea infusion samples and eliminate bias [21]. IRB approval (IRB#14-278) was received by Virginia Tech Office of Research Compliance. The Panelists were filled out a human subject consent form on IRB# 14-278 before preceding the evaluation. One set of three samples (n=3) was presented simultaneously in a balance order of presentation using a complete block design. Temperature of RTD green tea infusion samples were controlled at 4℃ to minimize flavor change of samples by temperature as the samples were stored in the refrigerator right before serving the samples to panelists. One set of three samples compares light blocked RTD green infusion treatment (A) to light exposed RTD green tea infusion treatment (B). The samples

were presented in random order to panelists using six possible orders (ABB, BAA, BBA, ABA and BAB) to minimize bias [21]. The panelists were asked to taste three samples from left to right and choose a different tasting sample within three samples and asked to indicate "odd taste sample" on the scorecards [21]. After completing one set of triangle test, panelists were requested to fill out a survey including demographics, age, race, frequent consumption and self-reported preference of RTD green tea infusion.

EXPERMENTAL DESIGN AND STASTISTICAL ANALYSIS

For difference test on the triangle sensory test, statistical parameters were defined at α=0.05, β=0.1 and P_d (proportion of discriminators) =30%. The number of subjects we needed was 53 at least. Sensory perception of RTD green tea infusion in light blocked and light exposed packaging were significantly different if the number of correct responses was more than 24 following in Table 17.8 of critical number of correct response in a triangle test (Table 1.1) [21].

Analysis of Variance was used to determine if EGCG level in RTD green tea infusion stored in two different packaging condition was significantly different after 10 days of storage under light exposure. Significant difference on mean values (n=2) of two treatments was compared by student t-test. Null hypothesis was rejected, and mean values were significantly different each other when p-value was smaller than 0.05 (Table 1.2).

Study 2. (-)-Epigallocatechin Gallate Stability in Ready to Drink Green Tea Infusion in TiO_2 and OA_TiO_2 PLA Film Packaging model under Fluorescent Lightening during Refrigerated Storage at 4 ℃

Ready to drink (RTD) green tea infusion preparation

Ground (8.42 g) dragon well green tea bush was brewed with 850 mL of spring water at 90 ℃ for five minutes, then 28.8 g of sucrose and 0.81 g of citric acid were added. The pH of the tea preparation was 3.74. The oxygen impermeable glass bottles were used due to investigate

only light blocking effects of the films for the green tea infusion. Fifteen ml of hot (82-85 ℃) RTD green tea infusion was filled into 20 ml glass bottles and capped tightly, then the bottles were placed upside down for two minutes. The bottles containing the RTD green tea were then cooled in an ice water bath. Films for testing (foil, PLA, 1% T-PLA, 1% OT-PLA, 3% T-PLA and 3% OT-PLA) were cut into uniform sizes of 5 cm x 9 cm for covering the glass bottles. Thickness of three sections of each film was measured by a digital micrometer (Mitutoyo 700-118-20 Digital Thickness Gage, Japan), then we averaged the thickness of the films. The glass bottles were covered by one layer of aluminum foil (complete light blocking), PLA (light exposed), 1% T-PLA, 1% OT-PLA, 3% T-PLA and 3% OT-PLA.

Storage conditions

Fluorescent light bulbs (1990 lux ± 365) produced by Sylvania (Designer cool white 30W, F30T12/DCW/RS, Ontario, Canada) provided light exposure to the glass bottles containing RTD green tea infusion in a walk-in cooler at 4℃ during 20 days. The light intensities and light spectrum were measured by Upertek MK350S (1B) (Miaoli County, Taiwan). The positions of the glass bottles were randomly rotated every 24 hours. Eighteen (6 treatments in triplicated) bottles containing RTD green tea infusion were taken from the storage every 10 days for EGCG analysis. The colors of the green tea infusion were measured on day 0 and day 20.

HPLC analysis

Level of EGCG was determined using an Agilent Technologies model 1260 series HPLC system (Santa Clara, CA) followed by the procedure described by Yoshida and others (1999) [13]. A Nucleosil 100-5 C-18 (25cm x 4.6mm) column, obtained from Machery-Nagel (Düren, Germany), was used for the analysis. Solvent consisted of mobile phase A (95.45% distilled water, 4.5% acetonitrile and 0.05% O-phosphoric acid) and mobile phase B (49.95% distilled

water, 50% acetonitrile and 0.05% O-phosphoric acid). The flow rate set to 1.0ml/min, and the column temperature was maintained at 40℃.

Color analysis

A colorimeter (Minolta Chorma Meter CR-200, Osaka, Japan) was used to analyze color changes of RTD green tea infusion on 0 day and 20 day. Calibration using a white calibration plate (CR-A44) was conducted first. The color values of the RTD green tea infusion in the glass packaging covered by the films were reported as L*=lightness (0=black, 100=white), a* (+a*=redness and –a*=greenness) and b* (+b*=yellowness and -b*=blueness).

STASTICAL ANALYSIS

One-way Analysis of Variance was used to determine if EGCG concentration changed in RTD green tea infusion stored under six different packaging models under the florescent light treatments. Significant differences on mean values were compared by Tukey's test at p-value ($p < 0.05$).

RESULTS AND DISCUSSION

Study 1. Light effects on sensory differences and degradation of (-)-Epigallocatechin gallate (EGCG) of Ready to Drink Green Tea Infusion
Sensory Analysis: Triangle discrimination sensory test

Difference for triangle test was conducted to determine if panelist detected taste difference between RTD green tea in clear glass packaging and in light blocked packaging when exposed to light.

Panelists (n=58) were consisted of male (24%) and female (68%). Panelists were range in age 18-24(59%), 25-34 (31%), 35-45(7%) and 45- older (3%). 83% of the panelists indicated positive responses on their liking on consumption of RTD green tea. 10% of the panelists

consumed green tea at least one time in a day. 57% of the panelists consumed green tea at least more than one time in a month.

In order to reduce Type 1 error, alpha value was set to low number 0.05 [21]. Null hypothesis (Table 1.1) was rejected since the number of correct response for the triangle test was 35 out of 58 respondents at α=0.05, β=0.1 and P_d=30%. Sixty (%) panelists were able to differentiate odd sample between RTD green tea samples stored in the packaging with and without light blocking during the storage. From the result of triangle discrimination sensory test, there was a significant flavor change of RTD green tea infusion between two different packaging when exposed to light during the storage.

Good quality of green tea has well balanced flavor of bitterness, astringency and constant sweetness after taste [22]. Narukawa, Kimata, Noga and Wantanbe (2010) reported that tea catechins were carrying astringency and bitterness in tea; especially, EGC and EGCG were recognized to bitter and astringency sensory attribute in green tea [23]. However, bitterness and astringency of green tea sensory perception was decreased after green tea extract were stored at 50℃ for 12 days of storage because of degradation of total phenolic contents [17]. The degradation of EGCG in RTD green tea infusion during the storage by HPLC analysis supported sensory triangle test result.

HPLC analysis

Light effect to degradation of EGCG in RTD green tea infusion was observed. HPLC analysis was conducted to evaluate stability of EGCG in RTD green tea infusion retained in clear glasses (light exposed packaging) and aluminum foil wrapped glasses (light blocked packaging) exposed to florescent light (2000-2500 lux) during 10 days storage at 4℃. A peak of EGCG on HPLC chromatogram was identified and quantified by comparison of retention times and areas

of peak using authentic standard of EGCG. Concentration of EGCG in RTD green tea infusion was attained by an external standard curve created by authentic EGCG standard solution (mg/ml) diluted to five times with distilled water using serial dilution.

In Figure 1, initial concentration of EGCG in RTD green tea infusion (0.51mg/ml) before the storage was decreased by 9% (0.47mg/ml) and 16%(0.43mg/ml) in glass packaging with and without light blocking respectively at 4℃ for 10 days of storage under light exposure. Null hypothesis ($H_0=\mu_{EGCG\ in\ light\ block\ glass}=\mu_{EGCG\ levels\ in\ clear\ glass}$) was rejected by one-way ANOVA ($p<0.05$) (Table 1.2), and mean values on levels of EGCG between two different packaging conditions were compared using student t-test. Significant differences on levels of EGCG were found between two different packaging at 4℃ during 10 days of storage ($p<0.05$).

Study 2. Study 2. (-)-Epigallocatechin Gallate Stability in Ready to Drink Green Tea Infusion in TiO_2 and OA_TiO_2 PLA Film Packaging model under Fluorescent Lightening during Refrigerated Storage at 4 ℃

HPLC analysis

EGCG stability in RTD green tea infusion retained in the glass bottles covered by foil, PLA, 1%T-PLA, 3%T-PLA, 1% OT-PLA and 3% OT-PLA under the fluorescent light (1990 lux ± 365) were evaluated during 20 days of storage at 4℃. A peak of EGCG on HPLC chromatogram was identified according to HPLC analysis described in the study 1.

Before the storage under fluorescent light, initial concentration of EGCG in the RTD green tea infusion was 0.83 mg/ml. After 10 days of the storage, amounts of EGCG were varied in RTD green tea depending on the packaging. EGCG in RTD green tea infusion was the most stable in the glass bottle covered by the aluminum foil (complete light protective film). The amount of EGCG in RTD green tea in the packaging covered by PLA (transparent light exposed film) shows the largest decrease of EGCG by 21.7% (0.65 mg/ml). The light protecting

packaging with foil wrap retained the most amount of EGCG in RTD green tea (0.77 mg/ml) on day 10. On day 20, level of EGCG in RTD green tea infusion in the glass packaging covered by PLA was decreased by 42.2 % (0.48 mg/ml) from initial level of EGCG in RTD green tea infusion. The result exhibited that the level of EGCG in RTD green tea infusion in the packaging covered by 3% T-PLA and 3% OT-PLA retained higher amounts than 1% T-PLA and 1% OT-PLA. Three % T-PLA packaging preserved higher levels of EGCG in RTD green tea infusion than 3% OT-PLA. 1% T-PLA and 1% OT-PLA had slight light protection to keep EGCG in RTD green tea infusion during 20 days of the storage as seen in Figure 2.

Oxygen and light influenced degradation of tea catechins and produced off-flavors of green tea significantly [5, 11, 12]. Scalia, Marchetti and Bianchi (2013) reported that EGCG in hydrophilic cream model system was degraded 76.9±3.7% under 1hr solar simulator emission at 500W/m^2 with controlled temperature below 37 ℃ [8, 14]. However, addition of vitamin C in the hydrophilic cream reduced less EGCG level of 20.4 ±2.7 % compared to the cream without vitamin C [14]. Hara (1989) reported green teas that were exposed to the lights produced unfavorable volatile compounds and reduce fresh flavor of green tea [15]. The fluorescent light used in this experiment had high light power at 430, 550 and 580 nm in the light spectrum (Figure 1). Chlorophyll has high excited peaks at the light wavelengths of of 430 nm and 660 nm [16]. As a result, chlorophyll might have acted as a photosensitizer in our model system. If this happened, chlorophyll photooxidation might have degraded catechins in the green tea. 3% T-PLA films had much higher light absorption in the visible region than OT-PLA films. EGCG level in RTD green tea infusion in the glass packaging covered by 3%T-PLA was higher than T-PLA and OT-PLA packaging. Further studies are needed to understand the specific wavelengths of light that cause degradation of catechins in tea [16].

Because RTD green tea drinks usually have long retail shelf life in retail stores and are displayed in retail cases under light, use of suitable packaging is important to preserve EGCG and other tea catechins and keep delicate green tea flavors.

Consumers would prefer to see foods through the packaging when they made food selections. Transparency of OT-PLA is quite similar as PLA due to well dispersion of TiO_2 nanoparticles by the surface modification in PLA. However, OT-PLA shows less effects in protection of EGCG compared to T-PLA when same concentrations of TiO_2 or OA_TiO_2 were incorporated into PLA. This study may suggest that higher amounts of TiO_2 loading in PLA retained level of EGCG better for light protection. However, it still limited complete protection of EGCG from light compared to the foil.

Color change

Color changes of the green tea infusion between six different packaging were measured on day 20. L (Table 3a), a (Table 3b), b (Table 3c) values of RTD green tea infusion stored in the packaging covered by foil, PLA, T-PLA and OT-PLA were recorded. On day 20, the RTD green tea infusion in the packaging with complete light protection had the least a value which means that the color of the RTD green tea was the most green and least red among the RTD green tea in six different packaging whereas RTD green tea in the PLA packaging had highest a value which means the most red. During 20 days of the storage, color of the green tea was changed significantly. These results showed that higher EGCG degradation in RTD green tea infusion in PLA packaging and 1% T-PLA and 1% OT-PLA had more reddish color than less degradation of EGCG in RTD green tea infusion in the packaging such as foil and 3%T-PLA. The color change of the green tea was obviously dependent on the films and storage time under the light exposure. Wang, Kim and Lee (2000) observed that oxidation of tea phenolic compounds led to a

development of brown color in green tea extract during 12 days of storage at 50℃ during the accelerated storage condition [17]. The a value of the color change results were agreed with previous research finding that the green tea color become more reddish in the result of oxidation of polyphenolic compounds. Chlorophyll is a green pigment in green tea and its amount decides final color of green tea infusion [24]. The light may degrade chlorophyll in RTD green tea infusion during the storage because light absorptions of photosensitizer chlorophyll are at the wavelength of 430 nm and 660 nm [16, 24]. Hence, the light may reduce green color of RTD green tea infusion in the packaging during the storage.

CONCLUSIONS

The first study showed that protection from light is essential to maintain EGCG and sensory quality of RTD green tea infusion. We found that EGCG levels in RTD green tea infusion in light exposed glass packaging significantly decreased during 10 days of storage at 4 ℃ under florescent light (2000-2500 lux). By using a triangle difference test (n=58), the taste of the green tea in light blocking and light exposed packaging during 10 days of the storage was significant different (α=0.05, β=0.1 P_d=30%). Sixty % of the panelists noticed differences in the green tea stored in the two different packaging conditions.

EGCG stability in RTD green tea in the glass packaging covered by foil, PLA, 1% T-PLA, 3% T-PLA, 1% OT-PLA and 3% OT-PLA was determined under the florescent light during 20 days of the storage at 4 ℃. The results suggested higher levels of TiO_2 incorporated into PLA may more effectively retard EGCG degradation than low concentration of TiO_2 and OA_TiO_2. OT-PLA was less effective than T-PLA for light protection assessed by EGCG stability in RTD green tea infusions. Color of RTD green tea infusion in glass packaging covered

by PLA displayed less green than RTD green tea infusion in the glass packaging with complete light protection.

Preservation of EGCG and other tea catechins is essential to retain antioxidant capacity and delicate green tea taste during the retail display. Commercial RTD green tea infusion should be sold in appropriate packaging provides not only high oxygen barrier property but also light protection in the retail case.

Table 1.1 The null hypothesis (H_0) and alternative hypotheses (H_a) for the triangle test for difference between light exposed RTD green tea samples and light blocked RTD green tea infusion samples when statistical parameters are α=0.05, β=0.1 and P_d=30%.

Triangle test	Hypothesis	Result
Difference test	H_0: Proportion of correct response is less than 24 in 53 respondents.	No significant differences
	H_a: Proportion of correct response is larger than 24 in 53 respondents.	Significant differences

Table 1.2 The null hypothesis (H_0) and alternative hypotheses (H_a) for EGCG level difference between light exposed RTD green tea samples and light blocked RTD green tea infusion samples.

EGCG level	Hypothesis	Result
	H_0: $\mu_{\text{EGCG in light block glass}} = \mu_{\text{EGCG levels in clear glass}}$	No significant differences
	H_a: $\mu_{\text{EGCG in light block glass}} \neq \mu_{\text{EGCG levels in clear glass}}$	Significant differences

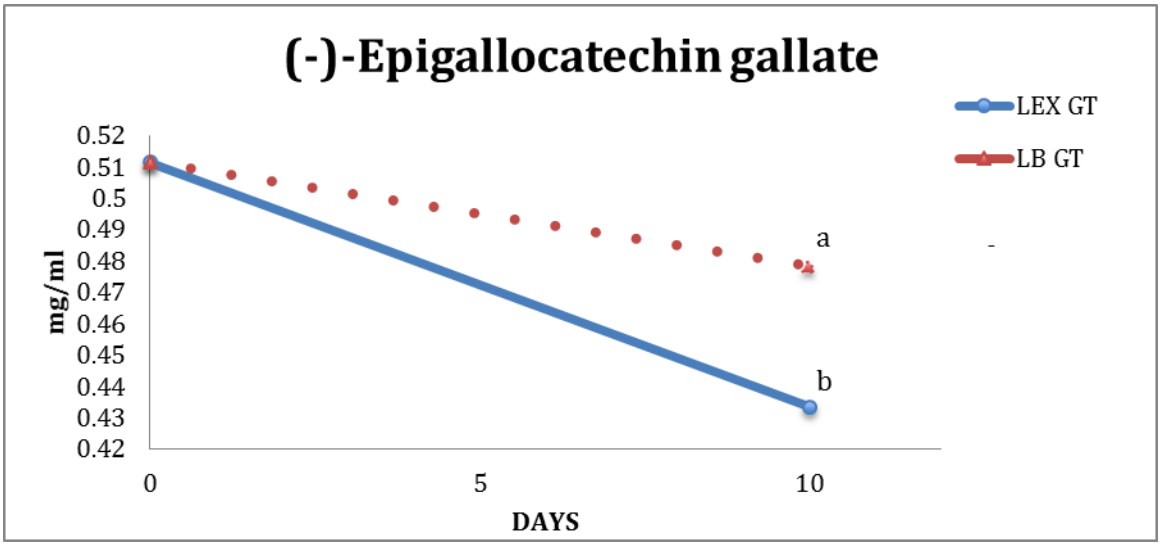

Figure1. Changes of EGCG (mg/ml) in ready to drink green tea infusion stored in light blocking glass packaging (LB GT) and clear glass packaging (LEX GT) under light exposure at 4℃ during 10 days of storage. Concentration (mg/ml) of LB GT and LEX GT was expressed with means (n=2). A significant difference between two treatments was expressed with different superscript letter (a or b) next to data ($p<0.05$).

Table 2. Thickness (Mean ± standard deviation) of PLA, 3%TiO_2 PLA, 1%TiO_2 PLA, 3% OA_TiO_2 PLA, 1%OA_TiO_2 PLA nanocomposite films covered the glass bottles (n=6).

Sample (n=6)	Mean (μm) ± Std Dev
PLA	70.6 ± 15.1
3%TiO_2PLA	62.2 ± 8.06
1%TiO_2PLA	61.1 ± 9.61
3%OA_TiO_2PLA	66.7 ± 4.7
1%OA_TiO_2PLA	62.2 ± 10.3

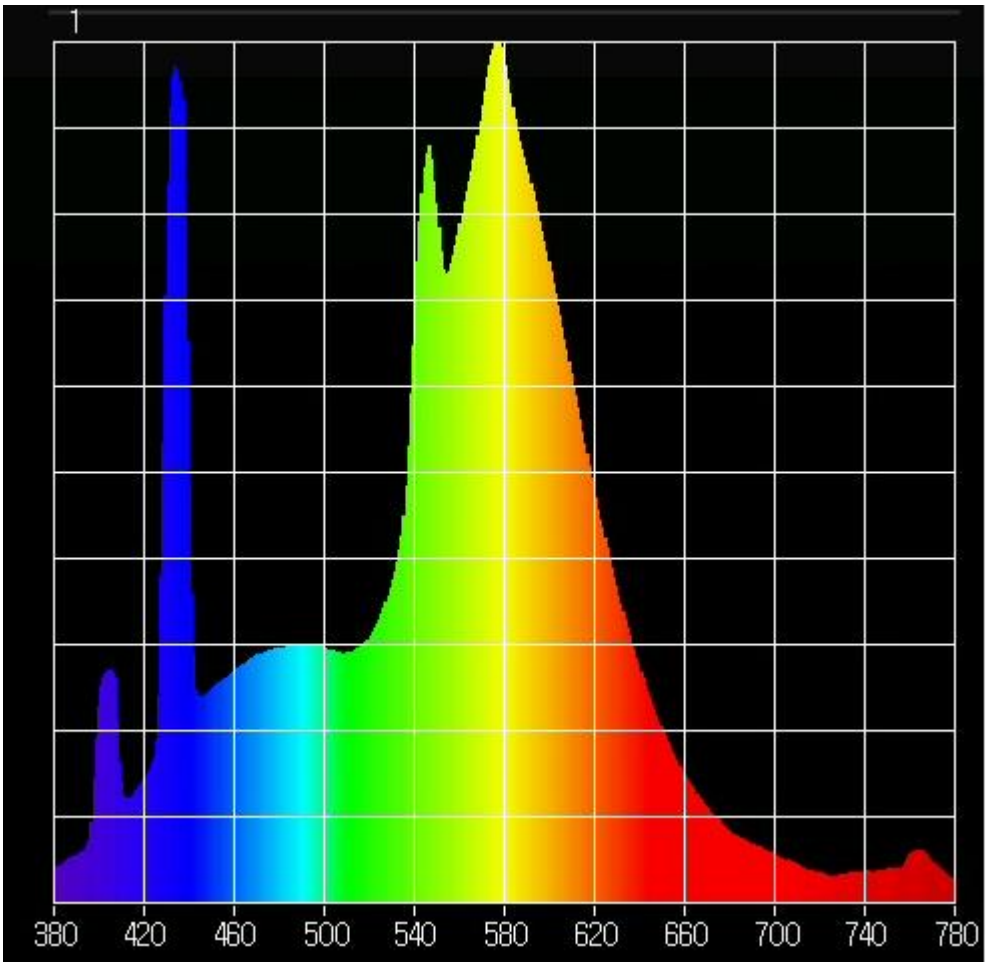

Figure 2. The Fluorescent light spectrum was taken at 2393 lux by a light measurement instrument Upertek MK350S (1B). The florescent light (1990 lux ± 365) was illuminated during EGCG stability test at 4℃.

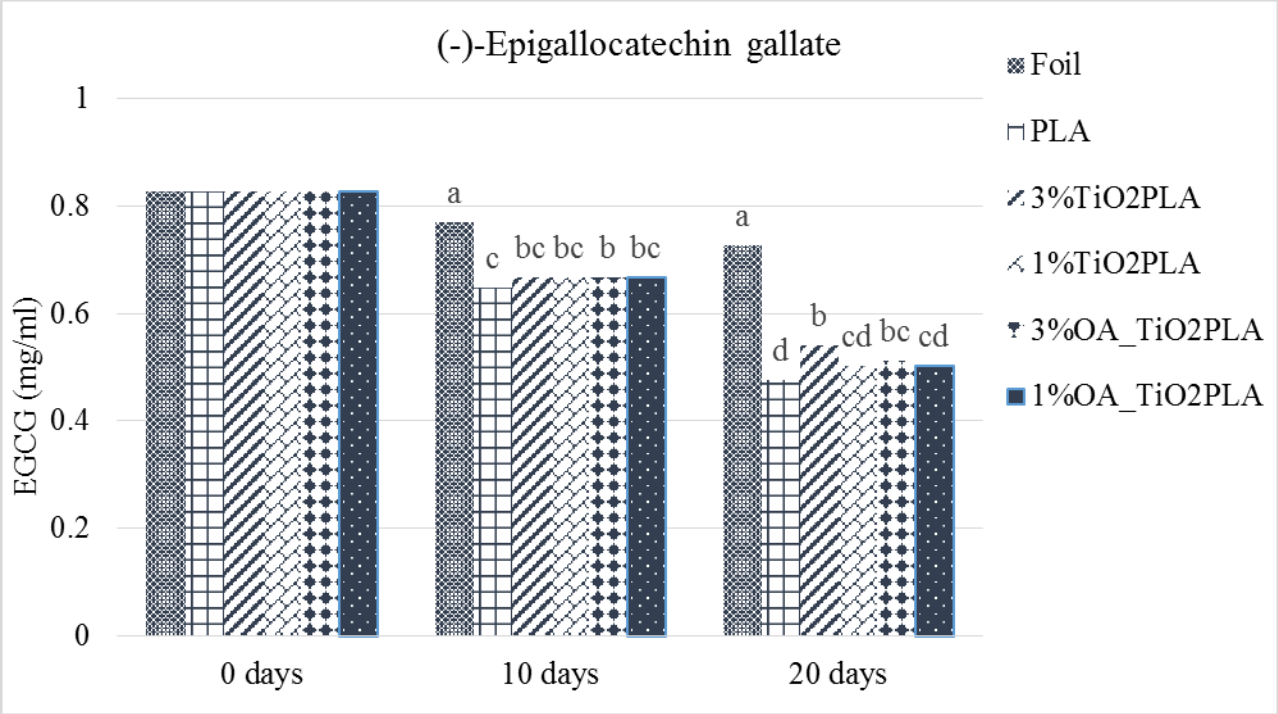

Figure 3. (-)-Epigallocatechin gallate concentration in the green tea infusion retained in glass bottles covered by foil, PLA, 3%TiO_2PLA, 1%TiO_2 PLA, 3% OA_TiO_2PLA, 1%OA_TiO_2PLA nanocomposite films at day 0, 10 days and 20 days under florescent light illumination at 4℃. Significant differences between the samples were expressed with different superscript letter above data by Tukey's analysis with p-value < 0.05.

Table 3a. Color changes (Mean ± standard deviation) was shown with L*value (L*:0=black, 100=white) of RTD green tea in the glass bottles covered by foil, PLA, 3%TiO $_2$PLA, 1%TiO_2 PLA, 3% OA_TiO_2 PLA, 1%OA_TiO_2 PLA nanocomposite films during the storage of 0 and 20 days at 4℃ under florescent lightening. Different letters next to data indicated statistical differences between L-values of the color.

	L-values					
Sample	Foil	PLA	3%TiO_2PLA	1%TiO_2PLA	3%OA_TiO_2PLA	1%OA_TiO_2PLA
0 days	92.3 ± 0.81	92.3 ± 0.81	92.3 ± 0.81	92.3 ± 0.81	92.3 ± 0.81	92.3 ± 0.81
20 days	96.9 ± 1.5^{a}	96.9 ± 0.05^{a}	94.59 ± 0.11^{bc}	96.1 ± 0.05^{ab}	96.2 ± 0.11^{ab}	94.2 ± 0.37^{c}

Table 3b. Color changes was shown with a*value: green- red (a*: + number, more red) of RTD green tea in the glass bottles covered by foil, PLA, 3%TiO_2 PLA, 1%TiO_2 PLA, 3% OA_TiO_2 PLA, 1%OA_TiO_2 PLA nanocomposite films during the storage of 0 and 20 days at 4℃ under florescent lightening. Different letters next to data indicated statistical differences between a-values of the color.

	a-values					
Sample	Foil	PLA	3%TiO_2PLA	1%TiO_2PLA	3%OA_TiO_2PLA	1%OA_TiO_2PLA
0 days	0.36 ± 1.3	0.36 ± 1.3	0.36 ± 1.3	0.36 ± 1.3	0.36 ± 1.3	0.36 ± 1.3
20 days	-1.38 ± 0.12^{c}	-0.46 ± 0.04^{a}	-1.14 ± 0.44^{bc}	-1.03 ± 0.23^{bc}	-0.72 ± 0.24^{ab}	-0.69 ± 0.25^{ab}

Table 3c. Color changes was shown with b*value: blue-yellow (b*: + number yellow) of RTD green tea in the glass bottles covered by foil, PLA, 3%TiO_2 PLA, 1%TiO_2 PLA, 3% OA_TiO_2 PLA, 1%OA_TiO_2 PLA nanocomposite films during the storage of 0 and 20 days at 4℃ under florescent lightening. Different letters next to data indicated statistical differences between b-values of the color.

	b-values					
Sample	Foil	PLA	3%TiO_2PLA	1%TiO_2PLA	3%OA_TiO_2PLA	1%OA_TiO_2PLA
0 days	3.76 ± 0.16	3.76 ± 0.16	3.76 ± 0.16	3.76 ± 0.16	3.76 ± 0.16	3.76 ± 0.16
20 days	2.43 ± 0.05^{a}	-2.04 ± 0.05^{c}	-0.96 ± 0.15^{b}	-1.28 ± 0.15^{bc}	-1.86 ± 0.08^{c}	-1.29 ± 0.26^{bc}

REFERENCES

1. Lambert, J. D., & Yang, C. S. (2003). Mechanisms of cancer prevention by tea constituents. *The Journal of Nutrition*, *133*(10), 3262S-3267S.

2. Zaveri, N. T. (2006). Green tea and its polyphenolic catechins: medicinal uses in cancer and noncancer applications. *Life Sciences*, *78*(18), 2073-2080.

3. Toschi, T. G., Bordoni, A., Hrelia, S., Bendini, A., Lercker, G., & Biagi, P. L. (2000). The protective role of different green tea extracts after oxidative damage is related to their catechin composition. *Journal of Agricultural and Food Chemistry*, *48*(9), 3973-3978.

4. Wang, R., Zhou, W., & Jiang, X. (2008). Reaction kinetics of degradation and epimerization of epigallocatechin gallate (EGCG) in aqueous system over a wide temperature range. *Journal of Agricultural and Food Chemistry*, *56*(8), 2694-2701.

5. Kim, Y., Welt, B. A., & Talcott, S. T. (2011). The impact of packaging materials on the antioxidant phytochemical stability of aqueous infusions of green tea (Camellia sinensis) and yaupon holly (Ilex vomitoria) during cold storage. *Journal of Agricultural and Food Chemistry*, *59*(9), 4676-4683.

6. Ananingsih, V. K., Sharma, A., & Zhou, W. (2013). Green tea catechins during food processing and storage: a review on stability and detection. *Food Research International*, *50*(2), 469-479.

7. Bazinet, L., Araya-Farias, M., Doyen, A., Trudel, D., & Têtu, B. (2010). Effect of process unit operations and long-term storage on catechin contents in EGCG-enriched tea drink. *Food Research International*, *43*(6), 1692-1701.

8. Bianchi, A., Marchetti, N., & Scalia, S. (2011). Photodegradation of (−)-epigallocatechin-3-gallate in topical cream formulations and its photostabilization. *Journal of Pharmaceutical and Biomedical Analysis*, *56*(4), 692-697.

9. Labbé, D., Têtu, B., Trudel, D., & Bazinet, L. (2008). Catechin stability of EGC-and EGCG-enriched tea drinks produced by a two-step extraction procedure. *Food Chemistry*, *111*(1), 139-143.

10. Wang, R., Zhou, W., & Jiang, X. (2008). Reaction kinetics of degradation and epimerization of epigallocatechin gallate (EGCG) in aqueous system over a wide temperature range. *Journal of Agricultural and Food Chemistry*, *56*(8), 2694-2701.

11. Zhen, Y. S. (2003). Tea: bioactivity and therapeutic potential. CRC Press.

12. Masuzawa, T. (1975). Effects of light on the qualities of green tea. Bulletin of the Shizuoka Tea Experiment Station (Japan).

13. Yoshida, Y., Kiso, M., & Goto, T. (1999). Efficiency of the extraction of catechins from green tea. *Food Chemistry*, *67*(4), 429-433.

14. Scalia, S., Marchetti, N., & Bianchi, A. (2013). Comparative evaluation of different co-antioxidants on the photochemical-and functional-stability of epigallocatechin-3-gallate in topical creams exposed to simulated sunlight. *Molecules*, *18*(1), 574-587.

15. Hara, T. (1989). Studies on the firing aroma and off-flavor components of green tea. Bulletin of the National Research Institute of Vegetables, Ornamental Plants and Tea. Series B. (Japan).

16. Bianchi, L. M., Duncan, S. E., Webster, J. B., Neilson, A. P., & O'Keefe, S. F. (2015). Contribution of chlorophyll to photooxidation of soybean oil at specific visible wavelengths of light. *Journal of Food Science*, *80*(2), C252-C261.

17. Wang, L. F., Kim, D. M., & Lee, C. Y. (2000). Effects of heat processing and storage on flavanols and sensory qualities of green tea beverage. *Journal of Agricultural and Food Chemistry*, *48*(9), 4227-4232.

18. Llorens, A., Lloret, E., Picouet, P. A., Trbojevich, R., & Fernandez, A. (2012). Metallic-based micro and nanocomposites in food contact materials and active food packaging. *Trends in Food Science & Technology*, *24*(1), 19-29.

19. Gumiero, M., Peressini, D., Pizzariello, A., Sensidoni, A., Iacumin, L., Comi, G., & Toniolo, R. (2013). Effect of TiO2 photocatalytic activity in a HDPE-based food packaging on the structural and microbiological stability of a short-ripened cheese. *Food Chemistry*, *138*(2), 1633-1640.

20. Palmer J. (1999). How to Brew. http://www.howtobrew.com/section1/chapter2-2-3.html.

21. Meilgaard, M. C., Carr, B. T., & Civille, G. V. (2006). *Sensory evaluation techniques*. CRC press.

22. Sanderson, G. W., Ranadive, A. S., Eisenberg, L. S., Farrell, F. J., Simons, R. O. B. E. R. T., Manley, C. H., & Coggon, P. H. I. L. I. P. (1976). Contribution of polyphenolic compounds to the taste of tea. In *ACS Symposim Series American Chemical Society*.

23. Narukawa, M., Kimata, H., Noga, C., & Watanabe, T. (2010). Taste characterisation of green tea catechins. *International Journal of Food Science & Technology*, *45*(8), 1579-1585.

24. Ošťádalová, M., Tremlová, B., Pokorná, J., & Král, M. (2015). Chlorophyll as an indicator of green tea quality. *Acta Veterinaria Brno, 83*(10), 103-109.

APPENDICES

Questionnaire for Sensory Study

Please answer all of the following questions.

Gender
Male
Female

Age
18-24
25-34
35-45
45 and older

Ethnicity origin (or Race): Please specify your ethnicity.

Hispanic
Caucasian
African or African American
Native American
Asian
Other

Do you like to drink a green tea?
Yes
No

How often do you consume green tea drinks?
More than one time in a day
At least one time in a day
Three times in a week
Once in two weeks
Once in a month
Seldom
Never

Scorecards

Panelist Number_____
Sample: Ready to Drink Green Tea Infusion

Characteristic Studied: Flavor

Instructions:
Taste samples from left to right. Two samples are identical; determine which one is the odd sample. If no difference is apparent, enter your best guess.

Sample Codes 653, 298, 455

Please circle or check mark on the odd sample.

Thank you for completing this sensory test. Please return the tray and scorecard to the researchers by sliding it through the booth. Please wait for demographics survey.

Virginia Polytechnic Institute and State University

Informed Consent for Participants in Research Projects Involving Human Subjects (Sensory Evaluation)

Title Project: Sensory Differences in Ready to Drink Green Tea Infusion during Storage at 4℃

Investigators: Susan E. Duncan, PhD, Sean O'Keefe, PhD, Naerin Baek, and Kristen Leitch

I. Purpose of this Research/Project
You are invited to participate in a study to determine whether consumers can detect overall sensory difference of green tea affected by packaging during storage at 4℃.

II. Procedures
You will be evaluating one set of green tea drinks for sensory quality. The set will have three samples. You will identify a sample that is different based on flavor, within one set and respond using a scorecard or a touch screen. You are encouraged to participate in the session, if possible.

III. Risks
There are only minimal risks associated to study participants with this project. Individuals with green tea allergy ,caffiene and acid sensitivity, iron deficiency anemia or pregnancy risk may have risks.

IV. Benefits
The goal of this research is to determine if packaging and storage condition affect sensory difference of green tea drinks during storage at 4℃. The information from this study will help determine appropriate packaging and storage condition for green tea drinks.

V. Extent of Anonymity and Confidentiality
The results of your performance as a panelist will be kept strictly confidential except to the investigator. Individual panelists will be referred to by a code number for data analyses and for any publication of the results.

VI. Compensation
You will be compensated with a small edible treat and a canned food at the end of the session.

VII. Freedom to Withdraw
If you agree to participate in this study, you are free to withdraw from the study at any time without penalty. Please withdraw from the study if you are less than 18 years of age.

VIII. Subject's Responsibilities
I voluntarily agree to participate in this study. I have the following responsibilities:

- Evaluate 1 set (3 samples of green tea drinks, as presented, and provide answers using a score card or touch screen.

IX. Subject's Permission

I have read the consent form and conditions of this project. I have had all my questions answered. I hereby acknowledge the above and give my voluntary consent:

Date: _____

Subject Signature: _____

Subject Printed Name: _____

- - - - - - - - - - - For Human Subject to Keep - - - - - - - - - - -

Should I have any pertinent questions about this research or its conduct, and research subjects' rights, and whom to contact in the event of a research-related injury to the subject. I may contact:

Susan Duncan, Faculty/Investigator	(540) 231-8675; duncans@vt.edu
Sean O'Keefe, Faculty/Investigator	(540) 231-4437; okeefes@vt.edu
Kristen Leitch, Graduate Student/Investigator	(540) 231-8675; kaleitch@vt.edu
Naerin Baek, Graduate Student/Investigator	(540) 231-8675; nbaek@vt.edu
David Moore Chair, Virginia Tech Institutional Review Board for the Protection of Human Subjects Office of Research Compliance Blacksburg, VA 24061	(540) 231-4991; moored@vt.edu